INIS-mf--13565

TEL AVIV UNIVERSITY אוניברסיטת תל-אביב
הפקולטה למדעים מדוייקים ע"ש ריימונד ובברלי סאקלר
בית הספר לפיסיקה ואסטרונומיה

ISRAEL PHYSICAL SOCIETY

1993

ANNUAL MEETING

Program and Abstracts

BULLETIN OF THE IPS, VOL. 39, 1993

אוניברסיטת תל-אביב TEL AVIV UNIVERSITY
הפקולטה למדעים מדוייקים ע"ש ריימונד ובברלי סאקלר
בית הספר לפיסיקה ואסטרונומיה

החברה הישראלית לפיסיקה

הכנס השנתי

תשנ"ג

תכנית ותקצירים

1993

אוניברסיטת תל-אביב TEL AVIV UNIVERSITY
הפקולטה למדעים מדוייקים ע"ש ריימונד ובברלי סאקלר
בית הספר לפיסיקה ואסטרונומיה

החברה הישראלית לפיסיקה

הכנס השנתי

תשנ"ג

תכנית ותקצירים

1993

ברוכים הבאים!

בית הספר לפיסיקה ואסטרונומיה וחברי הוועדה המארגנת שמחים לארח את באי הכנס של החברה הישראלית לפיסיקה. אנו מקווים מאד שתמצאו ענין רב בשמיעת ההרצאות במושבי המליאה ובמושבים המקבילים, ובקריאת התקצירים.

חברי הוועדה מודים מאד למארגני כל המושבים וצוות מזכירות ביה"ס לפיסיקה ואסטרונומיה שעמל רבות בארגון הכנס.

יואל רפאלי

Welcome!

The School of Physics and Astronomy and the organizing committee are pleased to host the participants in the annual meeting of the Israeli Physical Society. We hope that you will find great interest in the talks in the plenary and parallel sessions, and in reading the abstracts.

The organizing committee thanks all involved in the organization of the various sessions, and the staff of the School of Physics and Astronomy for all their work.

Yoel Rephaeli

ועד

פרופ' יצחק צרויה , נשיא - מכון ויצמן למדע
ד"ר טוביה בר נוי - קמ"ג
ד"ר יוסף ברק - ממ"ג
פרופ' שמואל גורביץ, מזכיר - מכון ויצמן למדע
פרופ' דוד גיל - אוניברסיטת בן-גוריון
ד"ר בנימין סבטיצקי - אוניברסיטת תל-אביב
ד"ר דב פאליק - רפא"ל
פרופ' צ'רלס קופר - (נציג Annals) - הטכניון
פרופ' דניס רפפורט, גזבר - אוניברסיטת בר-אילן
פרופ' דוד שאלתיאל - האוניברסיטה העברית
פרופ' גיורא שביב - הטכניון

גופים חברים

אוניברסיטת בר-אילן
אוניברסיטת בן-גוריון
האוניברסיטה העברית
הוועדה לאנרגיה אטומית
הטכניון - מכון טכנולוגי לישראל
אוניברסיטת תל-אביב
מכון ויצמן למדע

הוועדה המארגנת - אוניברסיטת תל אביב

פרופ' יואל רפאלי , יו"ר
פרופ' דוד אנדלמן
פרופ' סולאנג' אקסלרוד
ד"ר גדעון כלע
ד"ר יעקב זוננשיין
ד"ר בנימין סבטיצקי
פרופ' אלי פיאסצקי
ד"ר אלכסנדר פלבסקי

מידע כללי

דוכן ההרשמה לכנס יהיה בלובי של בנין שנקר מהשעה 08.30-10.00 בבוקר. משתתפים בכנס שלא שלמו עדיין את דמי החבר השנתיים לחברה הישראלית לפיסיקה (30 שקל; גמלאי או סטודנט 20 שקל) מתבקשים לעשות כך בהרשמה.

מושבי המליאה יתקיימו באולם לב. המושבים המקבילים יתקיימו באולמות אחרים, כמתואר בתכנית.

תצוגת הפוסטרים תערך לאורך הפרוזדור בהמשך ללובי של בנין שנקר ובחדר 104 בבנין שנקר. מומלץ שהפוסטרים יוצגו מוקדם ככל האפשר ובעל הפוסטר יעמוד על ידו בין השעות 15.45-16.15.

מזנון לב בקומת המרתף של בנין שנקר פתוח לשרותכם.

TEL AVIV UNIVERSITY אוניברסיטת תל-אביב
הפקולטה למדעים מדוייקים ע"ש ריימונד וברלי סאקלר
בית הספר לפיסיקה ואסטרונומיה

ISRAEL PHYSICAL SOCIETY

1993

ANNUAL MEETING

Program and Abstracts

BULLETIN OF THE IPS, VOL. 39, 1993

ברוכים הבאים!

בית הספר לפיסיקה ואסטרונומיה וחברי הוועדה המארגנת שמחים לארח את באי הכנס של החברה הישראלית לפיסיקה. אנו מקווים מאד שתמצאו ענין רב בשמיעת ההרצאות במושבי המליאה ובמושבים המקבילים, ובקריאת התקצירים.

חברי הוועדה מודים מאד למארגני כל המושבים וצוות מזכירות ביה"ס לפיסיקה ואסטרונומיה שעמל רבות בארגון הכנס.

יואל רפאלי

Welcome!

The School of Physics and Astronomy and the organizing committee are pleased to host the participants in the annual meeting of the Israeli Physical Society. We hope that you will find great interest in hearing the talks in the plenary and parallel sessions, and in reading the abstracts.

The organizing committee thanks all involved in the organization of the various sessions, and the staff of the School of Physics and Astronomy for all their work.

Yoel Rephaeli

COUNCIL

Prof. I. Tserruya - president - Weizmann Institute of Science
Prof. S. Gurvitz - secretary - Weizmann Institute of Science
Prof. D. Rappaport - treasurer - University Bar-Ilan
Prof. D. Shaltiel - Hebrew University
Prof. G. Shaviv - Technion
Prof. D. Gil - Ben-Gurion University
Dr. B. Svetitsky - Tel-Aviv University
Dr. Y. Barak - Atomic Energy Commission Yavne
Dr. T. Bar-Noy - Atomic Energy Commission Dimona
Dr. D. Falik - RAFAEL
Prof. C. Kuper - Annals representative - Technion

MEMBER ORGANIZATIONS

Bar-Ilan University
Ben-Gurion University
Hebrew University
Israel Atomic Energy Commission
Technion - Israel Institute of Technology
Tel-Aviv University
Weizmann Institute of Science

ORGANIZING COMMITTEE - Tel Aviv University

Prof. Y. Rephaeli
Prof. D. Andelman
Prof. S. Akselrod
Dr. G. Bella
Dr. J. Sonnenschein
Dr. B. Svetitsky
Prof. E. Piasetzki
Dr. A. Palevski

GENERAL INFORMATION

The conference desk will be open in the lobby of the Shenkar Building from 08:30 - 10:00 a.m. for registration. Participants who have not yet paid the annual membership fee (IS.30; IS.20 for retired members and students) to the Israel Physical Society are asked to do so at the time of registration.

The plenary sessions will be held at the Lev Auditorium; the parallel sessions will be held at various Lecture Halls, as indicated in the program.

The poster session will be held along the corridor adjacent to the lobby of the Shenkar Building, and in room 104 in the Shenkar Building. It is recommended that posters be displayed as early as possible. Please stay near your poster during the poster session (15:45 - 16:15 p.m.).

The Lev cafeteria in the basement of the Shenkar Building is open for lunch.

Table of Contents

(titles shown are of oral presentations)

Lasers and Optics

Israel Physical Society
Annual Meeting
Tel Aviv University
4 April 1993

החברה הישראלית לפיסיקה
הכנס השנתי
אוניברסיטת תל אביב
י"ג ניסן תשנ"ג

PROGRAM

08:30 Registration (Shenkar Lobby)

09:30 Opening Session (Lev Auditorium – אולם לב)
Formal opening: Yoel Rephaeli, Chairman, Organizing Committee
Welcoming remarks: Dan Amir, Rector, Tel Aviv University
Presentation of prizes: Itzhak Tserruya, President of the IPS

09:50 Morning Plenary Session (Lev Auditorium)
Chairman: Moshe Carmeli, Ben Gurion University

09:50 Yakir Aharonov, Tel Aviv University
Schrodinger waves are observables after all

10:25 Michael Finkenthal, Hebrew University
SARIT: A possible Israeli magnetic confinement fusion project

11:00 Coffee

11:30 Morning Parallel Sessions (see detailed program)

13:00 Lunch

14:15 Afternoon Parallel Sessions (see detailed program)

15:45 Coffee, Poster Session

16:15 Business Meeting of the IPS (Lev Auditorium)

16:30 Afternoon Plenary Session (Lev Auditorium)
Chairman: to be announced

16:30 Amnon Yariv, California Institute of Technology
Quantum well semiconductor physics in optoelectronics communication

17:05 David Gross, Princeton University
The status of the string

Morning Parallel Sessions 11:30–13:00

Particles and Fields **Lecture Hall 5**
Chairman: G. Alexander, Tel Aviv University

Invited Lectures:

11:30 A. Montag, Weizmann Institute
Initial results from HERA at DESY

12:00 S. Tarem, Weizmann Institute
Recent results from LEP

12:30 M. Leurer, Weizmann Institute
Mass matrix models

Medical Physics **Shenkar 222**
Chairman: S. Akselrod, Tel Aviv University

Invited Lecture:

11:30 Saul Stokar, Elscint
Functional mappings of the human brain by magnetic resonance imaging

Contributions:

11:55 Gideon Vennor, Tel Aviv University
Utilization of orientation in stereopsis within the human visual system

12:05 Yair Zimmer, Tel Aviv University
Assessment of cardiac function from short-axis cardiac magnetic resonance images using automatic boundary extraction

12:15 Y. Swirski, Technion
NMR imaging of dilute ^{3}He–^{4}He *mixtures on the melting curve*

12:25 Avidan Neumann, Santa Fe Institute (USA)
Low-dimensional chaos and localized oscillations in the immune network

Invited Lecture:

12:35 Aaron Lewis, Hebrew University
Unique ArF *excimer laser medical applications*

(Morning)

Astrophysics **Lecture Hall 6**
Chairman: Arigo Finzi, Technion

Invited Lectures:

11:30 Peter Biermann, Max Planck Institute for Radioastronomy, Bonn
The origin of cosmic rays

12:00 Noam Soker, Oranim (Haifa University)
Planets and elliptical planetary nebulae

Contributions:

12:30 Amotz Shemi, Tel Aviv University
Gammay ray bursts from binary neutron star mergers

12:45 Vladimir Usov, Weizmann Institute
Gamma-ray bursts as a cosmological phenomenon: observations, models, and tests

---

Condensed Matter Physics **Lecture Hall 7**
Chairman: David Bergman, Tel Aviv University

Invited Lectures:

11:30 Uri Sivan, Technion
Spectroscopy, electron-electron interaction, and level statistics in a disordered quantum dot

12:00 Yehoshua Levinson, Weizmann Institute
Ballistic quantum transport: Contact phenomena

Contributions:

12:30 Miriam Deutsch, Hebrew University
The optical Larmor clock: Measurement of photonic tunneling time as an analogy to electronic tunneling

12:45 Richard Berkovits, Bar Ilan University
Double barrier quasiparticles energy spectrum: Signs of chaos

(Morning)

Laboratory and Space Plasma Physics **Kaplun 118**
Chairman: S. Goldsmith, Tel Aviv University

Invited Lecture:

11:30 S. Wald, Soreq Nuclear Research Center
Plasma jet-liquid interaction in electrothermal launchers

Contributions:

12:00 M. Keidar, Tel Aviv University
The kinetics of macroparticles charging in strongly ionized plasma

12:15 N. Kleeorin, Ben Gurion University
A new kind of electromagnetic coupling in MHD

12:30 I. Rogachevski, Hebrew University
The modified renormalization group method for study of developed MHD turbulence

12:45 M. Gedalin, Ben Gurion University
Electron chaotic dynamics in quasiperpendicular shock front

Computational Physics **Orenstein 111**
Chairman: Giora Shaviv, Technion

Invited Lectures:

11:30 Amihai Silverman, Technion
Determination of semiconductor structures with simulated annealing

11:50 Ofer Shochet, Tel Aviv University
Nonequilibrium morphology transitions during diffusive growth

12:10 M. Sieber, Weizmann Institute
Examination of semiclassical approximations for chaotic systems

12:30 Sorin Solomon, Hebrew University
Visual study of Atiyah-Singer zero modes' role in PTMG convergence

Afternoon Parallel Sessions 14:15–15:45

Particles and Fields **Lecture Hall 5**
Chairman: Y. Frishman, Weizmann Institute

Invited Lectures:

14:15 B. Rusakov, Tel Aviv University
Large-N quantum gauge theories in two dimensions

14:45 N. Marcus, Tel Aviv University
Tachyon and W hair in 2D black holes

15:15 A. Davidson, Ben Gurion University
Threefold family of charged spin-1/2 Dirac bubbles

Laboratory and Space Plasma Physics **Kaplun 118**
Chairman: U. Samir, Tel Aviv University

Invited Lecture:

14:15 M. Mond, Ben Gurion University
MHD waves and instabilities in space plasmas

Contributions:

14:45 M. Balikhin, Ben Gurion University
Fine structure of the turbulence at a bow shock

14:57 A. Eviatar, Tel Aviv University
On statistical acceleration of particles near Venus

15:09 M. Harel, Tel Aviv University
Interactive model of the magnetosphere-thermosphere coupling

15:21 R. Schreier, Tel Aviv University
Modeling the Europa plasma torus

15:37 M. Filippov, Ben Gurion University
Coronal mass ejections: An attempt at a unified classification

(Afternoon)

Statistical Physics **Lecture Hall 6**
Chairman: Yacov Kantor, Tel Aviv University

Invited Lectures:

11:30 Henri Orland, Saclay
Some physical approaches to protein folding

12:00 David Kessler, Bar Ilan University
Spirals in excitable media

12:30 Jay Fineberg, Hebrew University
An instability in the propagation of fast cracks

Nuclear Physics **Orenstein 111**
Chairman: M. Kirson, Weizmann Institute

Invited Lectures:

14:15 L. Frankfurt, Tel Aviv University
Coherent hard diffractive processes off nucleons and nuclei

14:45 A. Leviatan, Hebrew University
Partially conserved quantum numbers in nuclear spectroscopy

Contributions:

15:15 R. Levy-Nathansohn, Tel Aviv University
A symmetrized ansatz for the dibaryon Skyrmion

15:25 Dror Nir, Tel Aviv University
Nuclear stimulated desorption

15:35 M. Paul, Hebrew University
Study of properties of rare negative ions by laser interaction and accelerator mass spectroscopy

(Afternoon)

Lasers and Optics **Shenkar 222**
Chairman: E. Marom, Tel Aviv University

Contributions:

14:15 A. Sharon, Weizmann Institute
Resonance phenomena in a grating/waveguide structure

14:27 Y. Weissman, Soreq Nuclear Research Center
Coherence effects in optical networks

14:39 V. D. Kugel, Tel Aviv University
Domain inversion in $LiNbO_3$ *optical waveguides*

14:51 E. Kogan, Bar Ilan University
Diffusion in a random system near resonance

15:03 M. Auslender, Ben Gurion University
The asymptotic of the time intensity fluctuations for light reflected by randomly moving point scatterers

15:15 A. Ben Amar, Negev Nuclear Research Center
Efficient copper vapor laser pumped Ti:*Sapphire laser*

15:27 E. Belotserkovsky, Tel Aviv University
IR fiberoptic radiometry for scientific, industrial, and biomedical applications

15:39 A. Saar, Hebrew University
Intersubband optical nonlinearities in GaAs *based quantum well structures*

(Afternoon)

Condensed Matter Physics **Lecture Hall 7**
Chairman: Ora Entin-Wohlman, Tel Aviv University

Invited Lectures:

14:15 Roman Mints, Tel Aviv University
Point-like vortices and magnetization relaxation in layered superconductors

14:45 Assa Auerbach, Technion
The theory of doped antiferromagnets

Contributions:

15:15 Leonid Shechtman, Tel Aviv University
Anisotropic superexchange interaction, frustration, and weak ferromagnetism

15:30 Issai Shlimak, Bar Ilan University
Crossover phenomenon for hopping conduction and density of states near the Fermi level

Plenary Lectures

Schrodinger Waves are Observables After all

Y. Aharonov

School of Physics and Astronomy
Raymond and Beverly Sackler Faculty
of Exact Sciences
Tel Aviv University
69978 Tel Aviv, Israel

It is universally believed that Schrodinger waves can be measured only statistically and therefore are observables only for ensembles. It is shown that this is not the case. New kind of experiments are discussed in which the wave functions of the individual particles may be observed. This fact demands a reevaluation of our interpretation of quantum mechanics.

SARIT: A Possible Israeli Magnetic Confinement Fusion Project

Michael Finkenthal

Racah Institute of Physics
The Hebrew University, Jerusalem

Moshe Rosenblum

The Israeli Atomic Energy Commission, Tel Aviv

SARIT stands for Small Aspect Ratio Israeli Tokamak. The tokamak line of research being the best understood among the magnetically confined plasmas (MCF), tokamak has been chosen by the international MCF community to be a precursor of an experimental test reactor (ITER project). However, several important questions related to tokamak confinement, steady state operation and the interaction of the fusion plasma edge with the plasma facing components, remain open at present. Small aspect ratio (SAR) tokamaks can significantly extend the data base concerning energy and particle confinement and stability in tokamaks; moreover, the expected high beta operation could lead to compact, steady state devices with extremelly high heat fluxes and neutron yields at the plasma edge. The talk will briefly discuss the physics problems related to SAR tokamaks, as well as the specifics of an Israeli program in the context of the present and future international MCF effort.

Quantum well semiconductor physics in optoelectronics communication

Amnon Yariv

Division of Engineering and Applied Science
California Institute of Technology
Pasadena, CA 91125, USA

The talk will show how fundamental quantum-well physical considerations of submicron electronic structures are used in a number of important new optical communication applications. The examples will include ultra-high-speed optical fiber communication, narrow-linewidth semiconductor lasers, and optical data storage.

The Status of the String

David J. Gross

Physics Department
Princeton University, Princeton, NJ 08540

I shall review the current status, promises and prospects of string theory, including recent attempts to construct a string theory of QCD.

Particles and Fields

Initial Results from HERA at DESY

Avram Montag

Department of Nuclear Physics
Weizmann Institute of Science
Rehovot 76100, Israel

Physics experimentation at HERA, the world's first electron-proton collider, began in June 1992. The supeconducting proton storage ring provides an 820 GeV beam that collides with 30 GeV electrons from a conventional ring. These energies open up a new kinematic regime for studying the proton structure through deep inelastic scattering. Other physics processes studied at HERA include measurements of photoproduction reactions and searches for electron-quark resonances known as leptoquarks. Two experiments are currently taking data at HERA, H1 and ZEUS. The latter has significant Israeli participation. Both experiments have published initial findings based on a low luminosity 1992 run. The deep inelastic scattering cross sections measured so far are consistent with extrapolations from lower energy data. The total photoproduction cross sections favor the lower range of theoretical predictions. Hard scattering in photoproduction has been observed. The hadronic activity in final states seems to be higher than was originally expected. No evidence has been found for leptoquarks.

Recent Results from LEP

Presented by

S. Tarem

Department of Nuclear Physics
Weizmann Institute of Science

The LEP experiments have been collecting data from Z^0 decays since 1989 and accumulated a total of 5.5 million visible Z^0 decays. From a subsample of this data collected in 1990-1991 by the four experiment, a precision measurement of the elecroweak parameters has been performed. This includes the Z^0 mass and width: M_Z= 91.187$\pm$0.007 , Γ_Z= 2.490$\pm$0.007. Combining these measurements with those of partial widths into leptons and hadrons and forward backward asymmetries, a fit to the standard model parameters was performed leading to a prediction of the top quark mass.

A limit is also presented on the mass of the standard model Higgs boson based on all the available statistics.

The average lifetime of B hadrons has been measured as well as lifetimes of specific B hadrons. Evidence has been found for the existence in our data of B baryons and the strange B meson.

The " τ decay puzzle" is on its way to a solution: Recent LEP measurements of the τ lifetime have significantly smaller errors than previous measurements. In conjunction with new mass measurements they are in good agreement with $\tau - \mu$ lepton universality.

LEP results on QCD include measurements of α_s, comparisons between quark and gluon jets, measurements of resonance production in jets and Bose-Einstein correlations.

Mass Matrix Models

M. Leurer and Y. Nir

Physics Department
Weizmann Institute of Science
Rehovot 76100, Israel

N. Seiberg

Department of Physics and Astronomy
Rutgers University
Piscataway, NJ 08855-0849, USA

It is possible that the hierarchy in the masses and mixing of quarks is a result of a horizontal symmetry. The smallness of various parameters is related to their suppression by high powers of a scale of new physics. We analyze in detail the structure of such symmetries in view of new experimental data and present explicit models consistent with all phenomenological constraints. We show that it is possible that the flavor dynamics can be at accessible energies – as low as a TeV.

Tachyon and W-hair in 2-D black holes

Neil Marcus and Yaron Oz

School of Physics and Astronomy
Raymond and Beverly Sackler Faculty
of Exact Sciences
Tel Aviv University
69978 Tel Aviv, Israel

We show that the two-dimensional black hole solution of $c = 1$ string theory can be perturbed by the tachyon of the theory with sufficiently small momenta, despite the usual "no-hair" theorems of black hole theory. The perturbed black hole has an infinite ADM mass, but its conformal structure is the same as that of the original black hole.

We make no approximations, other than taking the tachyon background to be weak. Asymptotically, the tachyons appear as a mixture of Seiberg and anti-Seiberg states, and so have a finite stress tensor only for momenta $|p| < |m_{\rm tach}|$. An analogous calculation for the discrete states of the $c = 1$ string shows that the black hole can not be perturbed by them and thus has no "W-hair."

The Aharonov-Bohm Effect as a Gauss' Law for Vortices

Michael Marcu[1] and Kornel Szlachányi[2]

[1] *School of Physics and Astronomy*
Raymond and Beverly Sackler
Faculty of ExactSciences
Tel Aviv University, 69978 Tel Aviv, Israel
[2] *Central Research Institute for Physics*
H-1525 Budapest 114, P. O. B. 49, Hungary

A Gauss' law is the possibility to identify a charge by measuring a gauge invariant quantity localized at infinity. On the example of scalar electrodynamics, a duality transformation is performed, and the generators of the dual gauge symmetry are used to formulate a Gauss' law for vortices. The corresponding charge is the magnetic flux. The appropriate measurement of this charge is identical to the measurement of the Aharonov-Bohm phase. In field theory, a vortex differs outside its core from the vacuum, but only in exponentially small fashion. This is enough to reconcile the Aharonov-Bohm phase with locality (as opposed to the case of quantum mechanics). We show which property of the vacuum allows for the measurement of such an exponentially small effect. Our discussion relies on calculations in both 3+1 and 2+1 dimensions. As a by-product, we conclude that in the Coulomb phase the magnetic flux is conserved in 4 dimensions, but it is screened in $4-\epsilon$ dimensions, thus clarifying the "photon as a Goldstone boson" discussion in the literature.

Simulations of 2-Dimensional Quantum Gravity Coupled to $c = 1$ Matter

M. E. Agishtein[1], T. Filk[2], I. Klebanov[3], M. Marcu[4], A. A. Migdal[1], S. Solomon[5]

[1] *Physics Department and*
Program in Applied and Computational Mathematics
Fine Hall, Princeton University
Princeton, NJ 08544-1000, USA
[2] *Fakultät für Physik, Universität Freiburg*
Hermann-Herder-Str. 3, 7800 Freiburg, Germany
[3] *Joseph Henry Laboratories*
Princeton University, Princeton, NJ 08544, USA
[4] *School of Physics and Astronomy*
Raymond and Beverly Sackler
Faculty of Exact Sciences
Tel Aviv University, 69978 Tel Aviv, Israel
[5] *Racah Institute of Physics*
Hebrew University, 91904 Jerusalem, Israel

We present results of a high precision Monte Carlo simulation of dynamically triangulated random surfaces coupled to one scalar field ($c = 1$). The dependence of the mean square extent $< X^2 >$ on the number N of triangles, i.e. on the area of the surface, is found to be in excellent agreement with the $< X^2 > \sim \ln^2 N$ law predicted theoretically by both conformal field theory and matrix models. For the integrated 2-point correlation function of vertex operators, a formula for the fixed area ensemble is derived and tested numerically. The agreement between prediction and simulation results is again impressive. However, the data are very accurate, and deviations from this theoretical form are in fact observed. This allows us to better understand the validity region of the formula, which in particular turns out to be smaller than the region where universal properties are exhibited. In order to better understand which features are universal and which are regularization dependent, we used two actions for the scalar field X: the Gaussian action and the absolute value action. The high precision measurements have been made possible by the use of the valleys-to-mountains-reflection (VMR) cluster algorithm for the update of the matter fields.

Fractional Charges in the XY and Sine-Gordon Models

Michael Marcu[1] and Kornel Szlachányi[2]

[1] *School of Physics and Astronomy*
Raymond and Beverly Sackler
Faculty of Exact Sciences
Tel Aviv University, 69978 Tel Aviv, Israel
[2] *Central Research Institute for Physics*
H-1525 Budapest 114, P. O. B. 49, Hungary

The two-dimensional XY model (O(2) sigma model) is known to have a massless phase at low temperatures, where the infrared behaviour is that of a $c = 1$ conformal field theory. We show that this behaviour is much more similar to that of a massless scalar free field theory than previously thought. Naively, the XY model has a U(1) global symmetry and therefore an additive *integer charge*. The free field theory on the other hand has the global symmetry of shifting the field by a real number, so the corresponding superselection sectors may carry any *real charge*. Here we construct the fractional charges for the XY model too. The symmetry of the model is *enhanced* dynamically, i.e. the U(1) symmetric model has sectors labelled by the characters of a group larger than U(1), the group of real numbers. Technically, the construction of the fractional charges is achieved by coupling the scalar field to an integer-valued gauge field. The resulting model has the same integer charges as the original XY model, but fractional charges may also be considered if a nontrivial electric flux is allowed. The existence of the fractional sectors is signalled by the VOOP (vacuum overlap order parameter). The XY model is obtained as the strong gauge coupling limit, the free field theory as the weak gauge coupling limit. The model with the integer gauge field is dual to the lattice sine-Gordon model. Another useful representation is that of a Coulomb gas, for which a multipole expansion exists in the massless phase. In the massive phase, for which a convergent expansion exists, the fractional charges are confined, thus absent.

Cosmic time in quantum cosmology and the quantum inflation-compactification era

E. I. Guendelman and A. B. Kaganovich

Department of Physics
Ben Gurion University
Beer Sheva 84105, Israel

We develop a new approach to the problem of time in quantum cosmology. We do this in the context of $1+D$-dimensional, toroidally compact Kaluza-Klein theories. Solving the Wheeler-DeWitt equation in the presence of a negative cosmological constant and dust, we find that there can be an avoidance of the cosmological singularity. Although cosmic time does not appear explicitely in the Wheeler-DeWitt equation, cosmic time dependence appears for the expectation values of certain variables when proper care of some subtle points concerning the definition of averages is taken. The anisotropy in the evolution of the Universe (which turns out to be quantized), is responsible for a "quantum inflationary phase" for some dimensions and simultaneously a "quantum deflationary contraction" for the rest.

Is 2d Turbulence a Conformal Turbulence?

Gregory Falkovich and Amihay Hanany

Department of Physics
Weizmann Institute of Science
Rehovot 76100, Israel

A critical analysis of the conformal approach to the theory of 2d turbulence is delivered. It is shown, in particular, that conformal minimal models cannot give a general turbulent solution, which should provide for constant fluxes of all vorticity integrals of motion.

Medical Physics

Functional Mapping of the Human Brain by Magnetic Resonance Imaging

S. Stokar

Elscint, Ltd.
Magnetic Resonance Imaging Area
P.O. Box 550
Haifa 31004, Israel

Until recently, applications of Magnetic Resonance Imaging (MRI) have been confined to the study of anatomy and physiology. Measurements of brain function have been performed by radionuclide techniques, primarily positron emission tomography (PET). Such measurements rely on the idea that brain functional activity, such as cognitive task performance, is localized in distinct processing areas of the brain and that such functional activity can be mapped by mapping changes in cerebral blood supply during performance of various tasks. Up until now, these mapping techniques have been hampered by the poor spatial resolution available with PET.

Recently, Belliveau et. al. have developed a technique for using the echo planar imaging technique (EPI) to map changes in regional blood volume during visual activation. This work stimulated a flurry of activity by other groups who used EPI to map brain function during a variety of motor cortex stimuli, including finger touching, passive word presentation, photic stimulation, etc. Subsequently, a number of groups developed "Turbo-Flash" techniques that allow acquisition of such maps on conventional high field MRI scanners.

We shall review the mechanisms responsible for this new realm of MRI. The signal imaged by these techniques is believed to reflect changes in local levels of deoxyhemoglobin and the associated change in magnetic susceptibility. We shall begin by reviewing different scan techniques (EPI vs. standard imaging), based on their respective strategies for scanning k-space. Next we shall review the differing sensitivity of spin-echo and gradient echo techniques to tissue magnetic susceptibility and we shall show how this sensitivity leads to the development of functional mapping techniques. Finally we shall briefly review the results obtained to date in the field of functional MRI and present a prognosis for future developments in the field.

Utilization of orientation in stereopsis within the human visual system

G. Vennor, Y. Yeshurun

School of Physics and Astronomy
Raymond and Beverly Sackler Faculty of Exact Sciences
Tel-Aviv University
69978 Tel Aviv, Israel

The role of orientation in stereopsis (binocular depth perception) was investigated under a variety of conditions. Several psychophysical tests were conducted, in which oriented stimuli and non-oriented stimuli were compared for their ability to facilitate depth perception. Direct evidence for the use of orientation was found with simple isolated contours. In contrast, orientation did not seem to be utilized with two-dimensional random dot stimuli, even when contours were added. The relatively small contribution of orientation to stereoscopic depth perception, as revealed by psychophysics, appears inconsistent with the physiological fact that a majority of binocular neurons in the visual cortex are orientation tuned.

Several complementary frameworks for explaining the above situation are presented. A spatial framework suggests that orientation is important only for local stereopsis, and that global stereopsis depends more on relations between elements than on individual element attributes. A temporal framework suggests that orientation is inherent in the preliminary stage of binocular matching, but not in creating a point by point disparity map. A computational framework offers two ways in which disparity-sensitive cells may be distributed among orientation-columns. "Inverse" physiological studies, in which the goal is to map all cells responding to a given stimulus (rather than map responses of a given cell to various stimuli), may provide valuable information on the way orientation is represented and utilized within stereopsis.

ASSESSMENT OF CARDIAC FUNCTION FROM SHORT-AXIS MAGNETIC RESONANCE IMAGES USING AUTOMATIC BOUNDARY EXTRACTION

Y. Zimmer, S. Akselrod

School of Physics and Astronomy
Raymond and Beverly Sackler Faculty
of Exact Sciences
Tel Aviv University
69978 Tel Aviv, Israel

Magnetic resonance images of the heart are an important source for cardiac related anatomical and physiological data. The recent advance in image processing induced an effort to handle magnetic resonance (MR) images automatically. Although several techniques for extracting data from cardiac MR images were described in the literature, the area is still intensively investigated.

In this work an almost fully automatic process, that provides images of the left ventricular boundaries and numerical values of the main cardiac functional parameters, is presented. The raw data for processing are short-axis cardiac MR images, obtained using different imaging protocols. The only non-automatic part of the procedure requires from the operator to supply the location of a single point within the left ventricle. The remainder of the process is fully automatic; it involves smoothing each image, thresholding it, extracting the left ventricular and myocardial boundaries, and finally combining this information from a set of short-axis processed images to assess the various cardiac parameters of interest. The parameters obtained can be used later by physicians to evaluate cardiac performance and to diagnose cardiac disease.

The quality of the edge images was visually assessed by three observers. Their evaluations show that the algorithm accomplishes good results in more than 60% of the inspected images (when only images of reasonable quality are included the method performs well in almost all the images). The values obtained for cardiac parameters seem to be within the normal range. Further evaluation work is required in order to fully assess the performance of the suggested method.

NMR Imaging of Dilute $^3He-^4He$ Mixtures on the Melting Curve

Y. Swirski[a], I. Shuster, E. J. Schmidt[b], E. Polturak, S.G. Lipson

Dep. of Physics
Technion, Israel Institute of Technology
Haifa 32000, Israel

Solidification and melting of dilute mixtures of $^3He-^4He$ (0.7% - 4.0% ^3He) at 0.4K–1.5K are investigated utilizing a 10 MHz NMR imaging system. The spatial distribution of ^3He, T_1 and T_2 relaxation times was mapped along the vertical direction, perpendicular to the liquid–solid interface. For all–solid samples, the relaxation times T_1 and T_2 agree with previously reported values, allowing for Larmor frequency differences. The different values of T_1 and T_2 for the liquid and solid were used to locate the liquid and solid regions in the cell. The results indicate that the relaxation of crystaline inhomogeneities speeds up considerably around the minimum of the melting curve.

[a] Present address: Raphael, P.O.B. 2250, Haifa, Israel
[b] Present Address: Elscint Co., Haifa, Israel

Low Dimensional Chaos and Localized Oscillations in the Immune Network

Avidan U. Neumann

Theoretical Immunology Group
Santa Fe Institute for Complex Systems
1660 Old Pecos Trail
Santa Fe, NM 87501, USA

Idiotypic network models of the immune system were shown to exhibit multiple stable steady states that can account for immune memory and immune tolerance. The trajectories leading to those steady states resemble the antibody kinetics observed in a normal immune response. On the other hand, the kinetics of auto-antibodies, antibodies directed against self components, were found to be oscillatory in several cases. Notably of interest is the difference in the nature of oscillations between healthy individuals and ones with an auto-immune disease.

Oscillations, both limit-cycles and chaotic attractors, are indeed found for some parameter regimes in models implemented on an x–y structure, i.e. isolated couples of idiotypic clones. However, when implemented on a full idiotypic network structure, the oscillations in the first levels stimulate the next levels and the response percolates all over the network. Thus, in contradiction to experimental results, correlation between the original stimulus and the kinetics of the lymphocyte populations is lost.

In this work we calculate the conditions for obtaining oscillations which are structurally stable, i.e. oscillations which stay localized at the first idiotypic levels of the network. Simulations, using parameter regimes set according to the above conditions, show two structurally stable behaviours in addition to point attractors. Limit cycles which give rise to localized periodic oscillations. Low-dimensional chaotic attractors, embedded in a high-dimensional phase space, which give rise to chaotic oscillatory behaviour of first idiotypic levels only. In these regimes of localized oscillations, the correlation between the stimulus and the idiotypic response is not lost. Thus a new mechanism of memory can be postulated, based upon the character of the oscillations.

Unique ArF excimer laser medical applications

Aaron Lewis,[1,2] Daniel Palanker,[1,2] Neri Laufer,[2] Itzhak Hemo,[2]
and Hanan Zauberman[2]

[1] *Division of Applied Physics*
and
[2] *The Hadassah Laser Center*
The Hebrew University of Jerusalem

A flexible, ultraprecise beam delivery system has been developed for the ArF excimer laser beam. The beam can be delivered even in biological media. These developments have generated a wide spectrum of unique new applications for this laser. Specific differences in ArF ablation mechanisms in air and biological media will be described.

Automatic Correction of Cardiac Displacement in Contrast Echocardiography

Victor Mor-Avi, Solange Akselrod

Medical Physics, Tel Aviv University, Tel Aviv 69978

Myocardial regions of interest tend to change their location due to respiratory translocation of the heart. Two different approaches were tried to enable the automatic frame-by-frame tracking of regions of interest, so as to allow reliable acquisition of contrast enhancement data free of translocation related noise. Both algorithms were based upon pattern recognition techniques: the minimum sum of differences (MSD), and the stochastic sign change (SSC), as the criteria for image alignment. The validity and accuracy of the developed algorithms were tested using computer simulation and experimental data in three stages.

(1) Six regions of interest within the coordinate system of the frame were selected. A single short axis image was randomly shifted in both x and y directions. The videointensity in each region was determined with and without the application of the tracking algorithm. Image shifting caused marked fluctuations in videointensity measured without tracking in all regions of interest, completely abolished by the tracking algorithm.

(2) This protocol was repeated under increasing levels of random noise (SNR 10 down to 2) dispersed throughout the entire image. Both tracking algorithm reduced the combined effect of translocation and noise to levels below the simulated noise.

(3) Following the validation of the algorithms using simulated noise and translocation, their accuracy was tested in 8 series of images obtained during experimental contrast injection (Albunex). The steady state, pre- and post-injection portions of the contrast enhancement curves were examined.

Both tracking algorithm significantly reduced the translocation related variations in videointensity ($p<0.025$). It was found that the SSC algorithm is considerably more robust with respect to the dynamic variations in the images produced by contrast injection, as compared with the MSD approach. Thus, automatic tracking of echocardiographic regions of interest improves contrast enhancement data distorted by translocation artifacts. The application of such algorithms can markedly enhance the reliability of myocardial blood flow assessment based upon contrast echocardiography.

The Scattered Radiation from Body Tissues During Therapeutic Irradiation

E. Loeventhal
Clinical Oncology and Radiation Therapy
Hadasa Hospital Ein Kerem,
Jerusalem ISRAEL
E. Bar-Avraham, S. Cremer
Rafael. P.O.Box 2250
Haifa, ISRAEL

ABSTRACT

The scattered X-ray radiation from simulated body tissue was measured and computed in a special configuration. A good fit between the calculations and the measurements was obtained. With the same model the scattered X-ray dose was computed for different therapeutic irradiations configurations. The scattered X-ray dose, 1 cm outside from the direct beam edge, was found to be 1-3% of the direct dose.

22

Fibroblasts Proliferation and Light-A Non Linear Interaction

R. Lubart *et al.*

Department of Physics
Bar-Ilan University
Ramat Gan 52900, Israel

The healing effect of low energy lasers is generally attributed to enhanced cell proliferation due to the irradiation. As it was not clear whether coherent radiation is essential, we examined the effect of various wavelengths from non-coherent light sources, on the rate of proliferation of fibroblasts and keratinocytes. We found that light at 360, 540 and 600-900 nm significantly accelerates the mitosis of these cells. Moreover, we have found that the effect is not only energy-dose dependent but depends non linearly on the intensity of the light source.

Accelerator mass spectrometry applications for the study of bone resorption

M. Paul[1], E. Boaretto[1], D. Berkovits[1], V. Sossi[1,2], R. Johnson[1,2]
E. Venzel[2], Z. Gelbart[2], R. Sutton[3], V. Walker[3], J. Prior[3]

[1] *Racah Institute of Physics, Hebrew University, Jerusalem*
[2] *TRIUMF, Vancouver, Canada*
[3] *Dept. of Medicine, Univ. of British Columbia, Vancouver, Canada*

Accelerator Mass Spectrometry (AMS) is mainly known for its applications in archeological and geological dating problems. The technique can also be used for tracer studies in biological systems over long-term periods. We have concentrated on studying calcium processes in the body that involve the resorption of bone. These studies are important to study calcium related diseases and their treatment.

Calcium participates in vital parts of the human metabolism. The calcium that is used comes from the daily diet but as well is obtained from stored calcium in the body. In cases where there are imbalances in hormones, there can be excessive resorption from bone and in extreme cases can result in diseases such as Osteoporosis. We have used tracer amounts of ^{41}Ca ($T_{1/2} = 1.04 \times 10^5$ yrs) as a bolus to imbed an identifiable amount of calcium in the stable bone pool. We have monitored the calcium in urine samples over time to establish the distribution of ^{41}Ca in the various body pools. About 100 ng of ^{41}Ca were injected into a subject at the beginning of the experiment. Because of the long radioactive half-life of ^{41}Ca , such an injection causes a lifetime radiation exposure considerably less than lifetime exposures from naturally occuring backgrounds. The urine samples are converted to CaH_2 where carrier ^{40}Ca is included to normalize the measurements. The samples are analyzed by AMS with the Rehovot Pelletron accelerator. The measurements that span over a year still indicate trace amounts of ^{41}Ca . We are now able to monitor bone resorption as the subject ages. In addition, bone resorption due to chemical intervention is also being studied. Such studies are important in clinical problems.

Fractal Analysis of Neuronal Growth

B.Vilensky[1], S.Havlin[1], T.G.Smith Jr[2]

[1] *Department of Physics, Bar-Ilan University, Ramat-Gan 52900, Israel*
[2] *Laboratory of Neurophysiology, NINDS, National Institutes of Health, Bethesda, MD 20892, U.S.A.*

We studied the fractal properties of various two dimensional neurons. The fractal dimension d_f, the chemical dimension d_ℓ, and the exponent $d_{min} = d_f/d_\ell$ has been analyzed. The chemical dimension d_ℓ represents the scaling of the mass M with the shortest path along the structure ℓ , i.e., $M(\ell) \sim \ell^{d_\ell}$. The exponent d_{min} was analysed using the relation $\ell \sim R^{d_{min}}$, where R is the Eucledean distance between two sites on the neuron. Our results suggest that the exponent d_{min} is a better parameter for characterization and classification neurons than the fractal and the chemical dimensions since the scaling relation $\ell \sim R^{d_{min}}$ is more accurate. From our results seems that the exponent d_{min} can be used as a measure of the morphological complexity of neurons from defferent populations, for more developed neurons d_{min} increases. Our results indicate that the chemical dimention d_ℓ is always smaller than the fractal dimention d_f and therefore d_{min} is larger than 1. This suggests that diffusion limited aggregation (DLA) model might not be sufficient to describe the neural growth mechanism.

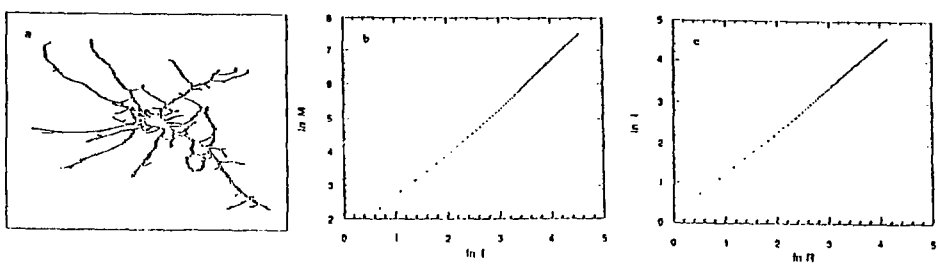

Fig.1. (a) Binary image of the neurons border; (b) ln $M(\ell)$ vs ln ℓ, the slope is d_ℓ=1.55; (c) ln $R(\ell)$ vs ln ℓ, the slope is d_{min}=1.09.

Astrophysics

The Origin of Cosmic Rays

Peter L. Biermann
Max Planck Institut für Radioastronomie
Auf dem Hügel 69
D-5300 Bonn 1
West Germany

The origin of cosmic rays is postulated to derive from three main sources, 1) supernova explosions into the interstellar medium, 2) supernova explosions into a stellar wind, and 3) radio galaxy hot spots. The key feature in this proposal is a new derivation of the energy gain of energetic particles at shock fronts where the magnetic field is perpendicular to the shock normal. For this we argue that there is diffusive transport in the shock region by fast convective turbulence, for which there is evidence in radio polarization observations. In addition to the energy gain from the Lorentz transformation across the shock interface we then have an additional energy gain from drifts in the electric field a particle experiences in the shock frame, but we have also energy losses from adiabatic losses from the curvature of the shock surface, as well as spectral changes due to the non-stationary nature of a spherical expansion. The predicted resulting spectrum and particle energy range for the three major sites of particle acceleration are as follows: a spectral index of -2.42 and a particle energy range up to 100 TeV (Hydrogen) for the supernova explosions into the interstellar medium; a spectral index of -2.33 below the knee in the cosmic ray spectrum, and -2.64 above the knee for the supernova explosions into a stellar wind, with a particle energy range up to 3 EeV (for Iron); the radio galaxy hot spots produce a spectral index of -2.00 up to the energy range near EeV where the spectrum steepens due to microwave background interaction, to cut off near 100 EeV. The galactic cosmic rays steepen due to diffusive losses from our galaxy by 1/3 in their spectral index. The cutoffs and the bend at the knee are rigidity dependent. The predictions were made in paper CR I (Biermann 1993, in press) and in paper UHE CR I (Rachen and Biermann 1993, in press): the predictions were tested against observations of Wolf Rayet stars and radio supernovae in paper CR II (Biermann and Cassinelli 1993, submitted), against observations of supernova remnants in paper CR III (Biermann and Strom 1993, submitted), and against cosmic ray airshower data in paper CR IV (Stanev, Biermann and Gaisser 1992, submitted) for the galactic component, and paper UHE CR II (Rachen, Stanev and Biermann 1993, in press) for the extragalactic component. The theory is basically analytical. One corollary derives from the sharpness of the knee feature of the cosmic rays, namely a suggestion as to the origin of the explosive energy of massive star explosions (paper CR I): This is argued to derive from the gravitational energy of the internal region of the star about to explode, of which the collapse is temporarily halted by rotational forces due to the conservation of angular momentum, but then renewed due to angular momentum transport by magnetic fields. We note that the proposal also explains the chemical abundances of cosmic rays both at low as well as at high particle energies, and for the first time, gives an adequate fit to the air shower data across the knee, i.e. from about 10 TeV to 100 EeV. Further tests of the theory proposed will be made with radio observations of novae, and the detailed chemical abundances of cosmic rays.

Planets and Elliptical Planetary Nebulae

Noam Soker

Mathematics-Physics
Oranim – University Division
Tivon 36910, Israel

I examine the evolution of Jupiter's orbit as the Sun evolves to form planetary nebula. I use an orbital synchronization mechanism, that was proposed by Tassoul (1987), and find that Jupiter is likely to deposit substantial fraction of its orbital angular momentum, in spinning-up the Sun, when the latter is on the upper AGB. This amount of angular momentum is likely to cause some small degree of axisymmetric mass loss from the Sun. In this case, the Sun will form an elliptical planetary nebula. The formation of elliptical planetary nebulae with the influence of massive planets and brown dwarfs, may explain the large fraction of elliptical planetary nebulae among the total number of planetary nebulae known today.

Tassoul, J.-L. 1987, ApJ, 322, 856.

GAMMA RAY BURSTS FROM BINARY NEUTRON STAR MERGERS

Amotz Shemi

School of Physics and Astronomy
Raymond and Beverly Sackler Faculty
of Exact Sciences
Tel Aviv University
Tel Aviv 69978, Israel

Gamma ray bursts (GRBs) are short and transient events in the energy range 1 KeV to $\sim$ 100 MeV that last from $\sim 10^{-2}$ to 10^3 s. Their sources are yet unknown, but new BATSE-CGRO observations suggest that they are at cosmological distances $\sim 10^{10}$ light years, rather than inter-galactic and emit $\lesssim 10^{51}$ ergs in one second (!), roughly 0.1% of a solar rest mass. A scenario in which GRBs originate in the merger of binary neutron stars (NSs) was studied. The universal merger rate was found to be 10^3 yr^{-1}. Black hole - NS mergers of similar rate are predicted.

The merger realeases an enormous $\nu\bar{\nu}$ burst, $\approx$ 0.3% of which is converted into e^+e^- pairs which annihilate to γ-ray photons, resulting in an opaque photon-lepton 'cosmic fireball'. Such a fireball is contaminated by baryonic mass but is dominated by the radiation pressure, thus expands adiabatically with a Lorentz factor $\gamma \approx 10^3$.

A radiation-hydrodynamics code was developed which calculates the relativistic conservation equations. The flow passes an initial short and strong acceleration phase in which the fireball rearranges into a narrow front. The acceleration continues until locally the energy density falls below the rest mass and the fireball coasts with a constant velocity profile along the Lagrangian shells. In an intermediate stage, depending on the initial (explosion energy)/(mass contamination) ratio, the fireball becomes optically thin and the photons escape on one crossing time. The spectrum is a modified black body.

Gamma-ray bursts as a cosmological phenomenon: observations, models and tests

V. Usov

Physics Department
Weizmann Institute of Science
76100 Rehovot, Israel

The spatial and luminosity distribution of γ-ray bursts obtained with the BATSE experiment on the Compton Gamma Ray Observatory (Meegan et al. 1992) indicates that the burst sources are at cosmological distances, i.e. at a redshift $z \sim 1$ (Usov and Chibisov 1975; Piran 1992). Observed durations of γ-ray bursts cover a range from ~ 0.1 to $\sim 10^3$ s, with a mean duration $\sim 10 - 20$ s. The luminosity in γ-rays which is needed to explain the cosmological γ-ray bursts is a few $\times 10^{51}$ ergs s^{-1}. This is $\sim 10^7$ times more than the total luminosity of our Galaxy. The density of photons near the γ-ray bursters is so high that γ-rays are absorbed and very dense electron-positron plasma is created. This plasma flows away from the γ-ray burster at relativistic speeds, and X-ray and γ-ray emission at the photosphere of this relativistic wind may reproduce the observational characteristics of a γ-ray burst. Available models of γ-ray bursters at cosmological distances are discussed. It is argued that among all these models the formation of rapidly rotating neutron stars with extremely strong magnetic fields (Usov 1992) and the merger of strange quark stars (Paczynski 1991) are the most promising. Observational tests to verify the cosmological origin of γ-ray bursts are considered.

Meegan, C.A. et al. Nature **355**, 143-145 (1992).
Paczynski, B. Acta astr. **41**, 257-267 (1991).
Piran, T. Astrophys. J. Lett. **389**, L45-L48 (1992).
Usov, V.V. Nature **357**, 472-474 (1992).
Usov, V.V. and Chibisov, G.V. Soviet Astr. **19**, 115-116 (1975).

RECONSTRUCTION OF CORONAL MAGNETIC CONFIGURATIONS - THE CASE OF STRONGLY NONLINEAR FORCE FREE FIELDS

by

S. Cuperman[1,2], C. Bruma[1], D. Zoler[1] and M. Semel[2]

[1]School of Physics and Astronomy,
Raymond and Beverly Sackler Faculty of Exact Sciences
Tel Aviv University, Ramat Aviv 69978, Israel

[2]URA 326, DASOP, Observatoire de Paris, Section de Meudon
92190, Meudon, France

A method for the reconstruction of force-free field coronal magnetic configurations above active regions is proposed. It is based on the mapping of the entire space surrounding the sun onto a rectangular box of dimensions $(1, 2, 2\pi)$, inside which the FFF Maxwell's equations are solved. The boundary conditions used are the field components observed at the photosphere, their vanishing at infinity and finitness of the magnetic potential components along the poles.

The solution is based on relaxation techniques and is illustrated for the 2 1/2 D case, that is the case in which all three field components B_r, B_θ and B_ϕ are finite and depend only on the polar coordinates r and θ. The equilibrium state is considered to be reached when the mean relative change in any of the field components, from one time step to another, is smaller than a prescribed infinitessimal number.

Faraday Rotation and Turbulent Dynamo in Clusters of Galaxies

O. Goldshmidt and Y. Rephaeli

School of Physics and Astronomy
Raymond and Beverly Sackler Faculty of Exact Sciences
Tel Aviv University 69978 Tel Aviv, Israel

Diffuse radio emission from clusters of galaxies indicates that the intracluster (IC) plasma is magnetized. Recently a statistical study of Faraday rotation (FR) in clusters [1] yielded a mean IC magnetic field of $1 \div 2\ \mu G$, if the coherence length of the field l_0 is of the order of 10 kpc. It had been suggested that IC magnetic fields could be generated by hydrodynamic turbulent flows excited by trans-sonic motion of galaxies through the IC gas. A detailed theory of the turbulent dynamo in clusters [2] led to a field value of $2\ \mu G$, though later it was argued [3] that the turbulent energy was lower, and the resulting field would be at most $0.1\ \mu G$ strong.

We suggest that even without going into details one can make a meaningful comparison of the predictions of the theory with the FR data. The comparison is based on the fact that the FR-derived IC magnetic field is sensitive to the coherence scale ($\sim l_0^{-1/2}$, from random walk considerations), while turbulent dynamo fields generically have a "thin rope" morphology, with main coherence scale $L \cdot Rm^{-1/2}$, where L is the energy scale of the hydrodynamic turbulence (typically $10 \div 20$ kpc), and Rm is the magnetic Reynolds number. Our analysis [4] shows that Rm is extremely large in IC space ($10^{26} \div 10^{28}$), so the "magnetic ropes" must be very thin. Since the polarization plane of a radio wave would be rotated only within the "ropes", and in random direction on different segments of the sightline, the strength of the field required to account for the FR would be proportional to $Rm^{1/4}$, and therefore prohibitively large. For instance, with $L = 20$ kpc, and $Rm = 10^{28}$, the required field is of the order of $15 G$, while the maximal field that can be generated by the turbulence is $\sim 10\ \mu G$.

We conclude that turbulent dynamo, even if viable in clusters, cannot generate magnetic fields that can account for the observed FR. Therefore, a different origin must be sought for IC magnetic fields. Most probably, the fields originate in either radio, or normal cluster galaxies.

[1] Kim, K.-T., Tribble, P. C., & Kronberg, P. P. 1991, ApJ, 379, 80
[2] Ruzmaikin, A. A., Sokoloff, D. D., & Shukurov, A. 1989, MNRAS, 241, 1
[3] Goldman, I., & Rephaeli, Y. 1991, ApJ, 380, 344
[4] Goldshmidt, O., & Rephaeli, Y. 1993, ApJ, to be published

Anisotropy of the Cosmic Microwave Background Due to Gas in Superclusters of Galaxies

Yoel Rephaeli

Raymond and Beverly Sackler Faculty of Exact Sciences
School of Physics and Astronomy
Tel Aviv University, Tel Aviv 69978

The large scale anisotropy in the spatial distribution of the Cosmic Microwave Background (CMB) radiation detected by the COBE/DMR experiment is of fundamental cosmological importance when interpreted as due to primordial density perturbations. It is reasonable to consider the possibility that the detected anisotropy is not of primordial origin, especially that it is due to superclusters (SC) of galaxies. Specifically, it is of interest to determine the level and angular scale of anisotropy due to Compton scattering of the radiation by hot gas in SC. Our systematic X-ray searches in the *HEAO-1* A2 database have yielded - for the first time - a direct bound on the properties of hot gas in SC. The bound translates to a mean Comptonization parameter whose value is typically lower than $few \cdot 10^{-7}$ in a SC. Using this bound, and the formalism developed by Rephaeli (Astrophys. J., **245**, 351, 1981), we have calculated the implied (temperature) anisotropy to be $\Delta T/T \leq 10^{-7}$ on a characteristic angular scale of a few degrees. This level of anisotropy is a factor of ~ 100 smaller than that detected by COBE.

32

Dust in the Narrow Line Region of Active Galactic Nuclei.

Marcella Contini

School of Physics and Astronomy
Raymond and Beverly Sacker Faculty of Exact Sciences
Tel Aviv University, 69978 Tel Aviv, Israel

Dust in Active Galactic Nuclei is directly investigated through the infrared (IR) bump in the spectral energy distribution. Composite models, which account consistently on shocks accompanying the outer radial motion of the clouds in the narrow line region (NLR) and on radiation from the active center, are successfully used for the calculations of line intensities, line profiles, and continua from the gaseous phase. They are calculated by the SUMA code. The SUMA code has been recently extended to consistent calculations of dust heating and reradiation and of grains sputtering.

The results show that the frequencies corresponding to the turnovers of the IR bump and to its peak depend strongly on the shock velocity, v, on the intensity of the radiation, F, and on the dust-to-gas ratio, (d/g).

The comparison with the observational data shows that a good fit is obtained for Seyfert 2 and intermediate Seyfert galaxies for v = 200 - 600 km s^{-1}, F = 10^{10}-10^{12} units, and d/g = 10^{-14}- 10^{-13} (see, for example Fig. 1). Moreover, it is noticed that the dip, observed in LINERS at λ = 4.8 μm, depends on rapid gas recombination and it is out of the range of the IR bump (Fig. 2).

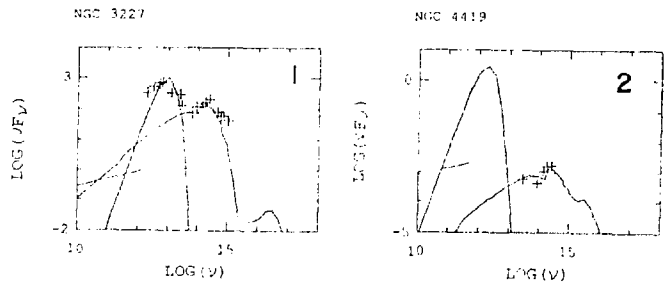

The Prediction of Stellar UV magnitudes

Georgy Mersov and Noah Brosch
The Wise Observatory and the School of Physics and Astronomy
Tel Aviv University, Tel Aviv 69978, Israel

In preparation for the TAUVEX experiment we produced a catalog of ~ 100000 stars with synthetic UV magnitudes accurate to 0.3 mag. The observational data used about 300 spectra from the International Ultraviolet Explorer (IUE) mission and the Hipparcos input catalogue (118209 stars with V magnitudes, B-V color, spectral type and luminosity). The TD1 catalogue (23328 star with UV magnitudes in four bands) was used to test the prediction quality of the routine. Theoretically, the prediction of UV apparent magnitudes for a given star is possible if the star visual magnitude, the observed (B-V) colour and intrinsic $(B\text{-}V)_0$, and the spectral type are known. As the spectrum for the given star we adopted the measured spectrum of a star with the same spectral type and luminosity from IUE data.

The computed UV magnitude for the given star from Hipparcos catalogue was compared with the measured UV magnitude of the star positional copartner (if any) in the TD1 catalogue. The results shows that it is possible to reach an accuracy of UV prediction of ~0.5 magnitude for longest TD1 band (2585-2895 Å). The error is the bigger in the shorter band (up to 1.5 magnitude for shortest band 1400-1730 Å). We estimated statistically the coefficients of the $(B\text{-}V)_0$ to UV transformation using all TD1 data as measurements. The results are in agreement with previous results and are used to select IUE spectral data for a more accurate synthesis of the UV star catalogue.

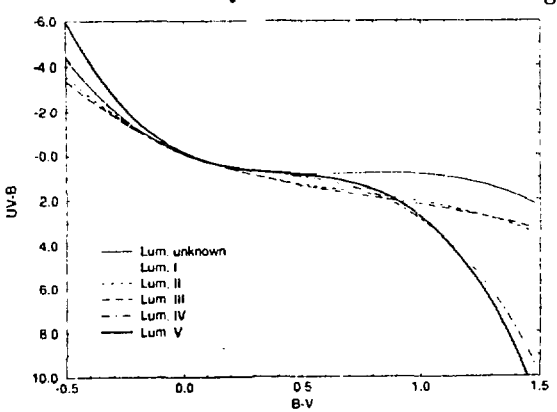

Properties of Galactic Dust in the UV

Benjamin Bilenko and Noah Brosch
The Wise Observatory and the School of Physics and Astronomy
Tel Aviv University, Tel Aviv 69978, Israel

The properties and spatial distribution of dust in the solar neighborhood are studied through the extinction of the UV light in different directions and distances in the Galaxy. The data base used to determine the UV magnitude of a star with known spectral type and visual magnitude is the TD-1 data set and the Hipparcos input catalog. This work will produce a three dimensional map of the dust in each TD-1 band, as a preliminary step in the construction of UV star maps for the TAUVEX experiment.

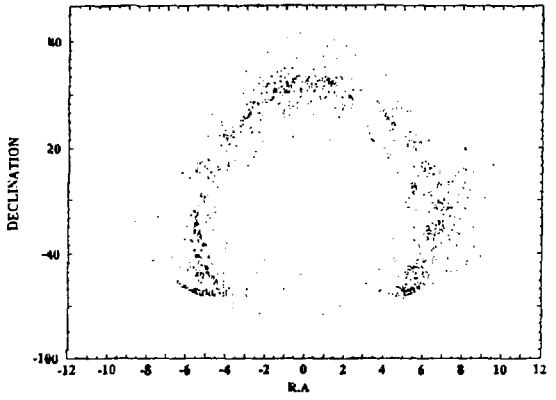

Figure 1: The sky in the UV (TD-1 catalog)

Far-UV Astronomy at the North Galactic Pole

Noah Brosch
The Wise Observatory and the School of Physics and Astronomy
Tel Aviv University, Tel Aviv 69978, Israel

An analysis of a far-UV image obtained during the ATLAS Space Shuttle flight in 1992 is presented. The star counts per magnitude are compared with a model of the distribution of stars in the Galaxy. Follow-up optical observations performed at the Wise Observatory indicate that most uncatalogued objects are normal stars. This study is a preparation for the TAUVEX experiment.

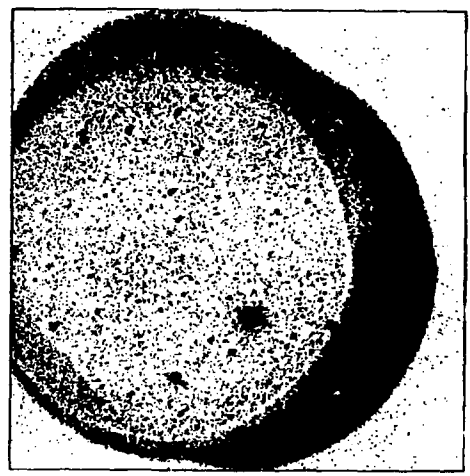

Figure 1: FAUST image of the North Galactic Pole

UV and Optical properties of Virgo Cluster Dwarf Galaxies

Elchanan Almoznino and Noah Brosch
The Wise Observatory and the School of Physics and Astronomy
Tel Aviv University, Tel Aviv 69978, Israel

We present observations of samples of Blue Compact Dwarf Galaxies (BCDGs) in the Virgo cluster obtained at the Wise Observatory, with the IUE satellite and with the FAUST UV Shuttle imager. The observations are interpreted in terms of star formation processes in the BCDGs.

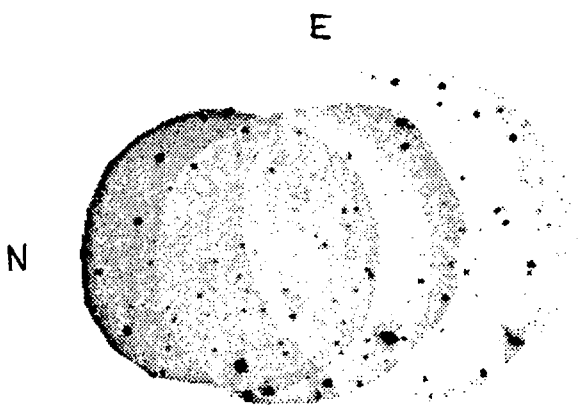

Figure 1: The Virgo cluster combined UV image from 3 FAUST images

TAUVEX Status Report

Noah Brosch and Amotz Shemi
The Wise Observatory and the School of Physics and Astronomy
Tel Aviv University, Tel Aviv 69978, Israel

Jeremy Topaz and Ofer Braun
El-Op Electro-Optical Industries, Ltd., POB 1165, Rehovot, Israel

The TAUVEX space astronomy experiment to image wide sky areas in the 1400-2800Å spectral segment passed a number of milestones during the last year. A thermal model was constructed and tested successfully under space conditions. Prototype detectors were fabricated and tested. An engineering model, identical to the flight model is in construction. These, and other achievements of the project, will be reported. A full-size mockup of the experiment will be exhibited.

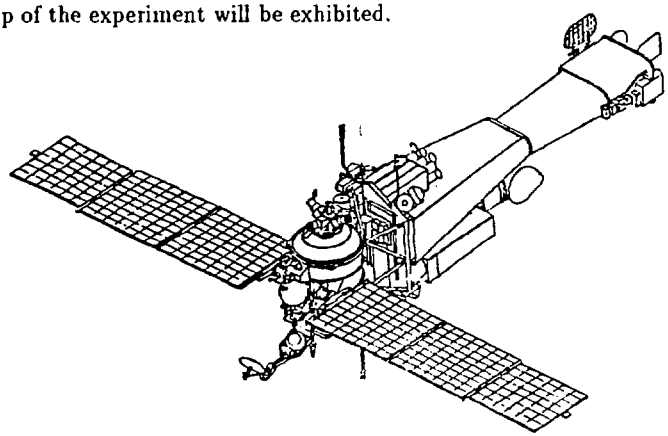

Figure 1: The Spectrum X-γ spacecraft will carry TAUVEX in orbit in 1995

Imaging Polarimetry of Comet P/Swift-Tuttle

Evgeny Goldberg and Noah Brosch
The Wise Observatory and the School of Physics and Astronomy
Tel Aviv University, Tel Aviv 69978, Israel

The Swift-Tuttle comet is the parent of Perseid meteor stream and could strike the Earth on its next perihelion pass. The comet was recovered only in 1992. We observed it with the 1 m telescope of the Wise Observatory with the FOSC ccd-polarimeter. The polarimeter uses polarizer filters at three discrete orientations of the polarization plane. The polarized images contain also the simultaneos image of an unpolarized, for the compaensation of atmospheric effects. The observation and reduction of polarimetric data from a comet, which is a fast moving object, required the development of new reduction techniques. Polarimetry of the comet was successful on November 30, 1992.

We obtained polarimetric maps of central and outer parts of the comet in red light. The orientation of the polarization plane in the the nucleus, coma and observed part of comet tail is perpendicular to the plane of sunlight scattering. Our resolution is 5 arcsec, ~3300 km at the comet. The polarization of the nucleus is 16±2%. In the coma and beginning of tail the polarization varied between 10 and 14%. We observe a spiral pattern of the degree of polarization in the coma, which can be seen on unsharp-masked total intensity maps and in the coma isophote. This pattern is interpreted as asymmetric ejection (jet) of dust from the rotating comet nucleus.

Map of the degree of polarization of comet P/Swift-Tuttle

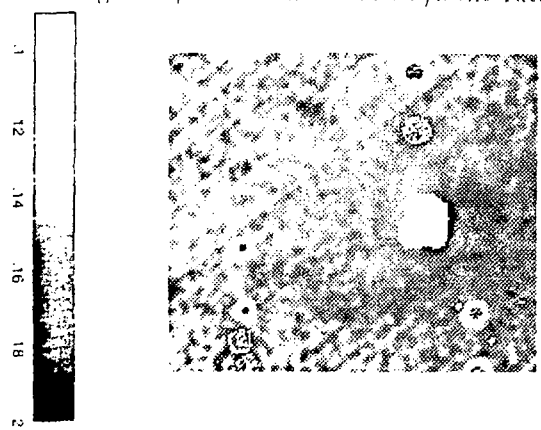

The IUE Uniform Low Dispersion Archives

Frieda Loinger and Elchanan Almoznino
The Wise Observatory and the School of Physics and Astronomy
Tel Aviv University, Tel Aviv 69978, Israel

The IUE Uniform Low Dispersion Archives (ULDA) has recently been installed on one of the TAUVEX UNIX workstations. It offers access to all low-dispersion spectra obtained from 1978 to 1989 with IUE, with all cameras, short and long wave. The ULDA is available on-line to any Israeli astronomers as a national facility.

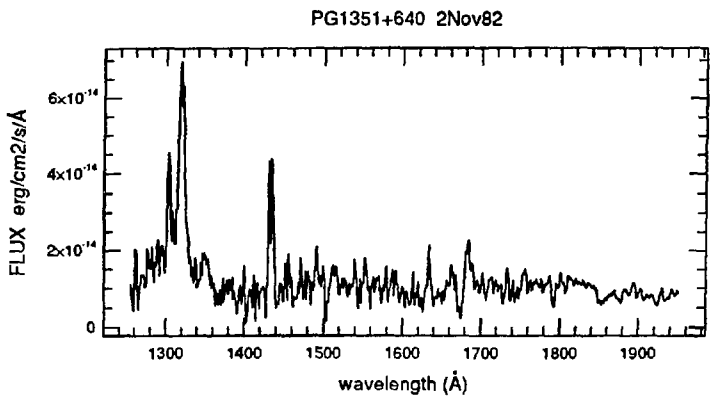

Figure 1: A sample spectrum extracted from the ULDA at Tel Aviv

Condensed Matter Physics

Spectroscopy, Electron-electron Interaction, and Level Statistics in a Disordered Quantum Dot

U. Sivan[a]
The Solid State Institute and Physics Department, Technion, Israel Institute of Technology, Haifa 32000, ISRAEL.

A novel spectrometer is employed to study the spectrum of heavily doped quantum dots in a regime where electronic motion is diffusive and the Fermi energy is much larger than the average level spacing. A single particle discrete spectrum is found to exist only in close vicinity to the Fermi energy. Levels further away are broadened beyond the average level spacing and merge to form a quasi continuos spectrum. Broadening is traced to electron-electron interaction in the dot. For the discrete part of the spectrum, level correlation is studied as a function of magnetic field and energy and found to agree remarkably well with recent calculations.

[a] Work done in collaboration with F. P. Milliken, K. Milkove, S. Rishton, Y. Lee, M. J. Hong, V. Boegli, D. Kern, and M. deFranza, IBM, T. J. Watson Research Center, Yorktown Heights, NY 10598, USA.

Ballistic quantum transport - contact phenomena

Yehoshua Levinson

Department of Physics, Weizmann Institute of Science
Rehovot 76100,Israel

Recent progress in crystal growth allows fabrication of GaAs/GaAlAs heterostructures with very high mobility two dimensional electron gas (2DEG), the elastic mean free path of the electrons being of the order of 10 microns. On the other hand progress in electronic beam lithography allows to patterning of structures with lateral dimensions of the order of few microns. As a result of these two technological achievements one can fabricate submicron 2DEG devices the dimensions of which are smaller than the elastic and inelastic scattering mean free path. Electrons move in such devices ballistically crossing the device without scattering and therefore conductivity is nonlocal.

The theory of nonlocal transport is based on the Landauer-Buttiker approach, where the contacts are treated as ideal ones. It means that the contacts absorb without reflection all electrons in incoming states and feed all outgoing states with equilibrium distribution.

Real contacts are heavily doped n^+-domains attached to the 2DEG and prepaired by alloying AuGe contacts. In such a contact electrons undergo strong scattering, while in the 2DEG the electrons can be treated as ballistic ones. It is known from neutron physics that a strongly scattering halfspace attached to a nonscattering halfspace is a *nonideal* contact.

Nowadays one has strong experimental evidence that properties of the Quantum Hall Effect (QHE) in small devices are also strongly contact dependent . This is supported by the new theoretical approach to the QHE, based on the concept of edge states.

We develop a microscopic model of a contact between a heavily doped disordered strongly scattering region(which is metal-like) and lightly doped pure ballistic region (which is semiconductor-like).The ingredients of this model are the elastic and inelastic scattering in the metal and different Fermi-surfaces in the metal and in the semiconductor.

Using the microscopic model of the contact we calculate the reflection of electrons in incoming states and the population of the outgoing states emitted by the contact.

The Optical Larmor Clock: Measurement of Photonic Tunneling Time as an Analogy to Electronic Tunneling

M. Deutsch and J. E. Golub

The Hebrew University
Racah Institute of Physics
Jerusalem, Israel

The concept of the time of tunneling through a potential barrier has been discussed over the past 60 years. The Larmor clock--one of several theoretical suggestions for defining and measuring tunneling times--is based on the spin precession of a polarized electron tunneling through a magnetic-field-permeated barrier. Though an electronic Larmor clock has not been realized, we show that an optical Larmor clock, suitable for the measurement of photonic tunneling times, may be constructed using thin films of birefringent materials. Other tunneling times, including the Büttiker-Landauer time, may similarly be implemented in optical analogy. We present experimental and theoretical results on an optical Larmor clock for transport over wells and through barriers.

DOUBLE BARRIER QUASI-PARTICLES ENERGY SPECTRUM: SIGNS OF CHAOS.

Richard Berkovits

The Jack and Pearl Resnick Institute for Advanced Technology,
Department of Physics, Bar-Ilan University,
Ramat-Gan 52900, Israel

The statistical properties of the many-body energy spectrum of a double-barrier hetrostructure are studied. Different types of interactions between the electrons in the structures are considered. For the cases where the interactions are homogenous the energy levels exhibit properties associated with regular system behavior. On the other hand, when interactions are limited to electrons in the well region the statistical properties of the energy spectrum are typical of systems which exhibit chaotic behavior.

Pointlike Vortices and Magnetization Relaxation in Layered Superconductors

R.G. Mints* and I.B. Snapiro†

*School of Physics and Astronomy, Raymond and Beverly Sacler Faculty of Exact Sciences, Tel–Aviv University, 69978 Ramat–Aviv, Israel

†Physics Department, Technion–Israel Institute of Technology, Haifa 32000, Israel

The energy of a point–like vortex is calculated for a layered superconductor with weak interlayer Josephson coupling. An energy barrier existing near the sample surface is found. The effect of the interlayer Josephson coupling on this barrier is considered. Magnetization relaxation due to thermally activated penetration of point–like vortices is considered. An initial avalanche–type decay of magnetization is predicted.

The Theory of Doped Antiferromagnets

Assa Auerbach
Physics Department
Technion, Haifa 32000

The large spin formulation of the t-J model allows a successful semiclassical expansion of the single hole problem. The effective Lagrangian for many holes in the physically interesting parameters regime is the t'-J model. This model has been argued to produce RVB superconductivity in the magnetically disordered phase. Currently, there is no satisfactory understanding of the disordering mechanism at low doping. We prove a Luttinger-like theorem for the staggered magnetization, which allows a systematic investigation of the dynamical effects of doping in $La_{2-x}Sr_xCuO_4$.

ANISOTROPIC SUPEREXCHANGE INTERACTION, FRUSTRATION AND WEAK FERROMAGNETISM

L. Shekhtman, O. Entin-Wohlman and Amnon Aharony
School of Physics and Astronomy
Raymond and Beverly Sackler Faculty of Exact Sciences
Tel Aviv University
Tel Aviv 69978, Israel

Abstract

Moriya's expression for the *single bond anisotropic superexchange interaction* is shown to possess an overlooked hidden symmetry, isomorphic to the symmetry of the isotropic case. For the unfrustrated case, this symmetry results in a degeneracy of the macroscopic state, implying no unique value for the Dzyaloshinsky weak ferromagnetic moment. A unique value emerges from superexchange *only* when more than a single bond is considered and *only* as a result of *frustration*. This implies that the symmetric part of the superexchange anisotropy tensor must vary among the bonds. The results are particularly relevant for the spin anisotropies in La_2CuO_4.

CROSSOVER PHENOMENON FOR HOPPING CONDUCTION AND DENSITY-OF-STATES NEAR THE FERMI LEVEL

I.Shlimak and M.Kaveh

The Jack and Pearl Resnick Institute for Advanced Technology and Department of Physics, Bar-Ilan University, Ramat-Gan, Israel.

M.Lea and P.Fozooni

Department of Physics, Royal Holloway University of London, Egham, Surrey, TW20 OEX, England.

The variable-range-hopping (VRH) conductivity of n- and p-type germanium prepared by a neutron-transmutation-doping technique, was measured at temperatures down to 30 mK and at magnetic fields up to 7 Tesla. For all samples studied the temperature dependence of VRH conductivity at low temperatures and weak magnetic fields is in agreement with the existence of a soft Coulomb gap (CG) at the Fermi level. We find that strong magnetic fields reduce the effectiveness of the CG. We propose a crossover phenomenon characterized by a temperature T_c with the CG being effective only below T_c. The value of T_c decreases as the magnetic field increases. It is shown that the temperature dependence of the VRH conductivity can be reduced to a universal curve for all samples and fields from which one can determine the density-of-states (DOS) near the Fermi level. The parameters of the CG were obtained for all the samples. The tendency to a constant DOS at higher energies is shown, which leads to the crossover phenomenon.

On the Auger and Autoionization Processes in 3d-Metals

E. Batkilin, R. Brener, S.Dorfman and J.Felsteiner

Physics Department and Solid State Institute,
Technion - Israel Institute of Technology, 32000 Haifa, Israel

There is a strong interest in the Auger and autoionization processes in solids, because of their sensitivity to the details of the band structure. Although these processes are quite related, no unified model has so far been proposed to explain them. The existing theory of Cini and Sawatzky explains the Auger line shape for the $3d$ metals with almost filled d-band. However, this theory fails in the case of $3d$ metals with less then half-filled d-bands. It is known that for the $3d$ series with increasing atomic number from Sc to Cu, the intensity of the autoionization line decreases and it comes closer to the Auger line. An explanation for the Auger and autoionization processes can be found using an appropriate many-electron model. We have constructed the corresponding diagramatic expansion for such processes in the valence band. We solve exactly the Bethe-Salpeter equation for the ladder and ring parts of the diagramatic expansion in the two-band model and show that for partially-filled bands the solution can have a bound state (negative binding energy). We also show the connection between the Auger and autoionization processes. Our theory satisfactorily explains many of the observed features of these processes and we find good quantitative agreement with the experimental results.

BACKSCATTERING ENHANCEMENT FROM INTERFACES WITH BOUND STATE

V.Freilikher, and I.Yurkevich

Department of Physics, Bar-Ilan University, Ramat-Gan 52900, Israel

Intensity enhancement in the retroreflection direction is studied for waves scattered by a random interface which has bound state (surface wave). It is shown that enhanced backscattered signal appears due to multiple scattering and localization of the surface waves. For these waves a closed equation of Schrodinger type with random potential and with effective attenuation is derived and investigated. The shape of scattering indicatrix is calculated. It is shown that the dependances obtained may be used for the determination of rough surfaces parameters.

Grain boundary migration and heterodiffusion in thin Pd/Ag films

A.N.Gladkikh [1], M.V.Karpovskiy [2]

[1]Faculty of Engeneering, [2]Faculty of Exact Sciences
Tel-Aviv University, Ramat Aviv

Interdiffusion processes in thin epitaxial Pd/Ag films in the temperature range 20-500°C are studied by the transmission electron microscopy, electron diffraction and electrical transport methods. Homogenization is investigated both during condensation and under conditions of postcondensation annealing.

As shown, in processes of mass transfer at these temperatures grain boundaries play a decisive role. "Cold" homogenization ($T<0,5T_m$) is found to be many-sided, dependent on initial structure and temperatures of condensation or annealing. Various mechanisms of "cold" homogenization can appear simultaneously or replace one another during diffusion experiment. They are diffusion induced grain boundary migration (DIGM), diffusion induced recrystallization (DIR), recrystallization induced diffusion (RID) and lattice diffusion activation in accumulations of fine grains.

Effect of Thickness Quantumization on Subsidiary Absorption Spectra

A.V. Pomyalov & I. Laulicht, Department of Physics, Bar-Ilan University, Ramat-Gan 52900, Israel.
J. Barak, Department of Solid State Physics, Soreq Nuclear Research Center, Israel.

Spin wave (SW) instabilities that take place at high power microwave pumping of yttrium iron garnet (YIG) subjected to a steady magnetic field are known to be a good example of nonlinear dynamics in solids [1,2].

We expect SW nonlinearities in thin films to have special features associated with the discreteness and low degeneracy of the SW spectra (resulting from thickness quantization of the wave lengths and anisotropy related to sample shape). Thin film studies can also help to find the active SWs and thus enable a quantitative theoretical treatment of the observed phenomena.

At the first stage of our research we investigated parametric excitations of SWs in tangentially magnetized films at the condition of perpendicular pumping – subsidiary absorption (SA). The threshold pumping power Pth of SA in tangentially magnetized films was taken as a function of magnetic field H (butterfly curve, figure 1) and film thicknesses ($0.33\mu m < S < 40\mu m$). The data shows a strong decrease of the upper field limit of SA with the thickness decreasing in the range $3 - 0.3\mu m$. Calculations revealed the upper limit in all the films to be less than that for bulk samples which means an increase of the lowest SW frequency in thin films compared to that of the bulk. The effect has been explained through the trade in between dipole and exchange contributions to the energy of SW in thin ferrite layer magnetized parallel to its surface (backward volume magnetostatic wave – BVMSW). Numerial calculations of the supposed effect were based on Damon-Eshbach dispersion relations modified to allow for exchange interactions. The good agreement with theory is shown in figure 2. The present results are consistent with a similar recent study by Polzikova etal [3].

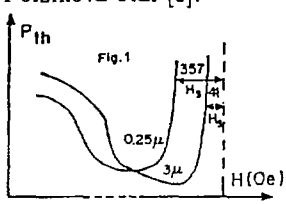

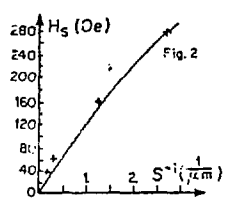

[1] H. Thomas *Nonlinear Dynamics in Solids* . Springer Verlag (1992)
[2] X.Y. Zang & H. Suhl *Phys Rev. B* 38,7, 4893, (1988)
[3] N.I. Polzikova, A.O. Raevskii & A.G. Temiryazev *Sov. Phys. Solid State* 26, 2113, (1984)

Scale Dependent Resistivity in Insulating 2D Samples

D. Kowal and Z. Ovadyahu
The Racah Institute of Physics, The Hebrew University Jerusalem

We have investigated the resistivities of thin crystalline and amorphous indium oxide films as a function of sample size and disorder. Sets of samples 500 μm in width and 0.5 μm to 200 μm in length were patterned from a common sheet of thin film (100–250 Å) deposit. In the liquid helium range of temperatures, significant and systematic differences in the samples 2D resistivities ($R_{\square}$) were found. For example, in the insulating regime, the longer the sample the higher the resistivity it exhibits. This length-dependent spread in resistivity becomes more pronounced at lower temperatures. The characteristic lengths pertinent for electronic transport in these samples (the hopping length, localization length and even the percolation length) are all appreciably smaller than any of the sample lateral dimensions. In this, macroscopic limit it is usually expected that a sample resistivity is independent of its specific geometry contrary to what is observed in our experiments. We suggest that the anomalous length dependence stems from the wide distribution of resistances inherent to the disordered sample on one hand and its geometrical shape on the other.

Equilibrium point defects in metals

Yaakov Kraftmakher

Department of Physics, Bar-Ilan University, Ramat-Gan 52900, Israel

I would like to consider once again two questions which seem to many authors not to be related each to other: (1) what is the reason of the strong nonlinear rise of the high-temperature specific heat (and thermal expansivity) of metals, and (2) what are the equilibrium concentrations of point defects in metals. Both questions are important, and it is surprising that they have no answers up to date.

What I claim is that there exists a direct relation between the two questions, namely: (1) the nonlinear rise of the specific heat (and of the expansivity) is caused by point defect formation, and (2) this phenomenon permits a very reliable calculation of the equilibrium defect concentrations which, in refractory metals, become of the order of 1% at the melting point.

It is possible now to compare data based on relaxation measurements of specific heat [1, 2], resistivity, and positron annihilation. Such a comparison may be useful even if the only result is evidence that the observed relaxation phenomena have a common origin. In measurements of the resistivity of platinum, the samples were rapidly heated to the desired temperature, maintained at this temperature for an adjustable time and then quenched [3]. The extra resistivity was studied as a function of time spent at high temperature. The relaxation time obtained for the region 1073 - 1223 K was of the order of 10^{-2} s. Extrapolation to the melting point gives times of the order of 10^{-6} s, which is in agreement with the results of the specific-heat measurements. Relaxation measurements of resistivity were performed also on gold [4] and aluminium [5]. Recently, the relaxation time of the defects in gold was measured by positron annihilation [6]. The lifetime of positrons in a sample was studied during fast changes of temperature. It follows from these data that at the melting point the relaxation time will be shorter than 10^{-3} s. Thus, recent data seem to support the statements formulated above.

[1] Ya.A.Kraftmakher. Fiz. Tverd. Tela 27 (1985) 235.
[2] Ya.A.Kraftmakher. Phys. Letters A 149 (1990) 284.
[3] F.Heigl and R.Sizmann. Crystal Lattice Defects 3 (1972) 13.
[4] D.N.Seidman and R.W.Balluffi. Phys. Rev. 139 (1965) A1824.
[5] K.Ono and T.Kino. J. Phys. Soc. Japan 44 (1978) 875.
[6] H.-E.Schaefer and G.Schmid. J. Phys.: Condensed Matter, Suppl. A (1989) 49.

Theory of the optical and microwave properties of metal-insulator films

Andrey Sarychev, David Bergman and Yoad Yagil
School of Physics and Astronomy
Raymond and Beverly Sackler Faculty of Exact Sciences
Tel-Aviv University, Tel-Aviv 69978, Israel.

The optical properties of metal–insulator semicontinuous films have been widely investigated, both theoretically and experimentally. Several effective medium theories and scaling arguments have been used to calculate properties of the films. All these theories are based on the assumption that electrical and magnetic fields can be treated as potential fields. This is not true for practically important case where the skin depth δ for metal grains is smaller than the thickness d of the semicontinuous film. To manage such a case we fix an electric field $\mathbf{E}$ and magnetic field $\mathbf{H}$ at some distance away from a film. Then we solve Maxwell equations to find the local fields inside the film and determine the electric current $\mathbf{I}$ and magnetic induction $\mathbf{B}$ averaged over the thickness of the film.

$$\begin{aligned} \mathbf{I}(x,y) &= \sigma\mathbf{E}(x,y) + g\mathbf{n}\times\mathbf{H}(x,y) \\ \mathbf{B}(x,y) &= \mu\mathbf{H}(x,y) + i\frac{4\pi g}{\omega}\mathbf{n}\times\mathbf{E}(x,y) \end{aligned}$$

where x and y are coordinates in the plane of the film, $\mathbf{n}$ is a unit vector normal to the film. The parameters σ, g and μ depend on the material of the particular grain, the thickness of the film and the frequency ω. We suppose that the typical size of metal islands in a semicontinuous film is smaller than the wavelength and away from the film fields are potential. Another equations can be obtained by taking into account the conservation laws $div\mathbf{I}(x,y) = 0$, $div\mathbf{B}(x,y) = 0$. All these equations have to be solved simultaneously to get the effective parameters of the semicontinuous metal–insulator film. So we propose that the films are characterized by three parameters— σ_{eff}, g_{eff} and μ_{eff}. These parameters are reduced to the usual electric conductivity σ_{eff} and magnetic permittivity μ_{eff} only for the quasistatic case when $d \ll \delta$ and parameter $g_{eff} \to 0$.
In this work we suggest the experimental procedure to determine the new parameters and calculate optical and microwave properties of semicontinuous films in terms of these parameters. For example, our theory reproduces the broad absorption peak observed in many experiments near a percolation threshold.

Quasiclassical theory of Shubnikov-de Haas effect in 2D electron gas

E.L.Altshuler

Department of Nuclear Physics
The Weizmann Institute of Science, Rehovot, 76100, Israel

and

B.Laikhtman

Racah Institute of Physics
Hebrew University, Jerusalem, 91904, Israel

A new approach to the theory of magneto-transport in 2D gas is developed. We make use of the Keldysh technique and introduce a modified Green's function which is translationally invariant and gauge invariant. The modification simplifies the calculation of diagram and allows us to obtain a new helpful addition theorem for the electron wave functions in magnetic field. The modified Green's function is very convenient to follow the transition between quantum magnetic transport and transport in zero magnetic field. For the calculation of conductivity we use the self-consistent Born approximation (SCBA). We carefully check its validity and show the physical meaning of the corresponding parameter. All specific calculations are made for the case when the separation between Landau levels, $\hbar\Omega$, is much smaller than the Fermi energy. At the same time no limitation is applied to the relation between $\hbar\Omega$ and the width of the levels induced by scattering, Γ. Specific attention is paid to the long range scattering potential. The evolution equation for the Green's function allows us to obtain magneto-oscillation effects carefully following the appearance of the single particle relaxation time and transport relaxation time. Analytical results for the conductivity tensor are obtained for both Shubnikov - de Haas effect, when $\hbar\Omega \ll \Gamma$, and quantum Hall regime, $\hbar\Omega \gg \Gamma$. In the last case the temperature dependence of the conductivity depends on the relation between the temperature and $\hbar\Omega$ and Γ. Although SCBA does not describe localization it, however, allows one to separate the Shubnikov - de Haas effect from the quantum Hall effect.

Photostructural transformations in the vitreous chalcogenide films stimulated by the excimer ArF-laser radiation

I. Bar, M. Klebanov, V. Lyubin, S. Rosenwaks, S. Shtutina, V. Volterra
Ben-Gurion University of the Negev

Photostructural transformations in the vitreous chalcogenide films are interesting physical phenomena (see review articles [1-3]). One of the peculiarities of these phenomena is the low quantum efficiency. This property is displayed in small photosensitivity limiting the practical application of the phenomena in micro- and optoelectronics.

It is shown in this paper that the photosensitivity can be increased greatly (more than a 1000 times) when excimer ArF laser pulses are used for irradiation. The comparative investigation of processes induced in the $As_{50}Se_{50}$ and $As_{40}S_{60}$ vitreous films by pulsed and continuous laser radiation allowed to conclude that the same structural transformations proceed in both cases. It is shown experimentally that the reason for the sensitivity increase is the intensive flux of light quanta and not the energy of quantum. A phenomenological explanation of the effect of photosensitivity increase is proposed and possible practical applications of the observed effect are discussed.

1. S.R. Elliott, J. Non-Cryst. Sol. 81, 71 (1986).
2. V.M. Lyubin, J. Non-Cryst. Sol. 97-98, 47 (1987).
3. Ke. Tanaka, Rev. Solid-State Science 4, 641 (1990).

Natural and photoinduced anisotropy and gyrotropy stimulated by the sub-band-gap light in bulk chalcogenide glasses

M. Klebanov, V. Lyubin, S. Rosenwaks, V. Tikhomirov, V. Volterra
Ben-Gurion University of the Negev

The finding that photoinduced anisotropy and gyrotropy in As-S and As-S-I glasses is stimulated by sub-band-gap light [1] contradicts the previous proposed mechanism. New experiments are, therefore necessary for understanding these photoinduced phenomena.

In this research the photoinduced and natural anisotropy and gyrotropy are studied simultaniously in two classes of chalcogenide glasses: arsenic-containing and germanium-containing having a substantial structural distinction. The spectra of the photoinduced phenomena were investigated for the first time. Comparatively large natural linear dichroism (up to 0.05) was observed in $GeS_{2.2}$ glass. The photoinduced linear dichroism in $GeS_{2.2}$ glass had a value close to the natural one and the form of the dichroism spectrum changed weakly during irradiation. Completely different behavior was found in the As-containing glasses where natural linear dichroism reached large values (0.5-0.7). The spectra of dichroism were changed drastically in the process of irradiation. The position of the dichroism maximum tended to the wavelength of the inducing light. The conclusion is reached that the localised states distributed widely in the gap of As-containing glasses are responsible for the photoinduced dichroism. The deep states are excited in the early period of irradiation and only after that the shallow states are displayed that determine the stationar value of dichroism. The narrow group of localised states is responsible for the dichroism in Ge-containing glasses.

Natural and photoinduced optical activity (gyrotropy) were discovered in the glasses. The characteristics of the optical activity were also very different in the glasses of both types.

1. V.M. Lyubin, V.K. Tikhomirov. J. Non-Cryst. Sol. 135, 37 (1991).

58

Theory of High Field Domain Structure in Superlattices

D.Miller and B.Laikhtman

Racah Institute of Physics
Hebrew University
Jerusalem. 91904, Israel

A number of experimental works provide evidences of the existence of a high field domain in superlattices when an applied voltage exceeds some critical value. A theoretical description of the structure of such domain is developed. It appeared to be quite different from that in Gunn diodes. We confine ourself to the case of narrow band superlattices, when electrons are strongly localized in the wells. In the interpretation of current-voltage characteristics it is usually assumed that for a voltage just above the critical value the high field domain occupies one period of the superlattice. Further increase of the voltage leads to the increase of the domain length. Our analysis shows that under typical experimental conditions a minimal size of the domain is not one but a few superlattice periods. A high field domain in the middle of the superlattice can exist only at relatively high electron concentrations. For low concentration the domain can appear only at the anode edge of the superlattice.

Conductance Fluctuations in Ballistic Cavities and Quantum Chaos

O. Millo,[a] M.W. Keller,[b] A. Mittal,[b] and D.E. Prober[b]
[a]*The Racah Institute of Physics, Hebrew University of Jerusalem, Jerusalem 91904*
[b]*Department of Physics, Yale University, New Haven CT 06520, USA*

We study electron transport in a two-dimensional-electron-gas system laterally confined to a small cavity. The cavity is small enough so that large angle elastic scattering is dominated by boundary scattering, but large enough that transport through it can be described semiclassically. We concentrate on studying cavities having shapes for which the classical dynamics is chaotic (e.g., stadium). Recent theoretical studies predict that for such devices the correlations in magnetic field and Fermi energy of the resistance fluctuations have a scale determined by the underlying classical chaotic scattering.[1]

The samples are fabricated from high mobility GaAs/AlGaAs heterojunctions. Electron beam lithography is used to pattern a metal mask, and the sample is then exposed to low energy ions which destroy the conductivity except under the mask. Submicron caviaties and leads less than 100 nm wide are fabricated with this technique. The metal mask serves also as a self-aligned gate, allowing the density of the electron gas to be changed over a significant range without changing the shape of the cavity. This is an important advantage of this fabrication technique over split-gate confinement methods. The samples are mounted in a dilution refrigerator and studied at temperatures from 4K to about 50 mK. We measure the four-terminal resistance of the cavities as a function of magnetic field and gate voltage, and focus on studying the resistance fluctuations as a function of these parameters.

We will present magnetic field and gate voltage results for stadia of different sizes. The scaling of the correlation fields and correlation energies of the conductance fluctuations with the size of the stadium and the width of the leads will be compared to theoretical predictions. The power spectrum of the fluctuations contains features which are related to particularly important scattering paths in the cavity, and this issue will also be discussed. Our data also show a large peak around zero magnetic field which we relate to a weak-localization effect in ballistic cavities.

[1] E. Doron, U. Smilansky, and A. Frenkel, Physica **D50**, 367 (1991); R.A. Jalabert, H.U. Baranger, and A.D. Stone, Phys. Rev. Lett., **65**, 2442 (1990).

Analysis of Time of Flight Signals Obtained by Charge Transport in Insulating Structures

N.R. Mirchin and A. Peled

Center for Technological Education Holon
affiliated with Tel-Aviv University
52 Golomb Street, Holon 58102, Israel

The Time of Flight technique[1] (TOF) used in the evaluation of hole mobilities in insulator structures involves the measurement of the induced currents appearing transiently on the electrodes as the charges drift through the device. The general shape of the transient current consists of an initial drop of the current to a near plateau level. Then it drops in a different form to zero as the charge is being collected. Due to various dispersion mechanisms involved in the charge transport such as diffusion, trapping, coulombic spread and detrapping, the current shape depends strongly on parametric values such as device thickness, temperature, doping level and electric field. In this work a theoretical analysis[2] has been initiated which involves the use of Poisson equation and a general scheme to account for any dispersion mechanism which is responsible for the transient current shape. The technique allows one to analyze the dispersive curves obtained experimentally in TOF charge transport investigations such as in Molecular Doped Polymers used in Laser Printers and Photoreprographics[3].

[1] L. Pautmeier, R. Richert and H. Basler, "Anomalous time-dependent diffusion of charge carriers in a random potential under a bias field", *Phil. Mag.* **B**, **63**(3), pp.587-601 (1991).
[2] N.R. Mirchina and A. Peled, "Induced Currents by propagating charge packets structures", *J. of Electrostatics* (to be published 1993).
[3] J.C. Scott, L. Th. Pautmeier and L.B. Schein, "Mean mobilities of charge carriers in disordered media", *Phys. Rev.* **B**, **46**, p. 8603 (1992).

Theory of Hall Effect and Magnetoresistance in a Periodic Composite for Arbitrarily High Magnetic Field

Yakov M. Strelniker and David J. Bergman

School of Physics and Astronomy
Raymond and Beverly Sackler Faculty
of Exact Sciences
Tel Aviv University
69978 Tel Aviv, Israel

A new method for calculating the bulk effective properties of a two-component composite with a periodic microstructure is applied to magneto-transport. For the first time it is possible to calculate the bulk effective magnetoresistance $\rho^{(e)}(p,H)$ and the Hall coefficient $R_H^{(e)}(p,H) = \rho_{xy}^{(e)}(p,H)/H$ for arbitrarily high magnetic fields, H, arbitrary volume fractions, p, and shapes of the inclusions. The method is based (as in Ref. [1], where the effective dielectric constant $\varepsilon^{(e)}(p)$ of two-components $(\varepsilon_1,\varepsilon_2)$ composite was evaluated) on a Fourier space representation of an integral equation $\phi = z+(1/s)\hat{\Gamma}\phi$ for the electric potential ϕ (z is the externally applied linear potential). In Ref. [1] the eigenvalues s_n of the integral operator $\hat{\Gamma}$ were real ($s_n \in [0,1)$), and $s \equiv \varepsilon_2/(\varepsilon_2-\varepsilon_1)$. In our case the eigenvalues of $\hat{\Gamma}$ are complex conjugate pairs ($0 < Re\ s_n < 1, |Im\ s_n| < H$), and the parameter s is introduced as a formal parameter which is set to 1 at the end of the calculation. The introduction of this parameter enables us to perform an analytic continuation and obtain expressions for $\rho^{(e)}(p,H)$ and $\rho_{xy}^{(e)}(p,H)$ as power series in $1/s$ that diverge (in the limit $s \to 1$) for large H. The divergence of these series is circumvented by using the methods of conformal transformations and of Padé approximants. We present results for cubic arrays of non-overlapping and overlapping spheres, as well as for other geometrical forms of inclusions: spheroids, cylinders, etc. We find that there is strong magneto-resistance for low and intermediate fields in two-component metal-insulator systems. For high magnetic fields the ohmic resistivity and the Hall coefficient both saturate. These results agree with results of the effective medium theory at low fields, and with recent numerical simulations of a percolating medium at high fields [2]. The method works for all ranges of volume fraction and can be used near a conductivity or superconductivity threshold.

[1] D. J. Bergman and K.-J. Dunn, Phys. Rev. **B45**, 13263 (1992-I).
[2] A. K. Sarychev, D. J. Bergman and Ya. M. Strelniker, sub. to Phys. Rev. B

Photostimulated phenomena in spin-coated vitreous $As_{40}S_{60}$ and $As_{50}Se_{50}$ films

S. Shtutina, V. Lyubin, M. Klebanov
Ben-Gurion University of the Negev

Vitreous chalcogenide films are intensively studied due to their interesting physical properties and the perspectives of their application in modern electronics. In most cases such films are prepared by the methods of vacuum evaporation or sputtering. Recently the new technique of films preparation by means of spin-coating was proposed and $As_{40}S_{60}$ films were produced. In this paper we report about the results of preparation and structural study of spin-coated vitreous $As_{40}S_{60}$ and $As_{50}Se_{50}$ films. The optical properties of these films and films of the same composition manufactured by the vacuum evaporation technique are compared. Two groups of photoinduced phenomena in the films: photodarkening and photoinduced diffusion of silver are studied. The polarized photodoping of the spin-coated films was observed and investigated for the first time. The conclusion is made that the photodarkening process is strongly dependent on the film structure but the details of film structure have very weak influence on the Ag photodiffusion and on the photoanisotropy.

Kosterlitz-Thouless Behavior and Scaling in Superfluid Helium Films

R. Brada*, H. Chayet and W.I. Glaberson

Racah Institute of Physics and Astronomy
The Hebrew University
Givat-Ram, Jerusalem, Israel

The results of a series of measurements of Kosterlitz-Thouless behavior in helium films are presented. Use is made of high Q piezoelectric crystals so as to probe the phenomena in a single flat substrate geometry at high frequencies. Variations of the superfluid density and dissipation in the vicinity of the transition were measured. Dynamical effects were probed by comparing transitions at two different frequencies. Results are compared with a comprehensive numerical calculation in which finite size scaling effects are explicitly introduced. A consistent picture for the dependence of critical thickness on temperature, of the scaling of the transition shape with temperature and of dynamical effects is obtained.

* current address: Department of Nuclear Physics, Weizmann Institute of Science, Rehovot, Israel.

Increase of Critical Current by External Electric Field in High-Temperature Superconductors.

L. Burlachkov, I. B. Khalfin and B. Ya. Shapiro

Department of Physics, Bar-Ilan University, Ramat-Gan 52900, Israel

An electric field directed perpendicular to the surface of a superconductor changes the superconducting properties near the surface and creates an additional barrier for flux penetration into the sample. This effect is characterized by the value l_D/ξ, where l_D is the Debye screening length and ξ is the coherence length, and can be neglected in conventional superconductors with $l_D<<\xi$. However, in high-temperature superconductors, where $l_D/\xi\sim1$, the effect is very pronounced and could be used for improvement of the transport critical current.

The Phase Diagram of $Pr_xY_{1-x}Ba_2Cu_3O_{7-\delta}$; Oxygen Depletion Versus Pr Doping

J. Genossar, B. Fisher, S. Israelit, C. Kuper,
L. Patlagan and G.M. Reisner

Department of Physics
Technion-Israel Institute of Technology
32000 Haifa, Israel

$PrBa_2Cu_3O_7$ is NOT a superconductor (while all the other $RBa_2Cu_3O_7$ compounds are HT superconductors - where R is a rare earth ion). We investigated the $Pr_xY_{1-x}Ba_2Cu_3O_{7-\delta}$ system, varying both the Pr and oxygen content; measured the resistivity as function of composition and temperature; and determined T_c and the crystal parameters. Using the literature data on T_N, a phase diagram was constructed, showing the variation of T_c and of T_N in the x, δ plane. In $Pr_xY_{1-x}Ba_2Cu_3O_{7-\delta}$ we find very close similarity between the dependence of transport properties: (T_c, T_N, $\rho(T)$, $S(T)$, $R_H(T)$, ...) on doping by Pr and by oxygen vacancies. We discuss the implications of these results for the proposed explanations concerning the unusual behaviour of $PrBa_2Cu_3O_7$.

Pair Transfer Superconductivity in the Anderson Model

B. Nathanson, and O. Entin-Wohlman

Raymond and Beverly Sackler Faculty of Exact Sciences,
School of Physics and Astronomy,
Tel aviv University,
Tel Aviv, Israel 69978

Superconductivity due to the transfer of electron pairs between the conduction band and a local impurity level is studied. Treating the Coulomb repulsion on the impurity site and the "pair transfer" term within the Hartree-Fock approximation for the non-magnetic case, it is found that superconductivity can occur due solely to interband interaction, with a transition temperature on the order of electronic energies. Single-electron hybridization with the impurity state reduces T_c when the pair transfer vertex is repulsive, whereas it can increase T_c at a very low impurity concentration for an attractive vertex. "Reentrance" to the normal state at low temperatures is obtained as is the case for alloys with a high Kondo temperature, in which superconductivity is driven by intraband attraction. Possible relevance to high T_c materials is discussed.

An explanation of the giant magnetoconductivity in La_2CuO_4

L. Shekhtman, I. Korenblit, and Amnon Aharony
School of Physics and Astronomy
Raymond and Beverly Sackler Faculty of Exact Sciences
Tel Aviv University
Tel Aviv 69978, Israel

Abstract

It is shown that the localization radius of the impurity hole wave function in La_2CuO_4 experiences a jump at the point of the weak ferromagnetic phase transition. [1] This jump may be related to the change in the *free* hole mass induced by the change in the underlying magnetic structure. This effect provides an explanation for the unusually big increase in the hopping conductivity associated with such transitions. Our approach explains the order of magnitude of the effect itself and accounts for its temperature dependence in a self-contained manner.

[1] Thio *et al.*, Phys. Rev. **B38**. 905 (1988).

Valence Subband Structure in <110> Quantum Wells

G. Shechter, L. D. Shvartsman, and J. E. Golub

Racah Institute of Physics
The Hebrew University of Jerusalem
Jerusalem 91904

We present Kohn-Luttinger calculations of the valence subband structure for <110>-oriented quantum wells of different cubic semiconductors. We show that in addition to the usual extremum at k=0, it is possible to obtain saddle point spectra with the result that the sign of effective mass depends on the crystallographic direction in the plane of quantum layer. We present an analytic expression for the effective mass tensor applicable to all cubic materials, and show the full subband dispersion for GaAs, Ge, and InGaAs. Finally, we discuss transport anomalies which may be associated with this band structure.

Persistent Currents and Spin-Orbit Coupling in The Anderson Model

E. Yahel and O. Entin-Wohlman

Raymond and Beverly Sackler Faculty of Exact Sciences,
School of Physics and Astronomy,
Tel aviv University,
Tel Aviv, Israel 69978

The average persistent current of single-channel and multi-channel rings is calculated numerically within the canonical ensemble, in the presence of spin-orbit interaction. We show that for a single-channel ring, the persistent current is paramagnetic after averaging over all possible directions of spin and different realizations of disorder. For a multi-channel ring, the average magnetic response of the ensemble depends on the coupling between the channels. We find that for an isotropic 2D ring, the persistent current changes its sign from diamagnetic to paramagnetic behavior upon averaging with respect to spin-orbit interaction. For weak coupling between the channels the current remains diamagnetic even upon this averaging.

Photoconductivity self-oscillations under impurity microwave breakdown in GaAs

B. Ashkinadze, E. Cohen and Arza Ron

Solid State Institute
Technion-Israel Institute of Technology
Haifa 32 000, Israel

We observed, for the first time, the selfoscillations of microwave absorption in pure epilayers of GaAs. This absorption is proportional to the ac photoconductivity when the sample is simultaneously excited by weak interband light and microwave (36GHz) radiation. The oscillations in absorption occur at temperature lower than 10K and when the microwave power increases above a certain threshold value. No oscillations are observed without light excitation. When the microwave power is high enough for selfoscillations we observe an abrupt increase of photoconductivity and strong quenching of donor-acceptor pair or donor-bound exciton luminescences.

The underlying physical mechanism is a microwave breakdown of impurities neutralized by light. Selfoscillations can arise if the impact ionization coefficient depends on electron density. The oscillation frequency varies with light intensity in the range of 100-10^4Hz. This is typical behaviour of nonlinear dynamical system.

The investigation of surfaces using the Scanning Tunneling and Atomic Force microscope

Eshel Ben-Jacov and Vladimir Wainstein

School of Physics and Astronomy
Raymond and Beverly Sackler Faculty
of Exact Sciences
Tel Aviv University
69978 Tel Aviv, Israel

We have developed and built an original Scanning Tunneling Microscope (STM) for air and liquid helium environment (CSTM) and also an Atomic Force Microscope (AFM). This devices can be used to study surfaces of materials up to atomic resolution. The STM is based on principle of quantum tunneling of electrons between two separated electrodes under an applied electric field. The feedback control unit maintans a constant current (near 1nA) between the two electrodes: an atomically sharp metal tip, mounted on a piezoelectric driver and the sample under study. We have studed neutron radiation damages on graffite surfaces. Surface distortions of the atomic were observed scale after the collision. This information can be used to for modify of the microstructure of materials. We compared the quality of different samples of HTSC thin films For the STM, was developed process of electrochemical hi-frequency tip etching . We also developed and built an original antivibration platform and cryogenic equipment with low vibration noise for our CSTM. The AFM can measure force (in the range 10^{-6}-10^{-10}N) between a tip and any surface, by means very flexible cateliver and laser deflection system. The feedback control unit maintans constant force imposed on the surface of the sample by sharp tip attached on the end of cateliver. This tool can measure friction, hardness,charge and other surface properties with atomic resolution.

A.C CONDUCTANCE OF AN INTERACTING QUANTUM DOT: SINGLE ELECTRON LEVEL SPECTROSCOPY

R. Berkovits, M. Abraham, and Y. Avishai*

The Jack and Pearl Resnick Institute for Advanced Technology,
Department of Physics, Bar-Ilan University,
Ramat-Gan 52900, Israel

* *Also at Department of Physics, Ben-Gurion University,*
Beer-Sheva, Israel

We calculate the a.c and d.c current through a quantum double barrier heterostructure taking into account Coulomb interactions in the well. The a.c conductance has a periodic dependence on the external field frequency corresponding to the single electron level spacing, and as a function of the leads chemical potential with a period determined by the interaction. These two different periods enable probing of the two characteristic energy scales of the quantum dot structure.

Sum Rule in the Luminescence of Doped Semiconductors

P. Dahan, V. Fleurov

School of Physics and Astronomy
Raymond and Beverly Sackler Faculty
of Exact Sciences
Tel Aviv University
69978 Tel Aviv, Israel

A relation between two zero phonon lines in semiconductors doped by transition metal impurities is discussed. The observation first made in $ZnS : Ni$ and $CdS : Cu$ where two lines complementing each other to the forbidden energy gap, $h\nu_1 + h\nu_2 = E_g$, had been found was called 'Sum Rule'. Since the first line ($h\nu_1 = 0.858$eV for ZnS:Cu) is known to be due to the intracenter transitions between the $^2T_2$ and ^2E states of the Cu atom in the zinc-blend lattice one has to explain the second line $h\nu_2 = 2.965eV$ which cannot be attributed to any known first order dipole transition. It is shown that this line can appear due to a second order process of the recombination of the electron - hole pairs in the presence of a transition (or noble) metal impurity. This process is a peculiar interference of dipole radiation and nonadiabatic radiationless transitions leaving the impurity in an excited state. The fact that the intensity of the complementing line is comparable with those of the usual dipole transitions is due to a specific Fermi-type resonance strongly enhancing the process.

The principal condition for the complementing line is the multielectron structure of the atomic shell playing role in the creation of the deep levels. This is the situation typical of the transition and noble metal impurities. The line becomes strong enough in the case of the strong enough interaction between the impurity electrons and the local vibrations. Such a situation is to be expected due to a rather strong Jahn - Teller interaction which is also typical of the transition metal impurities having degenerate electronic states of their d-shells. All this make us to believe that observation of the lines complementing intraatomic transitions in the impurities to the forbidden energy gap of the host semiconductor must be a typical situation for various semiconductors doped by transition or noble metal impurities.

STUDIES OF NANO-SCALE SCHOTTKY DIODES BY STM

L. A. Gheber, G. Gorodetsky and V. Volterra

Physics Department

Ben-Gurion University of the Negev

Beer-Sheva 84105, ISRAEL

The formation and electrical properties of discrete islands in discontinuous Au films on Si (111) were studied with a home built Scanning Tunneling Microscope (STM). Ohmic electrical contact between the STM tip and isolated gold islands was established and I-V characteristics of the Au - Si junctions were measured. A typical Schottky diode behaviour with ideality factor close to 1 was observed. The STM appears to be an appropriate probe for electrical measurements of nano-scale diodes.

DETERMINISTIC CHAOS IN HETEROSTRUCTURES

I. Khalfin, R. Berkovits, and M. Gitterman

Department of Physics, Bar-Ilan University, Ramat-Gan 52900, Israel

We have found chaotic behavior in a classical system of three particles moving on a one-dimensional ring, where the particles interact via a non-homogeneous Toda or Coloumb interaction. Chaos appears due to the spacial symmetry breaking induced by the non-homogeneous interactions. This system is the classical counterpart of the quantum double barrier hetrostructure, a system for which fingerprints of chaos in its energy spectrum were recently found.

Influence of the Initial Temperature of Melt on the Properties of its Quench State (Amorphous Alloys $Al_{91}La_5Ni_4$, $Al_{91}Ce_5Ni_4$).

V. Manov†, D. Shechtman†, A. Rubstein‡ and A. Voronel‡

† *Department of Materials Engineering*
Technion, 32000 Haifa, Israel
‡ *School of Physics and Astronomy*
Raymond and Beverly Sackler Faculty of Exact Sciences
Tel Aviv University, 69978 Tel Aviv, Israel

New low density amorphous alloy ribbons with high Al concentration have been produced melt spinning in vacuum. The metallic alloys were melted in alumina crucibles prior to their rapid quenching onto a copper drum surface. Contact of the molten alloys with the crucible and with residual gases in the vacuum was prevented by a layer of molten salts.

Ductile rapidly solidified ribbons (the thickness about 20 micrometers) have been prepared with different soaking times of the melt and under different melt temperatures (1273-1473K).

The amorphous structure of all the ribbons has been confirmed by an X-ray diffraction study. The specific electrical resistivity and its dependence on the preparation conditions was studied as a function of temperature over a large temperature range at heating rate of 0.05 K/s. The electrical resistivity of the ribbons varies from 35 to 50 $\mu\Omega \cdot cm$ for both alloy ribbons. The crystallization temperature (565K for $Al_{91}La_5Ni_4$ and 591K for $Al_{91}Ce_5Ni_4$) was surely detected by both differential thermal analysis and resistance measurements.

DOMAIN SWITCHING PHENOMENON IN A FERROELECTRIC WITH FREE SURFACE

G. Rosenman and V.D. Kugel
Department of Electrical Engineering - Physical Electronics, Faculty of Engineering, Tel-Aviv University, Tel-Aviv 69978, Israel

Stable ferroelectric state is characterized by complete screening of spontaneous induction field. Polar axis switching leads to uncompensated charges arising and to generation of two kinds of screening currents: internal screening current I_{in} and external one I_{ex}. Conventional experimental setup envisages a short external circuit with electrodes covering the polar surfaces. In this case $I_{ex} \ll I_{in}$. For free polar surface electron [1] or ion [2] emission occurs. Electron current is generated from negatively charged surface and ion emission may be observed from positively one. Calculations show that electron (ion) currents into vacuum contribute sufficiently to the depolarizing screening and this external emission screening current may be as large as internal bulk one or even much more [3]. For low conductivity ferroelectrics and under fast reorientation of the polar axis the electron (ion) current becomes the principal one. Thus for these conditions electron (ion) charge determines mainly a screening process of a new monodomain state and as a result the switching time.

Experimental studies were implemented by using some ferroelectrics such as $Pb_5Ge_3O_{11}$, $Gd_2(MoO_4)_3$ and TGS. Electron emission currents, charges and switching time were measured.

It was shown that for weakly conductive ferroelectrics $Gd_2(MoO_4)_3$ and TGS the switching time is determined by the emitting charge. The conductivity of $Pb_5Ge_3O_{11}$ crystals is 5 orders of magnitude more than conductivity of $Gd_2(MoO_4)_3$ and TGS. Internal screening current in lead germanate is much more than electron emission one. That is why its switching time is determined by Maxwell relaxation time.

<u>References:</u>

1. G. Rosenman, V. Okhapkin, Yu. Chepelev, and V. Shur, *Sov. Phys.-JETF's Letts.*,**39**, 477 (1984).

2. G. Rosenman, M. Urbach, *J. Appl. Phys.*, **71**, 1952 (1992).

3. H. Gundel, H. Riege, E.J.N. Wilson, J. Handerek, and K. Zioutas, *Nucl. Instrum. Methods*, **A280**, 1 (1989).

Laboratory and Space Plasma Physics

Plasma Jet-Liquid Interaction in Electrothermal Launchers

A. Arensburg and S. Wald

Propulsion Physics Laboratory
Soreq Nuclear Research Center
Yavne 70600, ISRAEL

The penetration of a plasma jet into liquid water was observed at successive time intervals by means of x-ray shadowgraphy. The plasma jet was generated by producing in a polyethylene capillary tube a high current pulsed discharge. The tube inner diameter and length are 0.64 and 22 cm, respectively. A pulse forming network delivered 121 to 182 kJ of electrical energy in 500 μs. The plasma jet emerged from the open end of the tube and interacted with a column of water gel. Jet velocities around $250m/sec$ were measured. The water ablation rate, estimated by calculating the radiative energy flux emitted by the plasma and reaching the water surface, is approximately 0.155 $kg/sec{\cdot}cm^2$. This rate is significantly lower than the measured average flux of mass lost by the water: 3.5 $kg/sec \cdot cm^2$. We propose that the main mechanism of the water loss is in the form of droplets which are ripped from the water surface by the shear force resulting from the plasma-water direct interaction. These droplets are entrained in the back flowing part of the plasma jet, which streams out of the interaction chamber. Peak pressures up to $3.5 \cdot 10^8 Pa$ were measured during the process.

THE KINETICS OF MACROPARTICLES CHARGING IN STRONGLY IONIZED PLASMA

I. Beilis,* R.L. Boxman, and M. Keidar
Department of Interdisciplinary Studies,
Faculty of Engineering

and

S. Goldsmith
School of Physics and Astronomy,
Raymond and Beverly Sackler Faculty of Exact Sciences
Tel Aviv University, Tel Aviv 69978, ISRAEL.

The erosion products of vacuum arc cathodes consist of ions, neutral vapor, and macroparticles. The macroparticles become electrically charged through their interaction with the interelectrode arc plasma. The charged macroparticles move in the arc plasma and affect the flow field of the plasma. Practical applications of the vacuum arc, and modeling of the plasma flow require the understanding of the macroparticle charging processes.
In this work the kinetics of macroparticle charging are studied using the following framework. The electron density is in the range of 10^{16} to $10^{17} m^{-3}$. The macroparticles have a spherical surface, and their radius is in the range of 0.1 μm to 1.0 μm. The ion and electron velocities have a Maxwellian distribution, but with different temperatures. As the electron temperature is assumed to be smaller than 10 eV, the macroparticle radius is much smaller than the Debey radius. Solving the equation for the electric field strength at the macroparticle surface, together with the equation for ion and electron flow, the charging time of the macroparticle and and the electric field near the macroparticles were calculated. The steady state charge of a macroparticle is between 10^{-16} to 10^{-17} C, and the charging time is smaller than 10^{-5} s. The model presented here agrees well with previous experimental studies of macroparticle charging.

*Supported by a grant from the Wolfson Foundation.

A NEW KIND OF ELECTROMAGNETIC COUPLING IN MHD

N. Kleeorin *, I. Rogachevskii ** and A. Ruzmaikin***

* *Department of Mechanical Engineering, Ben-Gurion University of Negev, POB 653, 84105 Beer-Sheva, Israel*

** *The Racah Institute of Physics, The Hebrew University of Jerusalem, 91904 Jerusalem, Israel*

*** *California State University Northridge, 18111 Nordhoff Street, Northridge, CA 91330, USA*

Flows of a conducting fluid between two concentric solid spheres rotating with different angular velocities can generate magnetic field. The Reynolds number of the flow is assumed to be large and the angular velocities of the spheres is only slightly different. The boundaries of the spheres have variable conductivities and the Ekman-Hartmann boundary layers near the spherical surfaces exist.

A new kind of the electromagnetic coupling between the conducting fluid and the solid rotating spheres is found. The coupling is due to a transfer of angular momentum of the basic flow of the conducting fluid to the solid parts of the system by means of the boundary layers. The torque of the coupling is determined by the magnetic field generated outside the boundary layers and neither depend on viscosity nor the differential rotation of the fluid.

The main difference of the new coupling from the classical electromagnetic one is that the torque is not zero even if the boundaries are perfect insulator. It is due to the basic flow of the conducting fluid contributes to the coupling, while the classical electromagnetic torque is determined by the surface effects. The Ekman-Hartmann layers stand duty as a mechanism of the exchange of the angular momentum of the basic flow of the fluid and the solid spheres. The coupling is important for the excitation of the differential rotation in the fluid. The results discussed in this report can be applied to the planetary physics.

THE MODIFIED RENORMALIZATION GROUP METHOD FOR STUDY OF DEVELOPED MHD TURBULENCE

Nathan Kleeorin* and Igor Rogachevskii**

* *Department of Mechanical Engineering, Ben-Gurion University of Negev, POB 653, 84105 Beer-Sheva, Israel*
** *The Racah Institute of Physics, The Hebrew University of Jerusalem, 91904 Jerusalem, Israel*

The modified renormalization group (MRNG) method was developed for the investigation of the MHD turbulence at the large magnetic Reynolds number (Kleeorin and Rogachevskii, 1993). The aim of the MRNG method is a study of the interaction between a regular magnetic field and a background MHD turbulence. The MRNG method comprises a change of real turbulence by a medium with effective turbulent transport coefficients. This procedure allows to derive equations for the turbulent transport coefficients: turbulent viscosity, turbulent magnetic diffusion and turbulent magnetic coefficients. The turbulent magnetic coefficients determine a contribution of the MHD turbulence in the mean magnetic force and describe an inverse energy cascade in developed MHD turbulence.

The MRNG method for this problem requires to find an equation invariant under the renormalization of the turbulent transport coefficients. The recent results (Kleeorin et al., 1990) with a simple model for the high order closure procedure were used for deriving the equation.

By contrast to the renormalization group (RNG) method (McComb, 1990), spectrum and statistical properties of the background turbulence (a medium with zero mean fields) are not studied, but assumed to be given. The background turbulence can be arbitrary. While an external random stirring force with a Gaussian statistics is introduced in the RNG method. A study of the energy spectrum of the hydrodynamic turbulence is the main aim of the RNG method.

It was found that the level of the magnetic fluctuations can exceed that obtained from the equipartition assumption due to the inverse energy cascade in developed MHD turbulence.

References

Kleeorin and Rogachevskii, *Phys. Rev. A*, submit. (1993).

Kleeorin, N., Rogachevskii, I. and Ruzmaikin, A., *Soviet Phys. JETP* **70**, 878 (1990).

McComb, W.D., *The Physics of Fluid Turbulence,* Clarendon, Oxford (1990).

ELECTRON CHAOTIC DYNAMICS IN QUASIPERPENDICULAR SHOCK FRONT

M.Balikhin, M.Gedalin

Department of Physics, Ben-Gurion University

Beer-Sheva, 84105, Israel

Electron dynamics in the stationary electromagnetic field structure typical for a colli sionless qusiperpendicular shock front is investigated. It is shown that the motion is chaoti when the potential electric field gradient is sufficiently steep. Physical implementations fo electron heating in shocks are analyzed. Possibility of ion stochastic dynamics in such structure is discussed.

MHD Waves and Instabilities in Space Plasmas

M. Mond
Ben Gurion University, Beersheva

The variety of plasmas available for observation in space environments provides a wide range of MHD wave phenomena. A survey is given of the various sources of free energy which drive unstable MHD modes. Nonlinear turbulence theory has advanced greatly in recent years and our understanding of the finite amplitude waves to be found in space plasmas has both contributed to and benefited from this advance. Modes of nonlinear stabilization are discussed.

FINE STRUCTURE OF TURBULENCE AT BOW SHOCK

M.Balikhin, M.Gedalin

Department of Physics, Ben-Gurion University

Beer-Sheva, 84105, Israel

Low-frequency turbulence at the terrestrial bow shock is studied in the basis of the experimental data obtained by AMPTE-IRM and AMPTE-UKS satellites. Several methods of separation of spatial and temporal variations are applied to mutlipoint measurements. Some basic characteristics of the turbulence are obtained: wave velocities, wavevectors and frequencies in the plasma rest frame. Conclusions are made about the nature of the turbulence.

On statistical acceleration of particles near Venus

Mordekhay E. Kovner and Aharon Eviatar

Department of Geophysics and Planetary Sciences
Raymond and Beverly Sackler Faculty
of Exact Sciences
Tel Aviv University
69978 Tel Aviv, Israel

Various gasodynamic and kinematic problems of the solar wind interaction with the ionosphere of Venus's on the day-side are investigated. On the assumption that in the transition region between the bow-shock and ionopause there exists an irregular magnetic field of B $\simeq$ 20 nT, we estimate typical plasma parameters such as: mean free path, internal scale of inhomogeneities, viscisities, plasma conductivity and dissipated energy.
A statistical acceleration mechanism in the transition region is investigated. We find that protons are accelerated in time at a rate proportional to $t^{\frac{2}{3}}$ up to an energy of $\sim$ 5 KeV and their distribution function is $n(E) \sim E^{\frac{1}{2}}$ [$n(v) \sim v^2$]. The acceleration of electrons up to relativistic energies is proportional to the acceleration time.

INTERACTIVE MODEL OF THE MAGNETOSPHERE - THERMOSPHERE COUPLING

Moshe Harel

Interdisciplinary Center for Technological Analysis and Forecasting
at Tel Aviv University, Tel Aviv Israel

The interactive Magnetosphere - Thermosphere model couples the Rice Convection Model of the inner magnetosphere with a thermospheric model that includes the effects of EUV- and convection-driven neutral winds under quasi-equilibrium conditions. We review results of work that was performed at the Jet Propulsion Laboratory in the past few years in collaboration with J. Forbes.

The Rice Convection Model (RCM) is reviewed in detail. The model was developed at Rice University and is presently the most sophisticated and complete model of its type. Thus, we are able to bring standard theoretical ideas about physical parameters such as plasma motion, electric fields, and current distributions, into more precise and meaningful confrontation with observations. For each event we model, some data are used to specify model inputs, while a variety of other data are used for comparisons with model predictions. Addition of neutral wind enhances the model capabilities especially in the mid- and low-ionospheric altitudes. It is found that the coupling between the neutral winds and plasma motion may be responsible for the observed low- and mid-latitude electric fields during and following storms.

The method of investigation involves combining the Rice Convection Model with a simple model for the neutral winds with convection and solar EUV- driven winds. It is shown that the parameters determining the coupling are the Pedersen and Hall "effective winds", which are the height integrals of the respective conductivity-weighted wind profiles divided by the respective layer conductivities. A unique aspect of the study is that the convection-driven winds are included self-consistently and interactively.

Substorm simulations results are reviewed. During the early phases of the disturbance, when the normal shielding from high latitudes breaks down, the neutral winds do not modify appreciably the disturbance electric field at middle and low latitudes. As the system approaches a quasi-equilibrium state, the neutral wind plays a much more significant role.

Modeling The Europa Plasma Torus

Ron Schreier and Aharon Eviatar
Department of Geophysics and Planetary Sciences
Raymond and Beverly Sackler Faculty
of Exact Sciences
Tel Aviv University
69978 Tel Aviv, Israel

Vytenis M. Vasyliunas
Max Planck Institut für Aeronomie
Lindau, Germany

John D. Richardson
Center for Space Research
Massachusetts Institute of Technology
Cambridge, MA 02139, USA

The existence of a torus of plasma generated by sputtering from Jupiter's satellite Europa has long been suspected but never yet convincingly demonstrated. Temperature profiles from Voyager plasma observations indicate the presence of hot, possibly freshly picked-up ions in the general vicinity of the orbit of Europa, which may be interpreted as evidence for a local plasma torus. Studies of ion partitioning in the outer regions of the Io torus have led to the result that the oxygen and the sulfur mixing ratios vary differently with radial distance, which has been taken as indicating injection of oxygen-rich matter from a non-Io source, most probably Europa. We have constructed a quantitative model of a plasma torus around the orbit of Europa, taking into account plasma input from the Io torus, sputtering from the surface of Europa, a great number of ionization and charge-exchange processes, and plasma loss by diffusive transport. When the transport time is chosen so as to predict correctly the observed total plasma density, the contribution from Europa is found to be significant although not dominant. The model predicts in detail the ion composition, charge states, and the relative fractions of hot Europa-generated and (presumed) cold Io-generated ions. The predictions are generally consistent with observations from Voyager and can in principle (subject to limitations of data coverage) be confirmed in more detail by Ulysses.

CORONAL MASS EJECTIONS: AN ATTEMPT OF A UNIFIED CLASSIFICATION

M. Filippov and E. Golbraikh
Physics Department
Ben-Gurion University of the Negev
84105, Beer-Sheva, Israel

We study characteristics of the CMEs assuming that the different forms of Coronal Mass Ejections (CMEs) are just different projections of a single 3-D object on the sky plane. Specific "X-ray delay", i.e. time detecting an X-ray precursor and a CME first appearance in the coronograph field of view , is considered as a very important characteristics of CME structure. That delay is defined by projection of CME velocity on the plane of the sky plane,according to experimental data. Such a velocity differs for the different classes of mass ejections. In terms of our model, this difference is connected with acceleration of the 3-D object. The average acceleration predicted by our model (0.3 km/s) is in agreement with experimental data. It is shown that the key structures of the CME, such as Loops, Curved front and Halo we unify within the scope of the model.

CONSISTENT TREATMENT OF CRITICAL PLASMA FLOWS IN HIGH PRESSURE DISCHARGE ABLATIVE CAPILLARIES

Sami Cuperman and David Zoler
Raymond and Beverly Sackler Faculty of Exact Sciences
School of Physics and Astronomy, Tel Aviv University
Tel Aviv, 69978, ISRAEL
and
Jossi Ashkenazy, Marc Caner and Zvy Kaplan
Soreq Nuclear Research Center, Yavne 70600, ISRAEL

A self-consistent solution of generalized, quasi-one dimensional non-ideal fluid equations describing the steady state critical plasma flows in high pressure capillary discharges is presented. All three equations used (continuity, momentum and energy) include ablative effects. No limitation to the case of ideal equation of state or to the spatial uniformity of the ionization degree is imposed. A numerical algorithm enabling the determination of self-consistent boundary conditions required for the integration of the differential equations is used. Illustrative results for typical physical parameters, namely, electrical current and radius and length of the capillary are presented for polyethylene capillaries. The effects of changes in the geometrical characteristics of the capillary as well as in the electrical and radiative characteristics of the discharge on the plasma parameters are also considered.

EXACT SOLUTION OF THE DISPERSION EQUATION FOR ELECTROMAGNETIC WAVES IN SHEARED, RELATIVISTIC, ELECTRON BEAMS

by

S. CUPERMAN[1,2] and D. HERISTCHI[1]

[1]URA 326, DASOP, Observatoire de Paris, Section de Meudon, 92190, Meudon, France

[2]School of Physics and Astronomy, Raymond and Beverly Sackler Faculty of Exact Sciences Tel Aviv University, Ramat Aviv 69978, Israel.

The transcendental dispersion equation for electromagnetic waves propagating in the slow mode in sheared, non-neutral, relativistic, cylindrical electron beams in strong applied magnetic fields is solved exactly. Thus, rather than using truncated power series for the modified Bessel functions involved, use is made of modern algorithms able to compute such functions up to 18 digits accuracy. Consequently, new and significantly more important branches of the velocity shear instability are found. When the shear-factor or/and geometrical parameter a/b (pipe to beam radii ratio) are increased, the unstable branches join, and the higher-frequency - larger wave number modes are significantly enhanced. Since analytical solutions of the exact dispersion relation cannot be obtained, it is suggested that in all similar cases, the methods proposed and demonstrated here should be used to carry out a rigorous stability analysis.

A THREE DIMENSIONAL MAGNETOHYDRODYNAMIC FORMALISM FOR CORONAL HELMET STREAMERS

by

S. CUPERMAN,[1,2] C. BRUMA,[1] T. DETMAN[2] and M. DRYER[2]

[1]Raymond and Beverly Sackler, Faculty of Exact Sciences.
School of Physics and Astronomy, Tel Aviv University, Ramat Aviv,
Tel Aviv 69978, Israel.

[2]Space Environment Laboratory, ERL, NOAA, Boulder, CO 80303

A three dimensional MHD formulation of the steady state coronal helmet-streamer problem is presented. It includes the simpler azimuthally symmetric ($\partial/\partial\phi = 0$) and two dimensional ($\partial/\partial\phi = 0$, $B_\phi = 0$) cases.

The major mathematical difficulty - the correct, iterative calculation of the transverse electrical currents, which are the sources of the fields in Maxwell's equations - is eliminated. This is achieved by the elaboration of an agorithm connecting four different coordinate spaces: (i) spherical, (r,ϕ,ϑ), in which the problem is defined and boundary conditions established; (ii) computationally convenient, (ν,μ,ξ), in which the entire space is represented by a rectangular box of sizes (1,2,1) ($\nu = r_0/r$, $\mu = \cos\vartheta$, $\xi = \phi/2\pi$), therefore allowing also the imposition of boundary conditions at infinity, $\nu = 0$ (e.g., vanishing of the magnetic field components, etc.); (iii) local Frenet's, (ℓ,c,n), defined by the orthogonal unit vectors $\underline{e}_\ell = \underline{B}/B$, $\underline{e}_c = R(\partial \underline{e}_\ell/\partial\ell)$ and $\underline{e}_n = \underline{e}_\ell \times \underline{e}_c$ (tangent to the field line, pointing toward the center of curvature of the field line and normal to the osculatory plane of the field, respectively; R is the curvature radius), required for the integration of the conductive, MHD equations along magnetic field lines; and (iv) cartesian, (x,y,z), in which Frenet's unit vectors as well as the derivatives along their directions are defined.

92

THE VELOCITY AND DISTRIBUTION OF VACUUM ARC CATHODE SPOTS LOCATED IN AN EXTERNAL MAGNETIC FIELD

A.A. Ishaaya and S. Goldsmith
School of Physics and Astronomy,
Raymond and Beverly Sackler Faculty of Exact Sciences
and
R.L. Boxman
Faculty of Engineering, Department of Interdisciplinary Studies

Tel Aviv University, Tel Aviv 69978, ISRAEL.

The motion and distribution of cathode spots were investigated on the surface of a 91 mm diameter cylindrical vacuum arc Cu, Ti, Sn and Si cathodes. The motion and distribution of the cathode spots on the electrode surface were affected by the magnetic field produced by a small solenoid (30 mm o.d.) mounted behind and close to the cathode surface. The solenoid produced a magnetic field $\vec{B}$, which had both axial and radial components on the cathode front. The axial component B_z of $\vec{B}$ changed direction at a radial distance of about 36 mm. Arcs with currents ranging from 30 to 480 A and voltages of 20- 30 V were ignited with an auxiliary electrode. An observation window and video camera were mounted on the axis facing the cathode. The video signal was recorded with a conventional video recorder and analyzed in the single frame mode to determine the location of the cathode spots for each frame. With arc current of up to 170 A, usually a single cathode spot was observed. With no applied magnetic field, the motion of the spots was random, and a velocity of about 20 cm/s was observed on the Cu electrode. When the magnetic field is applied the cathode spot motion becomes ordered and circular. The tangential spot velocity increases monotonically with the magnetic field. At magnetic field of 15 Gauss the rotational velocity of the spots on Cu cathode was 70 cm/s. Spot velocity on Ti cathodes exceeded markedly that of Cu, and being larger than 1500 cm/s could not be determined by our diagnostic method. When the magnetic field is applied, the cathode spots were narrowly distributed about an inner radial distance of 20 mm. The radial distance of the distribution peak moved to larger radial distances with increasing magnetic fields. At higher arc currents (320 - 480 A) multiple cathode spots were observed. Each cathode spot moved independently along its radial track, but at about the same radial distance.

GUIDING OF PLASMA BEAMS IN A TOROIDAL MAGNETIC FIELD

E. Gidalevich* and S. Goldsmith
School of Physics and Astronomy,
Raymond and Beverly Sackler Faculty of Exact Sciences
and
R.L. Boxman
Faculty of Engineering, Department of Interdisciplinary Studies

Tel Aviv University, Tel Aviv 69978, ISRAEL.

We consider here the transition of plasma beams through a magnetic field in a quarter torous collimator, assuming the diffusive fluid approximation. The system is described by a set of toroidal coordinates, and the magnetic field is assumed to be uniform at the entrance plane of the torous. Such system is used in our laboratory to filter out macroparticles from the plasma beam. The equations of motion and continuity for the three component isothermal plasma (ions, electrons, and neutrals) are solved numerically under the simplified assumption of complete plasma neutralization at the wall of the torous. The centrifugal force which is perpendicular to the magnetic field produces an electric polarization in the plasma, resulting with a $\vec{E} \times \vec{B}$ drift across the magnetic field. Plasma loss in the collimator is calculated for magnetic fields in the range of 200 to 600 Gauss, and initial electron density in the range of 10^{11} to 10^{13} cm^{-3}. We obtain that the plasma distribution at the exit plane of the torous is asymmetric, with the maximum of the plasma density shifted in the positive direction of torous major radius. The asymmetry is due to the plasma drift across the magnetic field. In our case, the asymmetry and plasma loss are maximum for a magnetic field of 200 Gauss and ion density of 10^{13} cm^{-3}.

*Supported by a grant from the Wolfson Foundation.

Vacuum Arc Deposition of Conductive Transparent Sn-0 Films, and the Influence of Post-Deposition Annealing on their Phase Composition, Structure, Resistance and Transparency.

A. Ben-Shalom, L. Kaplan, R.L. Boxman, S. Goldsmith, M. Nathan
Tel-Aviv University, Ramat-Aviv.

The deposition of transparent and conductive tin oxide (TO) 0.1-5μm films was carried out by using a filtered vacuum arc deposition (VAD) technique. The deposition apparatus included a vacuum arc plasma gun with a tin cathode and annular anode operated in an oxygen atmosphere. A 150-160A d.c. arc discharge was ignited with the aid of a mechanical trigger electrode and sustained between the tin cathode and anode. A highly energetic plasma jet ejected from the cathode passed through the anode into a quarter-torus magnetic filter that separated the tin macroparticles from the jet. Tin plasma jet combined with the background O_2 and produced TO films at the exit of the filter. The films were deposited on different substrates: glass, quartz, salt, GaAs, metal without heating and with the substrates heated to 150°C. The VAD parameters which produce optimal conductivity and transparency are as follows: oxygen pressure before VAD 0.5 Torr, pressure during arc $5 \cdot 10^{-3}$Torr. The best samples have a transmittance of about 90% at a thickness of 0.5μm and a resistivity of ~0.003 Ohm·cm.

The films were analyzed by X-ray diffraction, transmission and scanning electron microscopy (TEM, SEM), and resistivity and transparency measurements. The changes in the films under thermal treatment in vacuum, Ar, forming gas ($10\%H_2$ -$90\%N_2$) and air under slow and rapid annealing were also examined. According to X-ray and TEM diffraction data, as- deposited films on non-heated and 150°C heated substrates consist of an amorphous phase. Crystallization of the amorphous phase to tetragonal SnO_2 occurrs at 450°C. A rapid thermal annealing (RTA) in forming gas $10\%H_2$ -$90\%N_2$ at 500-700°C leads to reduction of the SnO_2 by hydrogen from the forming gas to form SnO and Sn. After an Ar RTA at 800-950°C we find tetragonal SnO_2 and also a SnO_2 orthorombic phase, which exists usually at high pressure.

Ar RTA at the crystallization temperature 450°C changes the resistivity and transparency. In addition, heat treatment of films deposited on a non-heated substrates decreases their stress, thus increasing their stability. The stress in the films is decreased by heating the substrate during VAD even to 150-200°C, where the film structure is still amorphous.

Fast Magnetic Field Penetration Into a Cylindrical Plasma of a Nonuniform Density Due to the Hall Field

K. Gomberoff and A. Fruchtman
Department of Physics
Weizmann Institute of Science
Rehovot 76100, Israel

Abstract

Fast magnetic field penetration into a cylindrical plasma has been the subject of many recent studies. This process is of special importance for the Plasma Opening switch (POS). For a plasma with uniform density that conducts current between two cylindrical electrodes, the penetration of the magnetic field at the bulk of the plasma is as a shock wave that propagates axially with a speed determined by the Hall field. The shock structure is defined by the low collisional resistivity. When the density is uniform the penetration occurs only when the anode is the external electrode. In this work the penetration of the magnetic field into a cylindrical plasma with density that varies both radially and axially is studied. The fast magnetic field penetration due to the Hall field is along constant nr^2 lines (n is the plasma density and r is the radial coordinate). It is shown that there is magnetic field penetration for both positive and negative polarity cases as long as there is penetration along the electrodes. The magnetic field evolution is found, analytically and numerically, for different time behaviors of the magnetic field at the boundaries.

Analysis of highly ionized gold spectra emitted from laser produced plasmas at varying Au/Be concentration ratios.

E. Behar, P. Mandelbaum and J.L. Schwob
Racah Institute of Physics, The Hebrew University
J.F. Seely, Naval Research Laboratory, Washington, D.C., USA
and D. Kania, Lawrence Livermore National Laboratory, USA

In a set of experiments held at the Nova facility at Lawrence Livermore National Laboratory, mixed Au-Be planar targets were irradiated with a 1ns, $5x10^{14}W/cm^2$ laser pulse at a wavelength of 0.35 μm. The emitted X-ray spectra were recorded for different Au/Be target concentration ratios (1.,.05,.01,.002) in the 3-6.5Å wavelength range using a set of flat crystal spectrometers. The spectra were analysed using previously published data[1] and *ab-initio* calculations with the RELAC atomic structure code[2]. Lines and Unresolved Transition arrays (UTA) of ions from Au^{46+} (AsI-like) to Au^{54+} (MnI-like) were identified.

Using intensity calibrated densitometer recording of time and space integrated spectra, the electron density sensitive line intensity ratio of the forbidden quadrupole ($3p^63d^{10}\ J=0 - 3p^5{}_{3/2}3d^{10}4f_{7/2}\ J=2$) to the electron dipole line ($3p^63d^{10}\ J=0 - 3p^5{}_{3/2}3d^{10}4d_{5/2}\ J=1$) of the NiI-like ion was deduced for each Au/Be concentration ratio. The experimental line intensity ratios were compared to the results of a collisional radiative model using the HULLAC package code for collisional excitation cross sections[3]. The deduced experimental electron density was found to *decrease* while the Au/Be ratio *increased*. This trend was confirmed by comparing theoretical and experimental intensity ratios of other strong NiI-like lines.

Comparing lines or UTA of 3d-5f transitions belonging to various ionization states for different target Au/Be concentration ratios, a clear shift towards *higher* ionization states was observed while the Au/Be concentration *increased*, indicating higher electron temperature.

Except for strong transitions from pure Au targets, it was shown theoretically that opacity effect could be neglected.

The observed trends are discussed and further spectroscopic diagnostics are proposed to improve the understanding of the atomic processes and dynamic of the mixed Au/Be plasma.

1. N. Tragin *et al.*,Phys. Scripta **37**,72(1988).
2. M. Klapisch *et al.*,J. Opt. Soc. Am. **17**,148(1977).
3. A. Bar-Shalom *et al.*,Phys. Rev. **A38**,1773(1988).

Calculation of Inner-Shell 3d-4l Excitation-Autoionization Effect on Ion Abundance Balance in Hot Coronal Plasmas

D. Mitnik, P. Mandelbaum, J.L. Schwob,

Racah Institute of Physics, The Hebrew University, (91904) Jerusalem,

A. Bar-Shalom and J. Oreg

Nuclear Research Center of the Negev, P.O Box 9001, Beer Sheva

Excitation of inner-shell electrons into highly excited autoionizing levels followed by autoionization (EA) can significantly enhance the total ionization rate. For ions isoelectronic to elements of the 4th row, our results show that the enhancements are much more important than those previously calculated for preceding sequences.

A large contribution of EA to the total ionization rates, is expected in these sequences through 3d-4l inner-shell excitations, due to the ten 3d M-shell electrons candidates to excitation, compared with the few outer electrons undergoing direct ionization[1,2]. Indeed, in contradistinction with the isoelectronic sequences of the three first rows, the lowest configurations populated by inner-shell excitation lie not well much above the first ionization limit, and are crossing down this limit while Z increases along the sequence. Because of the comparable inner-shell excitation and ionization energies, the rates for excitation become relatively important.

Detailed distorted-wave calculation of excitation rate coefficients were performed. Energy levels, radiative and autoionization coefficients were calculated using the HULLAC code based on the Relativistic Parametric Potential Method. These calculations have been done for all the relevant ions belonging to the CuI, ZnI, GaI and KrI isoelectronic sequences. For other sequences, calculations were made for a few elements.

A very rapid approximate but quite accurate procedure is presented, for the computation of the total 3d-4l inner-shell excitation rate coefficients, using analytical expressions. Also, a mean Branching Ratio toward autoionization has been introduced, allowing fast calculation of EA rates. Finally, results have been obtained for the sequences KrI to CuI for all the elements with $Z > 40$.

The EA rate coefficients were introduced in the coronal ionization rate equations. Results for Mo (Z=42), Xe (Z=54), Pr (Z=59) and Dy (Z=66) obtained with and without taking into account EA processes are compared.

A general consequence of the introduction of EA processes, is the drastic shift of the maximum fractional ion abundance for some ions toward low electronic temperatures (up to 40%). Moreover, the Z dependence of the effect, due to the crossing down of inner-shell excited levels below the ionization limit as Z increases, results in striking variations in fractional ion abundance maxima values and positions as a function of Te, for different elements.

1. P.Mandelbaum, et.al., Phys. Rev. A42 4412 (1990).
2. J. Oreg, et. al., Phys. Rev. A44, 3, 1741 (1991).

Computational Physics

Determination of semiconductor structures with simulated annealing.

Amihai Silverman*†, Joan Adler*, R. Kalish* and A. Zunger†

**Department of Physics, Technion, Haifa, 32000, Israel.*
†NERL, Golden, Colorado, USA.

In this talk we will introduce a new approach to the problem of finding the global minimum configuration of a cluster of particles interacting via two and three-body interatomic potentials. This approach is based on a combination of simulated annealing with interactive visualization in a workstation environment during the calculations. The interactive visualization is very helpful for determining optimal scheduling of temperature changes and of block moves.

We have applied this approach to the determination of the structure of superlattice layers and ternary compounds of semiconductor alloys. For Si-Ge phase diagrams our methods give the same results as, but are considerably faster than, the usual molecular dynamics methods based on the same two and three-body effective interatomic potentials. We intend to obtain results for InGaAs and InGaP systems which will be the first of their kind and will enable direct comparison with experimental measurements.

In order to study the behavior of our version of simulated annealing optimization, we first applied it to the 'test model' of 100 particles in two dimensions, interacting via a two body 6-12 Lennard-Jones interatomic potential. A demonstration of the visualization for this case will be given.

Acknowledgement This project is supported in part by the US-Israel Binational Science Foundation (BSF contract No 88-00295)and by the German Israel Foundation.

Non-equilibirum Morphology Transitions during Diffusive Growth

Ofer Shochet, Raz Kupferman and Eshel Ben-Jacob

School of Physics and Astronomy
Raymond and Beverly Sackler Faculty
of Exact Sciences
Tel Aviv University
69978 Tel Aviv, Israel

We present a diffusion-transition scheme to study the penetration of a stable phase into a meta-stable one in systems described by a conserved order parameter. This approach is inspired by the specific example of solidification from supersaturated solution, for which we can take advantage of new experimental observation on surface kinetics. The time dependence in the metastable phase (the concentration of solute) is evaluated by solving the continuous linear diffusion equation. The motion of the interface is described by the statistical mechanics of discrete phase transitions (solidification and melting) at the interface. Both processes are simulated alternatly each for a time period which is smaller than the characteristic time of both processes. First we will present the approach and a study of solid-liquid equilibrium. The average shapes are compared with the those evaluated by the Wulff construction. We calculate the fluctuations of the interface about the average shape as well as the temporal fluctuations in the diffusion field. Based on this, we propose a new strategy for experimental study of the kinetics of the phase transition. We describe and analyze four different morphologies observed during non-equilibrium growth with focus on the dense branching morphology (tip-splitting) and dendritic growth. We find that both morphologies have a well defined envelope that propagates at constant velocity. The envelopes shows 4-fold anisotropy, convex for dense branching morphology (DBM) and concave for dendrites. For both morphologies the asymptotic dimension is d=2. The transitions between the morphologies are studied as a function of the microscopic parameters (energy bonds) and the macroscopic driving force (the supersaturation). We compare the average velocity of growth and the growth of entropy production as response functions to characterize the morphology transitions. We show tha the transitions point found by change in the slope of the responce function (as function of the system control parameters) coincide with the transition between convex and concave envelopes. We shall also present preliminary results of mapping of the system and the morphology transition into a percolation problem. We further show coexistence of morphology for specific values of the control parameters.

Examination of Semiclassical Approximations for Chaotic Systems

M. Sieber

The Weizmann Institute of Science
Department of Nuclear Physics
Rehovot 76100, Israel

Semiclassical methods have been very helpful for a deeper understanding of the characteristic properties of quantum systems, whose classical counterpart is chaotic. However, the application of semiclassical theories for chaotic systems in general requires a large numerical effort. One example is the periodic-orbit theory of Gutzwiller, which is the basis for most semiclassical methods for the determination of quantum mechanical energies of chaotic systems. This theory supplies approximations to the energies by a sum over all periodic orbits of the classical system. A major difficulty which is connected to the periodic-orbit theory is due to the fact, that in a chaotic system the number of periodic orbits increases exponentially with the period of the orbits.

In this talk, the determination of periodic orbits and quantum mechanical energies is discussed on the example of a chaotic billiard system, the hyperbola billiard. Using these data, the properties of semiclassical theories are examined.

Visual study of Atyiah-Singer Zero-modes role in PTMG convergence

Sorin Solomon

Racah Institute of Physics, Hebrew University, 91904 Jerusalem, Israel

We present a visual study of the convergence of the Parallel Transported Multigrid (PTMG) in the presence of Atyiah-Singer lattice approximate zero modes (AZM). In particular, we explain the differences in the behavior of various PTMG variants and the divergence of the standard PTMG algorithm in the Dirac equation at nonphysically small masses m. To check our understanding we predict and verify at $m = 0$ a quite dramatic dependence of the convergence on the instanton size modulo 4.

Simulations of Vertex Models without Critical Slowing Down

Hans Gerd Evertz[1], Gideon Lana[2] and Michael Marcu[2]

[1] *Supercomputer Computations Research Institute*
Florida State University
Tallahassee, FL 32306, USA
[2] *School of Physics and Astronomy*
Raymond and Beverly Sackler
Faculty of Exact Sciences
Tel Aviv University, 69978 Tel Aviv, Israel

We present a new type of cluster algorithm that strongly reduces critical slowing down in simulations of vertex models. Since the clusters are closed paths of bonds, we call it the *loop algorithm*. The basic steps in constructing a cluster are the break-up and the freezing of vertices. We first concentrate on the case of the F model, which is a subset of the 6-vertex model exhibiting a Kosterlitz-Thouless transition. Then we use the framework of Kandel and Domany to generalize the algorithm to the full arrow flip symmetric 6 vertex model. Finally, we briefly discuss the application of our algorithm to simulations of quantum spin systems. In particular, all necessary information is provided for the simulation of spin one half Heisenberg and xxz models.

Simulations of Quantum Spin Systems

Michael Marcu

School of Physics and Astronomy
Raymond and Beverly Sackler
Faculty of Exact Sciences
Tel Aviv University, 69978 Tel Aviv, Israel

Following Suzuki, quantum spin systems may be simulated by using a path integral representation based on the Trotter formula. The technicalities of this approach are discussed in detail. Examples of high precision simulations are presented for spin S models in one dimension, with S ranging from one half to two, and for spin one half models in two dimensions. The one-dimensional results confirm the Haldane conjecture on the mass gap of Heisenberg antiferromagnets, while in two dimensions the existence of a low temperature phase with power-law correlations is exhibited in the easy-plane situation.

A Monte Carlo study of the random-bond Ashkin-Teller model

S. Wiseman and E. Domany

Department of Electronics
Weizmann Institute of Science
Rehovot 76100, Israel

The Ashkin-Teller model is an Ising type model possessing a line of continuously varying critical exponents (in d=2). Whether such critical behaviour will continue to exist when randomness is introduced into the model, is an interesting question which we try to address by a Monte Carlo (MC) study. First, a cluster algorithm, based on the idea of embedding an Ising model into the AT model, was devised for the latter. The dynamical behaviour, or efficiency of the algorithm was tested. Critical slowing down was found to be reduced to an extent that saturates the lower bound set by the model's static exponents (as is the case for Potts models). Secondly, duality was used to locate critical manifolds of the random-bond Ashkin-Teller model and of the anisotropic Ashkin-Teller model. Finally, MC simulations of lattices of linear size of up to $L = 128$, were performed at a few points on the critical manifolds of the two models. Finite size scaling was used to analyze the results. The critical behaviour of the two models is compared. The results indicate that a continuous variation of exponents still exists in the anisotropic model, while the results for the critical exponents of the random models are inconclusive. For the random models, the critical behaviour shows crossover, as a function of lattice size, from the anisotropic critical behaviour to some new random critical behaviour. The variation in the crossover length, and in the rate of crossover is attributed to the variation of the crossover exponent $\frac{\alpha}{\nu}$.

Statistical Physics

Some Physical Approaches to Protein Folding

Henri Orland

Service de Physique Théorique, CE-Saclay
F-91191 Gif-sur-Yvette Cedex
France
and
Groupe de Physique Statistique
Université de Cergy Pontoise
95806 Cergy Pontoise Cedex
France

Proteins are weakly branched polymers built out of 20 species of monomers (aminoacids). They undergo a phase transition from a high temperature coil phase to a low temperature compact native state. This folded state has a unique structure, closely related to the biological activity of the protein. We present simple statistical mechanics models for the folding transition. These models are inspired from spin-glass theory, and display several aspects characteristic of the folding transition, such as the unicity of the folded state, large number of metastable states, high barriers, etc... In addition, in the folded state, short range structure (known as secondary structure) settles in. We propose simple models, based on Hamiltonian walks, for the formation and stability of secondary structures.

Spiral Dynamics in Excitable Media

David A. Kessler

Dept. of Physics
Bar-Ilan University
52900 Ramat Gan, Israel

Spiral patterns are found in many physical, chemical, and biological systems. Many of these systems may be characterized as an excitable medium, i.e. one which is stable to small perturbations but which can be excited to a second long-lived state if sufficiently perturbed. We discuss a model of an excitable medium, and demonstrate the existance of steadily rotating spiral solutions. We also analyze the stability of these spirals.

An Instability in the Propagation of Fast Cracks

J. Fineberg

Racah Institute
The Hebrew University of Jerusalem
Givat Ram, Jerusalem, Israel

We report on experimental investigations of the propagation of fast cracks in brittle materials. Velocity measurements with resolution an order of magnitude better than previous experiments reveal the existence of a critical velocity at which the velocity of the crack tip begins to oscillate, the dynamics of the crack abruptly change, and a periodic pattern is formed on the fracture surface. Beyond the critical point the amplitude of the oscillations depends linearly on the mean velocity of the crack. The existence of this instability may explain the failure of theoretical predictions of crack dynamics and provides a mechanism for the enhanced dissipation observed experimentally in the fracture of brittle materials.

Application of Pulse Photothermal Surface Deformation Method for Studing the Pase Boundary Movement in a First-Order Transition.

S.V.Vintzentz [†], V.Sandomirsky[‡], A.Voronel[§]

[†] *Instutute of Radio and Electronics of Russian Academy of Sciences, 141120 Fryazino, Sq.acad.Vvdenskogo, 1, Russia*

[‡] *The Research Institute of College of Judea and Samaria, 44804, Ariel, Israel*

[§] *School of Physics and Astronomy Raymond and Beverly Sackler Faculty of Exact Sciences Tel Aviv University 69978 Tel Aviv, Israel*

The photothermal surface deformation method (PSDM) , a well-known photoacoustic technique, is extended and used for characterization of the first-order phase transformation (PTr) for the first time. The advantages of PSDM are demonstrated experimentally for the "model" system, VO_2 - film undergoing the metal-semiconductor PTr. It is found that near the PTr-temperature the PSDM pulse in the VO_2 - film has a sign opposite to that of the thermoelastic response. Analysis shows that in the PSDM kinetics one can "separate" a law for the metal-semiconductor interface movement. PSDM may be used for the non-destructive test of a laser surface treatment too.

The theory of motion of spiral waves in oscillatory media

I. Aranson

The Hebrew University of Jerusalem, Israel

L. Kramer and A. Weber

Universität Bayreuth, Germany

We present a new method for the calculation of the interaction between spiral wave and external perturbations (local inhomogeneity of the media or other spiral waves) in oscillatory media. This method is based on the evaluation of the perturbations of an isolated spiral. For the complex Ginzburg-Landau equation the existence of bound states is identified with the parameter range where the perturbations behave in an oscillatory manner. The results for the equilibrium distance for two spirals in the bound state and also the dependence of the velocity of the spiral versus the distance are in good agreement with numerical simulations. In the equally-charged case we find multiple bound states which may be interpreted as multiple-armed spirals. Outside the oscillatory range well-separated spirals appear to repel each other regardless of topological charge.

The stability of symmetric two spiral states in respect of spontaneous symmetry breaking is investigated. The existence and the stability of symmetric and asymmetric lattices of spiral waves is discussed.

The interaction of the spiral wave with the local axisymmetric inhomogeneity is investigated. It is shown that in the oscillatory range the stable rotation of the spiral around the inhomogeneity is possible. The radius of the equilibrium orbit is estimated analytically.

Surface Melting of Ice Induced by Hydrocarbon Films

R. Bar-Ziv* and S.A. Safran

Department of Materials and Interfaces
Weizmann Institute of Science
Rehovot, Israel 76100

We apply the continuum theory of van der Waals interactions to a system composed of a thin hydrocarbon film below vapor and above a water layer which is in equilibrium with bulk ice, at the triple point. We find that for *thin* hydrocarbon films, these interactions result in a finite film of water at the ice surface with a thickness which increases with the hydrocarbon film thickness, d, reaching a value of about $1000\mathring{A}$ for $d \approx 300\mathring{A}$. This corresponds to incomplete surface melting of ice but with a relatively thick wetting layer. However, for larger d, we predict a discontinuous wetting transition as the water film thickness jumps to infinity, indicating complete surface melting of ice.

*Present address: Department of Nuclear Physics, Weizmann Institute of Science, Rehovot 76100, Israel.

Transitions in MC Simulations of Polyelectrolytes

Chava Brender
Department of Physics
Bar-Ilan University
Ramat Gan 52900, Israel

From the MC simulations of the modified LBW lattice model for polyelectrolytes at various physical conditions, we studied the polyelectrolyte chain behavior. New thermal and screening effects were found and described [1-4]. The chain unfolding under cooling was found to be a new critical phenomenon [2-4]. The mechanism of the unfolding process was studied using new parameters: the contacts, and presented in a matrix format [2]. New rules for the unfolding process were proposed, and a new view of contacts as a type of physical statistical bond was presented [2]. A new parameter, the mean straight length, $< \ell, >$, was defined and shown to represent the persistence length of the cubic lattice polymer [3].

The new family of physical statistical bonds was found to include not only contacts but also kinks, which were found to be more important than the contacts due to their large numbers [4]. Critical value of λ for the coil to rod transition was found via percolation concepts. Size effects were found in polyeletrolyte chains through the kink fraction, a new parameter which is connected to the previous parameters [4].

These are part of the results that have broadened our understanding of the charged macromolecules, and they will be described.

[1] C. Brender *J. Chem. Phys.* 92, 4468, (1990)

[2] C. Brender *J. Chem. Phys.* 94, 3213, (1991)

[3] C. Brender *J. Phys. Chem.* 96, 5553, (1992)

[4] C. Brender & M. Danino *J. Chem. Phys.* 97, 2119 (1992)

Membrane Deformation and Induced Interactions

N.Dan, P.A. Pincus* and S.A. Safran
Department of Materials and Interfaces
Weizmann Institute
Rehovot, Israel

We investigate short range interactions between rigid bodies embedded in a thin fluid membrane. The membrane deforms in the vicinity of these objects, thereby increasing the system energy. As a result, the force between the rigid bodies is always attractive. However, we find that there is a metastable state where the objects may adopt a crystalline order.

*Department of Materials, University of California, Santa Barbara, CA 93106, USA.

Anomalous Fluctuations of Random Walks in Random Systems

E. Eisenberg and S. Havlin

Department of Physics
Bar-Ilan University
Ramat Gan 52900, Israel

We study the fluctuations of the probability density [1] $P(r,t)$ of random walks on regular lattices with random distribution of transition rates, w_{ij} between sites i and j. We find that for both quenched and annealed disorder in any dimension, one can relate all the moments of the distribution to its first moment by $< P^q(r,t) >= < P(r\sqrt{q},t) >$. Thus, from the form of the average probability density, one can conclude the cases where the behavior is multifractal corresponding to a broad distribution of $N(\log P)$, in which a single exponent cannot describe the moments of $P(r,t)$.

For exponential distribution of waiting times, $t_{ij} = w_{ij}^{-1}$, it is known that $< P(r,t) > \sim e^{-ar^2/t}$ and therefore $< P^q(r,t) > \sim < P(r,t) >^q$ and there would be no multifractality. For systems with anomalous diffusion in which $< P(r,t,) > \sim \exp[-(r/t^{1/d_w})]^\delta$ with $\delta = d_w/(d_w - 1)$ one gets multifractal behavior, $< P^q(r,t) > \sim < P(r,t) >^{\tau(q)}$ with $\tau(q) = q^{\delta/2}$. Moreover, we find an explicit criterion for the broadness of the distribution $N(\log P)$ where multifractality exists. We show that when $N(\log P) \sim |\log P|^{-\alpha}$ ($|\log P| >> 1$) there will be multifractal behavior in the small q domain only when $\alpha < 2$.

[1] For general review on fluctuations of the probabilities density on random fractals see e.g., *Fractals and Disordered Systems* (Springer, New York, 1991) Eds: A. Bunde and S. Havlin, p133.

Topological Quantum Numbers in Chaotic Systems

M. Feingold

Dept. of Physics, Ben-Gurion University, Beer-Sheva 84105, Israel

The Harper equation describes the quantum mechanics of a 2D periodic potential, $V(x,y)$, in a strong (or weak) perpendicular magnetic field, $\mathbf{B} = B\hat{z}$. While its spectrum is a fractal in the $(\alpha \equiv \phi/\phi_0, E)$ plane (ϕ=flux per plaquete, ϕ_0=flux quantum), the Hofstader butterfly,[1,2] it can be mapped onto an integrable one-degree of freedom problem with periodic phase space, the Harper Hamiltonian, $H = \cos p + \cos q$. For rational α, the Hall conductances of the corresponding minibands are integer multiples of e^2/h.[3] These integers are of topological origin and are known as Chern numbers.

The Harper Hamiltonian can be modified into a nonintegrable system which is still defined on a 2D periodic phase space. This is achieved by adding periodic time dependence, in the form of a periodic train of δ-functions multiplying the $\cos q$ term, $\cos q \sum_{n=-\infty}^{\infty} \delta(t - nT)$. This is the Kicked Harper Hamiltonian.[4,5] In the limit $T \to 0$, the integrable problem is retrieved. Therefore, $\gamma \equiv 2\pi T$ is a measure for the degree of nonintegrability. In particular, for $\gamma > 0.6$, the system is strongly chaotic (basically no regular trajectories). In the Figure bellow, the evolution of the Chern numbers with γ is shown for $\alpha = 1/9$. The behavior is symmetric with respect to the center miniband and therefore only the first five are shown. The Chern nrs., C_i, change only when the minibands pass through degeneracies. At generic degeneracies (two levels on a *diabolo*), $\Delta C_i = \pm 1$.

To summarize, two aspects are to be stressed: a) in strongly chaotic systems the Hall conductivities of minibands are typically non-vanishing (for $\gamma \ll 1$ the C_i are large) and therefore, the corresponding states are extended, b) the Chern numbers represent a new type of quantum numbers (of topological nature) which in contrast to the usual ones are equally valid for both integrable and nonintegrable systems.

1) M. Azbel, Sov. Phys. JETP **19**, 634 (1964).

2) D.R. Hofstader, Phys. Rev. B**14**, 2239 (1976).

3) D. Thouless, M. Kohomoto, M. Nightingale, and M. den Nijs, Phys. Rev. Lett. **49**, 405 (1982).

4) P. Leboeuf, J. Kurchan, M. Feingold and D.P. Arovas, Phys. Rev. Lett. **65**, 3076 (1990).

5) P. Leboeuf, J. Kurchan, M. Feingold and D.P. Arovas, Chaos **2**, 125 (1992).

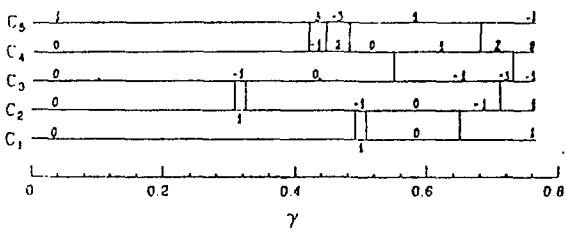

Premelting Phenomena within Computer Simulated Clusters of Alkali Halides

A. Frenkel, E. Shasha, O. Gorodetsky and A. Voronel

School of Physics and Astronomy
Raymond and Beverly Sackler Faculty of Exact Sciences
Tel Aviv University 69978 Tel Aviv, Israel

The method of molecular dynamics (MD) simulation of alkali halides and computer code CLUSTER were developed. The interionic potentials were chosen as a superposition of Coulomb and Born - Mayer potentials. The cluster sizes were $5 \times 5 \times 5$ and $6 \times 6 \times 6$ ions, however, all the characterics were evaluated over the inner core clusters $3 \times 3 \times 3$ and $2 \times 2 \times 2$, respectively. The method was applied to calculate structural and kinetic characteristics of RbBr, NaBr, NaI, NaCl, KI and KCl from 10 K to their melting points (T_m). The resultant values of melting points (except NaI) and bond lengths obtained for small clusters of atoms are in good agreement with the corresponding bulk properties. The relative mean square vibrational amplitudes in the vicinity of T_m satisfy the Lindemann criterion of melting. The anomalous behavior of NaI at 200 K below its melting point is interpreted in terms of fast ion conductivity observed previously for this salt.

This work was supported by the US - Israel BNSF Grant 90-00152/1.

Local Deviations from the Average Stucture in Mixed Alkali Halides

A. Frenkel[†], E. A. Stern[‡], A. Voronel[†], M. Qian[‡] and M. Newville[‡]

[†] *School of Physics and Astronomy*
Raymond and Beverly Sackler Faculty of Exact Sciences
Tel Aviv University 69978 Tel Aviv, Israel
[‡] *Physics Department FM-15*
University of Washington 98195 Seattle WA, USA

X-ray-absorption fine structure (XAFS) data of RbBr, RbCl, KBr and the two kinds of their solid solutions $Rb_xK_{1-x}Br$ and $RbBr_xCl_{1-x}$ at 30 K and 125 K were measured and analysed. Pure salts RbBr, RbCl and KBr were analysed to demonstrate the accuracy of an ionized atom multiple-scattering calculation used for fitting of the theoretically calculated normalized absorption $\chi(k)$ to the data. The vibrational information was determined through at least 10 $\AA$ around the central atom. The results demonstrate the domination of single - scattering and focusing paths in XAFS.

The mixed salts $Rb_xK_{1-x}Br$ and $RbBr_xCl_{1-x}$ XAFS data were analysed using the paths found important in the analysis of the pure salts. Both mixtures were prepared with the concentration x of their congruent melting points, corresponding to the highest degree of solubility of components. It was proved by XAFS composition analysis that the components were homogeneously mixed. The structure of mixed salts was found to deviate from the average NaCl structure. While the first nearest neighbor distances significantly ($\Delta R \approx 0.03 - 0.06\AA$) deviate from the average ones defined by X-ray diffraction, the second nearest neighbor distances remain to obey the Vegard law of a linear interpolation between those of pure components in accordance with composition. It means a break of collinearity between the two adjacent bonds occurs. The root mean square angles Θ were determined from the best fit of the theoretical $\chi(k,\Theta)$ to the data. The obtained values of these angles ($\Theta \approx 7^\circ - 9^\circ$ for both mixtures) are in good agreement with those found for the investigated mixtures by molecular dynamics computer simulations.

This work was supported in part by DOE grant DE-FG06-90ER45425 and by the US - Israel BNSF Grant # 90-00152/1.

The Most Accurate Method for the Roughening (Kosterlitz-Thouless) Transition

Martin Hasenbusch[1], Michael Marcu[2] and Klaus Pinn3

[1] *CERN Theory Division*
CH-1211 Genève 23, Switzerland
[2] *School of Physics and Astronomy*
Raymond and Beverly Sackler
Faculty of Exact Sciences
Tel Aviv University, 69978 Tel Aviv, Israel
[3] *Institut für Theoretische Physik I*
Universität Münster, Wilhelm-Klemm-Str. 9
4400 Münster, Germany

For a large class of two-dimensional statistical models, the unambigious verification of the Kosterlitz Thouless (KT) scenario is still an open problem. The most recent large scale Monte Carlo studies of the XY model and the Villain model clearly favor a KT against a second order transition. However, systematic errors are not yet under control. Here we present an alternative approach, based on the solid-on-solid (SOS) formulation of the same models. Our method exploits the fact that the BCSOS (body centered SOS) model can be solved exactly and has been proven to exhibit a KT (roughening) transition. The idea is to verify the KT scenario for an SOS model by demonstrating that its asymptotic renormalization group (RG) flow matches with the flow of the BCSOS model. The flows are conveniently parametrized in terms of physical quantities that are functions of block spin averages. Concretely, we considered several SOS models: DGSOS (discrete Gaussian SOS), ASOS (absolute value SOS), the dual of the XY model, and the BCSOS model. In the BCSOS case the roughening point is known exactly, so by taking blocks of increasing size we can map out the critical trajectory. For each of the other models we found an RG trajectory identical to the critical trajectory of the BCSOS model. In itself, this constitutes a spectacular test of universality. In the process of matching trajectories, the transition temperatures are determined with an accuracy exceeding by far the best previous results. We also show how to test some critical laws and how to extract some other nonuniversal quantities that characterize the critical behaviour. The necessary numerical accuracy was achieved by using cluster algorithms. As compared to other methods for determining the KT transition point, ours is by far the least computer time intensive. For the Ising interface, similarly accurate results were obtained by M. Hasenbusch.

Large Picosecond Energy and Coordinate Fluctuations of Single Atoms in Molecular-Dynamics Studies

Yu.L. Khait†, Yu. Kurskii† and Joan Adler*

**Department of Physics, Technion, Haifa, 32000, Israel.*
†Solid State Institute, Technion, Haifa, 32000, Israel.

Molecular-dynamic (MD) simulations on samples modeling nanometer regions of ideal gas solids in 2D lattices at finite temperatures are described. These reveal short-lived large energy fluctuations (SLEF's) and large transient coordinate fluctuations (LTCF's) of single atoms of lifetime $\Delta\tau = 10^{-13} - 10^{-12}s$. Although a few of these were observed [1] in our previous MD studies of 3D amorphous silicon solids, this is the first time that they have been seen in the simple 2D system where statistics about the behaviour of many fluctuations can be gathered. Both studies support the predictions of the kinetic many-body SLEF theory [2-4] about:

(i) The existence of SLEF's and SLEF-induced large picosecond deviations in coordinates of fluctuating atoms (FA's) from their mean positions that cause the formation of transient point defects of lifetime $\Delta\tau$ and leads to many large experimentally observed effects in various solids [**2**,3,4].

(ii) The characteristic energies, time intervals and frequencies of observed SLEFs and LTCFs.

(iii) The correlated many-body motion of the FA and its nanometer surroundings during $\Delta\tau$, which can be described analytically by coupled kinetic integro-differential equations [2].

Taking into account the SLEFs and LTCFs which play a key role in an extremely broad range of rate processes, and cause a strong electron-lattice interaction enables one to explain many previously puzzling observations [**2**,3,4].

1. Yu.L. Khait, A. Silverman, R. Weil and J. Adler, Phys. Rev. B **44**, 8308 (1991).
2. Yu.L. Khait, Phys. Reports **99**, 237 (1983); In Recent Progress in Many Body Theories, eds. A.Y. Kalio et al. (Plenum N.Y. 1988).
3. Yu.L. Khait, R. Brener and R. Beserman, Phys. Rev. B **33**, 2983 (1986); Yu.L. Khait and R. Beserman, Phys. Rev. B **38**, 8107 (1988); Yu.L. Khait, R. Weil, R. Beserman, W. Bayer and W. Wagner, Phys. Rev. B **42**, 9000 (1990); Yu.L. Khait, Semiconductor Sci. Techn. **6**, C-84 (1991).
4. Yu.L. Khait, J. Salzman and R. Beserman, Appl. Phys. Lett. **53**, 2135 (1988); ibid **55** 1170 (1989).

STATISTICS OF WAVES TRANSMITTED THROUGH A RANDOM MEDIUM

Eugene Kogan, Rene Baumgartner, Richard Berkovits, and Moshe Kaveh

Jack and Pearl Resnick Institute of Advanced Technology,
Department of Physics, Bar-Ilan University
Ramat-Gan 52900, Israel

The interest in problems relating to the propagation of light through disordered media was revived after the discovery that strong UCF (universal conductance fluctuations) exist also for classical waves. In contrast to electronic measurements which can measure only the conductance of a system, light experiments have the advantage of being able to measure the angular transmission coefficients. The angular transmission coefficient t_{ab} is defined as the ratio of the energy carried away by the transmitted wave with the transverse wave vector $\vec{q}_b$ to the energy of the incident wave with the transverse wave vector $\vec{q}_a$.

In the framework of the diagrammatic approach we calculate the statistics of t_{ab} and total transmission coefficient $t_a = \sum_b t_{ab}$ for a random medium. It is shown that the distribution function $P(t_{ab})$ is given by:

$$P(t_{ab}) = \frac{1}{\sqrt{2\pi < \tilde{\delta} t_{ab}^2 >}} \int_0^\infty dv \exp\left[-\frac{(v - < t_{ab} >)^2}{2 < \tilde{\delta} t_{ab}^2 >} \right] \frac{1}{v} \exp\left(-\frac{t_{ab}}{v} \right), \quad (1)$$

where $2 < \tilde{\delta} t_{ab}^2 > \equiv < t_{ab}^2 > - 2 < t_{ab} >^2$. The distribution function we got can be described as the Rayleigh distribution function but with some effective averaged value which in its turn fluctuates around the real averaged value (and is distributed according to Gaussian law). The distribution function $P(t_a)$ is a simple Gaussian:

$$P(t_a) = \frac{1}{\sqrt{2\pi < (\delta t_a)^2 >}} \exp\left[-\frac{(t_a - < t_a >)^2}{2 < (\delta t_a)^2 >} \right] \quad (2)$$

From Eq.(1) it follows, that only for $t/< t > \ll \sqrt{g}$, where g is the dimensionless conductance, does one obtain Rayleigh statistics for the angular transmission coefficient distribution function: $P_R(t_{ab}) \sim \exp(-t_{ab}/ < t_{ab} >)$. Outside this regime the distribution function greatly exceeds $P_R(t_{ab})$. For $t_{ab}/< t_{ab} > \gg g$ the distribution function is the stretched exponential:

$$P(t_{ab}) \sim \exp\left[-\frac{3}{(4\Delta)^{1/3}} \left(\frac{t_{ab}}{< t_{ab} >} \right)^{2/3} \right]. \quad (2)$$

These results are confirmed by numerical simulation.

Universal properties of current distributions on fractal resistor networks

Zvi Lev and Amnon Aharony

School of Physics and Astronomy
Raymond and Beverly Sackler Faculty
of Exact Sciences
Tel Aviv University
69978 Tel Aviv, Israel

We investigate the distribution of currents on a family of ordered fractal resistor networks. We quantitatively analyze the effect of binning on such distributions and on the calculation of the moments of these distributions. We use the Laplace and Fourier transform formalisms to derive formulae for the binned distributions' moments, and it is shown that the application of binning inevitably results in an approach to a Gaussian envelope for sufficiently large fractals. The "fine structure" sometimes observed in such distributions is also easily explained in terms of this formalism.

It is also shown that approximations fitted to the binned distribution are not necessarily good descriptions of the original distributions, especially for the very small currents' regions. Specifically, the claim that for the Mandelbroit Given fractal one can derive a power law behaviour for the distribution of small currents is shown to be wrong.

We extend the integral transform formalism to handle the case where the resistances of the bonds comprising the fractal structure are randomly distributed. We then proceed to show that the resulting $f(\alpha)$ curve has a negative region, and that even for narrow distributions the "fine structure" observed in the ordered case disappears.

Another possible form of randomization is to make the fractlization process itself random - that is, to randomly choose in every iteration of the fractal one fractal rule out of a given set. We show that the $f(\alpha)$ function for this case is simply related to the same functions for the fractals which compose the set, and that under certain conditions negative $f(\alpha)$ values are obtained.

Numerical Study of the Effective Response in Nonlinear Random Resistor Networks

Ohad Levy and David J. Bergman
School of Physics and Astronomy
Raymond and Beverly Sackler Faculty of Exact Sciences
Tel-Aviv University, Tel-Aviv 69978, Israel.

The nonlinear properties of small-particle composites have been extensively studied in recent years. The composites of interest are usually made of nonlinear (metal or semiconductor) particles embedded in a linear host. They are of particular interest because their nonlinearities may be strongly enhanced relative to bulk samples of the same materials.

We studied numerically the effective response of nonlinear random resistor networks consisting of two different types of resistors. One type of resistors is assumed to be ohmic, while the other is assumed to have a nonlinear $I-V$ response of the form $i = \lambda v^{\beta+1}$. The effective response is calculated by numerically solving the Kirchhoff's equations for the voltages at each node of the network. Numerical results, for $\beta = 2$ and $\beta = 4$, are compared to theoretical predictions of a recently derived Clausius - Mossotti approximation for such networks. The Clausius - Mossotti results are found to represent a reasonable description of the simulation results only in cases of law contrast between the two components or a small fraction of the nonlinear component in the network. However, it is found that the range of validity of this nonlinear Clausius - Mossotti approximation is larger than that of the classical Clausius - Mossotti approximation for linear two-component random resistor networks.

Multiple Cracking and Fragmentation Model

V. Chertkov

The problem is considered about accumulation of different size cracks in brittle medium under given stress action up to fragment formation and body decay on parts (or up to second fragmentation by compressive stresses).

The physical foundation of the approach to the problem solution is the tracing in each small volume of the correlations chain : stresses - microcrack concentration - macrocrack concentration - fragments characteristics. The problem solution are based on the next principle notions:

- fragmentation and fragment characteristics - probabilistic results of crack formation (probabilistic approach);
- general fundamental feature of preexisting and additional cracking - their multiple character (multiple crack formation);
- mechanism of crack formation - accumulation and coalescence of cracks, beginning from microcracks (kinetic model);
- under inhomogeneous conditions of crack formation the fragments characteristics are determined by local conditions (locality).

Main results are expressions and calculation algorithms for probabilistic correlations of cracking, fragmentation and fragment characteristics: micro- and macrocrack concentration, crushing probability, fragment distribution on size and shape, fragment strength. It is given generalization of kinetic approach to estimation of mean microcrack concentration time dependance on the case of complex stress state and high stresses.

For check up and ground of above results the present data for rocks from fields of geophysics and mining as well as data of physical experiments on explosion cracking and fragmentation in model monolithic brittle medium (colophony) are used.

Received results have general character and can find immediate practical application in such fields of science and technology as explosion and impulse action mechanics, materials properties exploration, materials engineering, soil and rock mechanics, geophysics, construction, building materials production, mining and other.

Quantum Theory of Delayed Fracture

R.L. Salganik

Department of Solid Mechanics, Materials and Sturctures
The Iby and Aladar Fleischman Faculty of Engineering
Tel Aviv University
69978 Tel Aviv, Israel

An overview will be given on delayed fracture, its theory and relevant mathematical problems. Delayed fracture (DF) is rupturing of the material after some time from the moment of its loading.

DF can be caused by the action of environmental agents penetrating into edge regions of cracks. Also it can be due to internal viscosity leading to gradual transmittance of the applied stress to structural elements responsible for strength and rupturing almost without any delay. Even if this is not the case significant DF is nevertheless observed under suitable conditions. It is produced by atomic fluctuations of stretched atomic bonds.

According to the traditional point of view these fluctuations are of a purely thermal nature. Then, the dependence of longevity on absolute temperature is of Arrenius' type, e.g. logarithm of longevity depends linearly on inverse absolute temperature. The role of tensile stress is only in reducing the activation energy. So, DF is in essence a kind of solid state chemical reaction accelerated by the tensile stress.

However, when the temperature decreases, quantum fluctuations affect fracture kinetics more and more. They become dominant below a characteristic quantum temperature which may be rather high. This was theoretically predicted and then experimentally substantiated (on fibers) down to liquid helium temperature. Taking the phonon spectrum into account is an important part of the theory (simplest form of the phonon spectrum, i.e. cut off of its linear part was assumed).

Thus, below the characteristic quantum temperature, there exists fracture kinetics practically independent of temperature but dependent on tensile stress. It means that damage accumulation, gradual crack growth, and DF under constant or even decreasing loads, should be observed at both normal and low temperatures, down to absolute zero. This fact is of importance for material science and engineering applications. Interesting applied mathematical problems are associated with different aspects of DF. A number of interesting problems associated with different aspects of DF will be considered.

Nuclear Physics

Coherent hard diffractive processes off nucleons and nuclei

L. Frankfurt

School of Physics and Astronomy
Raymond and Beverly Sackler Faculty
of Exact Sciences
Tel Aviv University
69978 Tel Aviv, Israel

The significant role of color coherent effects in high energy processes is explained. Diffractive production of minijets by pion projectiles off nucleons and off nuclei is calculated in QCD and suggested as the method to illuminate color transparency. Violation of the factorization theorem in hard diffractive processes is found.

Partially-Conserved Quantum Numbers in Nuclear Spectroscopy

A. Leviatan

Racah Institute of Physics, The Hebrew University, 91904 Jerusalem, Israel

Symmetry plays an important role in analyzing spectroscopic properties of nuclei. When an exact symmetry occurs, the Hamiltonian admits a block structure in a basis labeled by the irreducible representations (irreps) of the symmetry group. Eigenstates which belong to the same irrep are degenerate. In a dynamical symmetry, the Hamiltonian is written in terms of the Casimir operators of a chain of subgroups. The labels of irreps of the groups in the chain serve as quantum numbers to classify all the eigenstates of the Hamiltonian. States in a given irrep are no longer degenerate but different irreps are not mixed and the Hamiltonian still retains its block structure. The wave functions, eigenvalues and other observables (e.g. transition rates) are known analytically. The merits of a (dynamical) symmetry are self-evident, however, in detailed applications of group theoretical methods to the spectroscopy of nuclei, one often finds that the assumed symmetry is fulfilled by only some of the states but not by other. For example, certain degeneracies implied by the symmetry are not observed experimentally, as is the case with SU(3) assignments to rotational bands in deformed nuclei. At times requiring the Hamiltonian to be invariant under a certain group poses constraints which are too restrictive. This will be shown to be the case with a proton-neutron SU(2) symmetry (F-spin) of collective states in nuclei. Different types of experiments seem to justify associating F-spin labels as quantum numbers for some states. In contrast, microscopic arguments based on the nature of effective interactions in nuclei, do not support F-spin invariant Hamiltonians. These and other observations motivate one to consider particular breaking of the symmetry that would result in mixing of representations in some part of the spectrum while retaining a good symmetry to specific eigenstates. We refer to such a situation as partial (dynamical) symmetry. Within such a symmetry construction only a subset of eigenstates are pure and preserve the desired features of a dynamical symmetry (e.g. solvability). The notions of exact, dynamical and partial symmetry will be explained in relation to nuclear spectroscopy. Explicit forms of Hamiltonians with partial symmetries will be presented in the framework of algebraic models of nuclear structure. This will lead to a formulation of a general algorithm for constructing Hamiltonians with such property. The relevance of partial symmetries to a variety of nuclear phenomena will be pointed out, as well as to studies of dynamical systems which exhibit both regular and irregular (chaotic) behavior.

A SYMMETRIZED ANSATZ FOR THE DIBARYON SKYRMION

R. Levy-Nathansohn and J. M. Eisenberg

School of Physics and Astronomy
Raymond and Beverly Sackler Faculty
of Exact Sciences
Tel Aviv University
69978 Tel Aviv, Israel

We investigate a symmetrized ansatz for the dibaryon system in the Skyrme model. The ansatz obeys the same reflection symmetry that is observed in the complete, static numerical solution for the $B = 2$ sector. The baryon–baryon potential between two skyrmions is calculated as a function of the separation distance.

Although it is believed that Quantum Chromodynamics (QCD) is the elementary theory of strong interactions, our understanding in the low-energy range still remains a challenging problem. However, it can be shown that in the limit of a large number of colors QCD yields an effective lagrangian that describes a nonlinear field theory of interacting pions. In this context the Skyrme model has proven to be a successful effective theory of QCD in the long-wavelength limit, which is the nonperturbative regime. In the Skyrme model baryons emerge as stable field configurations characterized by a nontrivial topological structure. The model enables the study of single-baryon properties, a study which yields an appealing picture of the nucleon and delta and their static properties. It also offers a framework for investigating the interaction between classical baryons.

In the present work a symmetrized ansatz for dibaryon system in the Skyrme model is studied. The ansatz obeys a reflection symmetry that was observed in the numerical solution of the equation of motion for the sector $B = 2$. Using that ansatz a static Skyrmion-Skyrmion potential is calculated as a function of the separation distance and is compared to parallel results obtained with other ansätze. For the purpose of checking the validity of the ansatz in describing the dibaryon system we carefully verify that the baryon number is equal to two at all separation distance.

Generally, the results exhibit repulsion at all separation distances; specifically they show a divergent pattern of the potential for separation distance less than 1 fm. This result can be interpreted as a reflection of the hard core feature of the physical dibaryon potential. Regarding the intermediate range, the energy values are higher than those obtained with the Product Ansatz. For that reason it seems that the Symmetrized Ansatz fails to suggest a good alternative to the Product Ansatz.

Nuclear Stimulated Desorption

Dror Nir
School of Physics and Astronomy
Raymond and Beverly Sackler Faculty
of Exact Sciences
Tel Aviv University
69978 Tel Aviv, Israel

Nuclear Stimulated Desorption (NSD) is a new mode of experimentation in thin film and surface science. It is based on the interplay between nuclear phenomena (reactions and spontaneous decays), and atomic-scale induced effects on surfaces and very thin films. Implementation of NSD is based on radio active isotopes which undergoes two consecutive decays (normally Weak decays or isomeric transition). The first of these decays causes the nucleus (i.e. the atom or molecule containing it) to desorb from a surface onto which it had been placed; the second serves to determine the position of the daughter and thereby the characteristic of the primary desorption.

The essential feature in NSD is that it occurs almost exclusively from the outmost surface layer. This is because the recoil energy of the isotopes in use, is of the same order of magnitude of the binding energy of the atom to the surface ($\sim$10eV). Furthermore, the desorption probability and its angular and temporal characteristics,depend on the features (topology,morphology) of the nucleus immediate neighbourhood.

Note, that quite independently of the above, NSD provides us with an outgoing flux of radioactive atoms. If NSD is the only effective desorption mechanism, then this constitutes an ultra-clean flux of radioactive markers, of precisely known time dependence, which can be put to use in different applications.

References:

1) I.Kelson, D.Nir & A.Zidon, Identification of Nuclear Delayed Desorption in Physical Systems,Physics LetterA,139(1989)406
2) I.Kelson, D.Nir & G.Ringler, Study of the Charged component in Nuclear Stimulated Desorption, J. of Phys. D.,25(1992)1545
3) I.Kelson,D.Nir & A.Zidon, Ultra-Clean Radioisotope Marking by Nuclear Stimulated Desorption, J. of Appl. Phys., 69(1991)

Study of properties of rare negative ions by laser interaction and accelerator mass spectrometry

D. Berkovits[1], E. Boaretto[1], O. Heber[2], G. Hollos[3] and M. Paul[1]

[1] *Racah Institute of Physics, Hebrew University, Jerusalem 91904*
[2] *Nuclear Physics Dept., Weizmann Institute of Science, Rehovot 76100*
[3] *Accelerator Laboratory, Weizmann Institute of Science, Rehovot 76100*

Most elements are able to form free stable negative ions by binding an extra electron to their atomic shells. The electron affinity defined as the binding energy of this electron, is experimentally known for most of the elements [1]. However, for some cases, when the negative ion formation is very weak and the ion is difficult to identify, no experimental knowledge exists for the electron affinity, a fundamental physical property. Such is the case for a few sparse elements and for the whole region of the lanthanides (4f) and the actinides (5f).

We present here a method for measurements of properties of rare negative ions . The method involves the use of ultra-high sensitivity accelerator mass spectrometry (AMS) where individual atoms are counted after thorough identification, in combination with excitation of the negative ion in laser light. Study of the photoelectric detachment of the extra electron as function of the wavelength gives then information on the binding energy of the electron. The experimental setup [2] is based on the Rehovot Pelletron tandem accelerator. Absolute cross-sections of photodetachment in negative ions of La,Ce,Th and U have been measured [3] with the second harmonic (532 nm) and fundamental wavelength (1064 nm) of an Nd:YAG laser and will be extended to the near infra-red region, in which the electron affinity of these elements is predicted. Experimental knowledge of the electron affinities in a region where no information exists, will contribute to the understanding of the atomic physics involved and be a test for numerous theoretical calculations which have been performed.

[1] H. Hotop and W. C. Lineberger, J. Phys. Chem. Ref. Data 14(1985)731.
[2] D. Berkovits, E. Boaretto, G. Hollos, W. Kutschera, R. Naaman, M. Paul, and Z. Vager, Nucl. Inst. Meth. B52(1990)378.
[3] D. Berkovits, E. Boaretto, M. Paul, and G. Hollos, Rev. Sci. Instrum. 63(1992)2825.

Lasers and Optics

130

Resonance Phenomena in a Grating/Waveguide Structure

A. Sharon, D. Rosenblatt, Y. Noifeld, and A.A. Friesem

Department of Electronics
Weizmann Institute of Science
76100 Rehovot, Israel

An optical resonance phenomenon, based on an interference effect that occurs when a plane wave is incident on a dielectric grating/waveguide structure which supports a guided electromagnetic mode, is presented. The incident wave excites a guided mode which in turn is partially diffracted by the grating in the direction of the transmitted zero order beam, interfering destructively. As a result most of the light energy is contained in the reflected zero order beam. The resonance phenomenon is explained with a ray picture of the multiple interference. A computer algorithm which solves Maxwell's equations for the exact eigenfunctions in a rectangular grating on a dielectric waveguide structure, for both TE and TM polarizations, has been developed. Computer simulation results reveal that the bandwidth of the resonances can be as narrow as 0.1 nm, with a corresponding angular beamwidth on the order of minutes of arc. The beamwidth and bandwidth depend strongly on the parameters of the grating/waveguide structure.

Coherence Effects in Optical Networks

Yitzhak Weissman

Department of Atmospheric Optics
Soreq NRC, Yavne 70600, Israel

The technology of optical networks has advanced rapidly in the past few years. This development is driven by needs in the fields of communication, metrology, sensing, and signal processing.
Typically, in optical networks there are two scales of length: one scale, denoted by L_c, measures the typical size of a component, and the other, denoted by L_i, measures the typical length of the interconnects. In many applications, L_c and L_i differ by an order of magnitude or more.

One of the characteristics of an optical source is its coherence length L_s. Physically speaking, this quantity measures the spatial distance along the propagation direction over which the second-order correlation function of the field decreases significantly.

The qualitative features of the output field depend on the relations between L_s, L_c, and L_i. A case which is both practically important and lends itself to a simple analytic treatment is the case in which $L_c << L_s << L_i$. This case is called the "incoherent limit". Simple expressions which qualify the output field in the incoherent limit will be presented.

DOMAIN INVERSION IN $LiNbO_3$ OPTICAL WAVEGUIDES

V.D. Kugel and G. Rosenman
Department of Electrical Engineering,
Physical Electronics, Faculty of Engineering,
Tel-Aviv University, Tel-Aviv 69978, Israel

Some ferroelectrics $LiNbO_3$, $LiTaO_3$, KTP are widely used in integrated optics for the development by second harmonic generation of solid state coherent light sources in the visible spectrum. The light generation occurs by frequency doubling in quasiphasematched intergrated waveguides. Quasiphasematching technique uses alternative sign of a nonlinear coefficient which in its turn is linked with spontaneous polarization direction of a ferroelectric crystal. Thus high efficient frequency doubling achieves in ferroelectric waveguides by means of domain periodical structure formation.

Domain inversion takes place under some diffusion and ion-exchange treatments. The domain inversion phenomenon is observed on a +C-surface of $LiNbO_3$, -C-surface of $LiTaO_3$ and on +C-surface of KTP. Reorientation of a spontaneous polarization in ferroelectric crystals without application of external electric field is not yet understood.

We develop a new microscopic mechanism of the domain reversal phenomenon in diffused layers and studied some ferroelectric properties of a domain inverted structure in heat treated $LiNbO_3$ crystals. Diffusion process leads to a nonuniform distribution of incorporated atoms in a $LiNbO_3$ crystal matrix. They represent donors (acceptors) centers which are ionized at elevated heat treatment temperature. As a result a built-in electric field arises. Computed data show that the field is large enough for the domain reversal, at the heat treatment temperature. For unelectroded $LiNbO_3$ crystal Li_2O outdiffusion process leads to the domain inversion on +C-surface only and inverted layer thickness may be as large as a half of the sample thickness.

Pyroelectric current, electron emission and domain structure were investigated. "Head to head" domain structure was observed for treated crystals. Domain inversion leads to drastic changes of the pyroelectric currents and to a total suppression of the electron emission. Experimental data were in a good agreement with computed ones.

DIFFUSION IN A RANDOM SYSTEM NEAR RESONANCE

Eugene Kogan and Moshe Kaveh

Jack and Pearl Resnick Institute of Advanced Technology,
Department of Physics, Bar-Ilan University
Ramat-Gan 52900, Israel

Recently, the first experiments were reported where the diffusion constant and transport mean free path for light propagating in a disordered medium were measured independently on the same sample . The medium consisted of dielectric balls situated in air. The results show an order-of-magnitude decrease of the diffusion constant D in comparison with the naive equation $D = c\ell/3$, where ℓ is a mean free path and c is the velocity of light in vacuum. To describe this slowing down of the diffusion of optical waves we propose a modification of the traditional Boltzmann equation when scatterers are near resonance. This modification takes into account the scattering delay time and can be written in the form:

$$\partial f_k(t)/\partial t + v_k \nabla f_k(t) + \sum_{k'} P_{kk'}[f_k(t) - f_{k'}(t - \tau^D_{kk'})] = 0, \qquad (1)$$

where v is the velocity, $P_{kk'}$ is the transition probability and $\tau^D_{kk'}$ is the delay time for the scattering channel $k \to k'$. When applied to the propagation of light in a disordered medium consisting of dielectric balls in air, this modified equation leads to the renormalization of the diffusion constant:

$$D = D_0/(1 + X_D), \qquad (2)$$

where D_0 is the traditional diffusion constant $D_0 = v_g^2\tau/3$ (v_g is the group velocity and τ is transport relaxation time). The parameter X_D is expressed through the phase angles of the Mie-scattering theory:

$$X_D = \frac{3f}{2x^2}\sum_{n=1}^{\infty}(2n+1)\left[\frac{\partial\alpha_n}{\partial x}\sin^2\alpha_n + \frac{\partial\beta_n}{\partial x}\sin^2\beta_n\right] \qquad (3)$$

where f is the volume fraction of the Mie-spheres, and $x = kd = \omega d/c$ is the size parameter (d is the ball radius).

The results thus obtained agree with the experimental results and also with theoretical results obtained using a different approach.

The Asymptotic of the Time Intensity Fluctuations for Light Reflected by Randomly Moving Point Scatterers

M.Auslender

Department of Electrical and Computer Engineering,
Ben-Gurion University of the Negev, Beer-Sheva 84105, POB 653

The diffusive reflection in the direction $\vec{n_r}$ of plane monochromatic wave with the propagation vector $k_0\vec{n_i}$ incident on a medium containing randomly moving point scatterers is considered. The movement of the scatterers is supposed to be diffusive on macroscopic level.

The quantity of interest is the asymptotic at $t \to \infty$ of reflected intensity-intensity time correlation function $\Gamma_2(\vec{r},t)$ which in factorization approximation is expressed in the terms of field-field correlator $\Gamma(\vec{r},t)$ [1]. The asymptotic of $\Gamma(\vec{r},t)$ is found within real space approach developed by Kaveh *et al* [2], which represents $\Gamma(\vec{r},t)$ via the sum over $N = 1,2,...\infty$ of the contributions from the real space light trajectories with N scattering events, which start and finish outside the medium. On account that after each scattering act the light wavevector is randomized but its initial and final values are fixed at $k_0\vec{n_r}$ and $k_0\vec{n_i}$ the following series representation in far field zone is obtained

$$\Gamma(t) = \sum_{N=1}^{\infty} W_N Z_N(D_s k_0^2 t; \vec{n_r}, \vec{n_i}), \tag{1}$$

in which D_s is the diffusion coefficient of the scatterers, W_N is the statistical weight of the N-th trajectory and $Z_N(J;\vec{n},\vec{n'})$ is the conditional partition function of classical ferromagnetic Heisenberg chain of $N+1$ spins with dimensionless exchange integral J and fixed first and last spins equal $\vec{n}$ and $\vec{n'}$ respectively. By means of transfer matrix formalism and classical summation methods an integral representation of the series (1) is obtained, which allows to get the asymptotic at $t \to \infty$

$$\Gamma(t) = \gamma(\frac{t}{\tau_0},\theta)\exp[-\theta\sqrt{\frac{t}{\tau_0}\ln(\frac{t}{\tau_0})}], \quad \frac{1}{\tau_0} = D_s(2k_0)^2. \tag{2}$$

Here θ is the angle between $\vec{n_r}$ and $\vec{n_i}$ and $\gamma(z,\theta)$ is the function depending upon the explicit form of the probabilities W_N [3]. However, irrespective to this the asymtotic of $\gamma(z,\theta)$ at $z \to \infty$ is power-like, the power being strongly dependent on the relation between $\pi - \theta$ and $1/z$.

REFERENCES

1. M.J.Stephen and G.Cwilich, Phys.Rev **B 34**, 7564 (1986)
2. M.Kaveh, M.Rozenblue and I.Freund, Nature **326**, 778 (1987)
3. I.Edrei and M.Kaveh, J.Phys. **C 21**, L971 (1988)

Efficient Copper Vapor Laser Pumped Ti:Sapphire Laser

A. Ben Amar, J. Kagan, M. Lando, and E. Miron

Laser Department

A. Cohen, and M. Nahmani

Crystal Growth Department

Nuclear Research Center Negev
P.O.B. 9001
84190 Beer Sheva, Israel

A high-average power, efficient Ti:Sapphire laser, pumped by an oscillator-amplifier configured copper vapor laser is reported. The ϕ 9 x 15 mm Ti:Sapphire rod was made out of a boule grown by the Czochralsky method using the Cambridge Instruments Autox machine and annealed in a home-made annealing furnace.
The Ti:Sapphire measured slope efficiency was 38% and the total efficiency was 25% at 3 W broad band output. To the best of our knowledge these are the highest figures reported for both slope and total efficiencies for a copper vapor laser pumped Ti:Sapphire laser.
The polarized pump beam diameter was 28 mm and its full divergence angle, including spatial dither, was 0.26 mRad. Ti:Sapphire laser beam divergence was 2.7 mRad (M^2 = 7).
Ti:Sapphire laser pulse buildup time was 25 nsec and its pulse width was 8 nsec FWHM.

IR Fiberoptic Radiometry for Scientific, Industrial and Biomedical Applications

E.Belotserkovsky, O.Eyal, and A.Katzir

School of Physics and Astronomy, Tel-Aviv University,
Tel-Aviv, 69978, Israel

Temperature distribution monitoring is essential in many scientific, industrial and biomedical applications. IR fiberoptic radiometry offers several advantages over refractive optic radiometry; and it does not need a direct line of sight to the controlled thermal area. It also has advantages over the standard fiberoptic temperature sensors because of the capability of non-contact temperature measurements.

We developed a fiberoptic radiometric system based on IR silver halide ($AgCl_xBr_{1-x}$) fibers for monitoring non-uniform temperature distributions. These fibers are highly transparent in the wavelength range of 2 to 20μm, flexible, non-toxic and insoluble in water.

The monitoring of different kinds of non-uniform temperature distributions in different applications were carried out. Glass, metal and plastic samples were non-uniformly heated and the surface temperature distribution was monitored. We also controlled surface temperature distribution of gelatine phantoms of different form and biological tissues heated in a MW oven. The developed system allowed us to map the temperature of samples during heating in a MW oven.

The system was also applied to monitoring temperature during drilling and cutting processes. In addition, the fiberoptic radiometer was utilized for real time temperature monitoring of a CO_2-laser irradiated target.

State-to-State Photodissociation Dynamics of Rovibrationally Excited H_2O

D. David, A. Strugano, I. Bar and S. Rosenwaks

Department of Physics , Ben-Gurion University of the Negev, Beer-Sheva 84105, Israel

Triatomic molecules are particularly appealing objects for both theoretical and experimental studies of photodissociation. This is because they are small enough to allow *ab initio* calculations of potential surfaces and photodynamics and yet retain the complexity of different vibrational degrees of freedom. However, quantitative comparison with theory requires experiments that prepare reactant molecules in specific initial states to avoid the averaging over different quantum states. Also, it is necessary to determine accurately the populations in the various final quantum states of the photofragments. We report on studies of state-to-state photodissociation at 193 nm of the fundamental symmetric stretch vibration of water, H_2O (1,0,0). Stimulated Raman excitation and coherent anti-Stokes Raman scattering are used to prepare and detect, respectively, particular rotational states of H_2O (1,0,0). Laser induced fluorescence is used for monitoring the OH species which are formed from particularly selected rotational states of the H_2O (1,0,0) and also from photodissociation of all occupied rotational states of the ground vibrational state, H_2O (0,0,0), at room temperature. The cross section for photodissociation from the particular rotations of H_2O (1,0,0) at 193 nm is found to be ~ 550 times greater than that for H_2O (0,0,0). The formation of the OH product in different rotational, Λ-doublet and spin-orbit states is analyzed for the photodissociation of H_2O (0,0,0) and for the photodissociation of the 1_{01}, $1_{10} + 1_{11}$, $2_{12} + 2_{11}$ and 3_{03} rotational states of H_2O (1,0,0). The rotational distribution of the OH resulting from photodissociation of H_2O (1,0,0) shows a structured distribution that is dependent on the particular rotation of the vibrationally excited state, while that resulting from photodissociation of H_2O (0,0,0) presents a smooth distribution. The Λ-doublet ratio in the two spin-orbit states shows preference of the A" component for photodissociation from the above rotational states of H_2O (1,0,0), while only a small preference at high N is observed for photodissociation from the ground vibrational state. The preliminary results of a study of the correlation between the polarization of the photodissociation laser and the angular momentum of the OH fragment indicates that the correlation depends on on the particular rotational state of the H_2O (1,0,0). The experimental rotational distributions are compared to available theoretical calculations based on the Franck-Condon model and show qualitative agreement between experiment and theory.

The effect of mixing on the operation of a chemical oxygen-iodine laser

B.D. Barmashenko, A. Elior, E. Lebiush and S. Rosenwaks.

Department of Physics, Ben-Gurion University of the Negev, Beer-Sheva 84105, Israel.

The mixing rate between the flows of iodine and oxygen in a chemical oxygen-iodine laser (COIL) has an influence on the processes of iodine dissociation, population inversion and lasing. For the usual subsonic COILs characterized by low pressure and low I_2 concentration such an influence is moderate. However, for the future generation of COILs characterized by higher densities of singlet oxygen or/and supersonic flow in the cavity (requiring higher I_2 concentrations) the effect of mixing becomes predominant. The iodine injected into the oxygen flow is concentrated initially in narrow jets. Therefore the local $[I_2]$ is initially of the same order of magnitude as $[O_2(^1\Delta)]$. This on the one hand accelerates the dissociation of iodine. On the other hand high local $[I_2]$ causes fast quenching of excited $O_2(^1\Delta)$ and $I(^2P_{1/2})$ by iodine molecules in the jets and hence leads to retardation of dissociation. Competition between the two alternative processes governs the dependences of the characteristic dissociation length and the maximum gain on the iodine flowrate nI_2. Low mixing rates affect also the lasing power of the COIL, leading to low efficiency of lasing. This is because the iodine is concentrated in the narrow jets and most of the singlet oxygen passing the cavity remains unreacted.

In the present paper the effect of mixing in the COIL is studied theoretically with the aid of the leak flow tube model which was earlier successfully applied to different types of IR chemical lasers. Several I_2/He jets are assumed to be injected into parallel stream of $O_2(^1\Delta)$/He. In a short distance from the injection point, initially circular iodine jets merge turning into the thin plane jet flowing parallel to the main flow of $O_2(^1\Delta)$/He. Kinetic processes inside the iodine jets were studied taking into account entrainment of the surrounding oxygen into the jet.

The model makes it possible to calculate the distributions along the flow of the average (over a flow cross section) iodine dissotiation fraction, gain and power of lasing as functions of iodine flow rate, yield of singlet oxygen and pressure in the cavity. Both maximum gain and characteristic length of the iodine dissociation are shown to be nonmonotonic functions of the iodine flow rate nI_2. Maximum nI_2 for which the lasing is possible is less than 1 - 2% of the oxygen flow rate which is in agreement with experimental data and can not be explained by premixed flow models. Analytical expressions are obtained for all the parameters. In particular the model predicts a linear relationship between iodine dissociation ratio and the square root of the distance in the case of high nI_2 corresponding to diffusion limited reaction. This dependence agrees with the results of two-dimensional calculations of dissociation in the COIL. The model is applied also to the mixing in the nozzle and cavity of supersonic COILs. Experiments on a supersonic COIL are now in progress in this laboratory. The experimental results for laser power are in qualitative agreement with theoretical calculations.

The Operator Representation of the Coupled Wave Approach for Electromagnetic Calculations of Lamellar Gratings: Application to Silicon Gratings.

S. Hava, M. Auslender and D. Rabinovich

Department of Electrical and Computer Engineering,
Ben-Gurion University of the Negev, Beer-Sheva 84105, POB 653

Optical gratings are constantly of interest because of their great importance in device applications.The mathematical techiques for electromagnetic calculations of general profile gratings based upon solving the appropriate differential and integral equations were indicated to fail numerically in particular important case of non shallow lamellar gratings [1].

The coupled wave scheme proposed by Knop [2] based on matching the Rayleigh wave expansions outside and inside the grating region, being applicable irrespective of grating material and dimensional relations, is most useful for lamellar gratings since it reduces the problem to solving the linear (though infinite) system.

When solving this system numerically by proper truncation one frequently meets the ill-conditioning problem. This is especially the case for materials with rather large dielectric constant where a large number of the Rayleigh waves have to be retained in the scheme to ensure convergence. The empirical method of handling the problem by the extraction of the evanescent waves was proposed initially [2].

We present a new operator/matrix formulation of Knop's scheme and perform some exact transformation to avoid rigorously possible ill-conditioning problem on initial stage. To speed up the convergence for deep gratings the exact modal expansion in the grating region [3] is inserted. On this basis a very compact MATLAB program (m-file) to calculate the reflectance, transmittance (for each order and total) and absorptance of lamellar gratings for both TE and TM polarizations is developed.

The calculations are performed for Si grating material both intrinsic and doped up to metallic concentrations. It is shown that the spectral resonance extema of reflectance are very sensitive to the imaginary part of dielectric function whatever is. The experimental data for intrinsic Si and Drude-Lorentz fit (including its generilized form [4]) for doped Si complex refractive index are used.

REFERENCES

[1] *Electromagnetic Theory of Gratings*, ed. by Petit, Springer-Verlag 1980
[2] K. Knop, J. Opt. Soc. Am. **68**, 1206 (1978)
[3] P. Cheng, R.S. Stepleman and P.N.Sanda, Phys. Rev. bf B 26, 2907 (1980)
[4] M. Auslender and S.Hava, Physica Status Solidi (b),**174**,565 (1992)

Two Proposals for Optical Experiments Demonstrating Quantum Interference Effects

LEV VAIDMAN

School of Physics and Astronomy
Raymond and Beverly Sackler Faculty of Exact Sciences
Tel-Aviv University, 69 978 Tel Aviv, ISRAEL

I. Amplification of effective index of refraction using polarization filters.

It is natural to assume that if a prism made out of birefringent material with indices of refraction n_1 and n_2, then the light ray which passes through polarization filters is deflected due to the prism by an angle corresponding to an index of refraction n such that $n_1 < n < n_2$. We have found that using filters of appropriate polarization before and after the prism, we can get deflection corresponding to the index of refraction far away from the region $[n_1, n_2]$. The method might be useful for improving sensitivity of measurements of small differences between indices of refraction of birefringent materials.

II. Detection of an atom in a certain excited state without disturbing it in any way whatsoever.

Let us assume that an atom in a certain excited state absorbs photons of appropriate energy with high probability. Thus, if such a photon was absorbed, we know that the atom *was* in this state. Now, can we find out that the atom *is* in excited state? The measuring procedure proposed by Elitzur and Vaidman for quantum interaction-free measurements allows us to detect excited atom using only the ability of excited atoms to absorb the photon (and the fact that unexcited atom cannot absorb this photon). The procedure is not always successful, but frequently it is, and then the excited atom remains absolutely undisturbed.

A small scale, supersonic oxygen-iodine chemical laser

A. Elior, E. Lebiush, W.O. Schall* and S. Rosenwaks

Department of Physics, Ben-Gurion University of the Negev, Beer-Sheva 84105, Israel

A supersonic oxygen-iodine chemical laser of 5 cm long active medium has been operated utilizing a simple sparger-type $O_2(^1\Delta)$ chemical generator and a medium size pumping system. A grid nozzle was used for iodine injection and supersonic expansion. 3 W of cw laser emission at 1315 nm were obtained in the present experiments. The small size and the simple structure of the laser system makes it a convenient tool for studying operation parameters which are important for high power supersonic iodine lasers.

*DLR - Institute for Technical Physics, D-7000 Stuttgart 80, Germany

Cr^{4+} Solid State Passive Q-Switch for Pulsed Nd:YAG Laser

Y. Kalisky and Y. Shimony

Laser Department
Nuclear Research Centre-Negev
P.O. Box 9001 Beer-Sheva 84190, Israel

Cr^{4+} doped garnets are emerging as novel, simple, efficient and photochemically stable saturable absorbers for 1.06 μm emission of Nd^{3+} lasers. This is due to the tetrahedral Cr^{4+} absorption band in the 0.95-1.25 μm spectral regime.

In particular, using Cr^{4+}:YAG as a passive Q-switch for a pulsed Nd:YAG laser yielded a suppression of the relaxation oscillations and the appearance of short (FWHM of 28nsec) multispike lasing having an intensity peak of up to 30 times greater than the free running spikes.

These results combined with the simplicity as well as the good optical, thermal and mechanical properties of YAG host indicate the potetial use of Cr^{4+} doped YAG passive Q-switch for extracting high average or high peak power from small size laser systems.

Analysis of the experimental results according to the existing theories will also be presented.

STRAIGHT TRAJECTORIES: AN ALTERNATIVE TO SNELL'S LAW OF REFRACTION OF RAYS

by

Dan Loewenthal

Raymond and Beverly Sackler Faculty of Exact Sciences
Department of Geophysics and Planetary Sciences
Tel Aviv University, Ramat Aviv 69978, Israel.

Snell's law of refraction of rays, which are the normals to the wave fronts, shows how the rays are broken upon passing through parallel layers of different propagation velocities. We wish to stress an alternative point of view which states that the source emits straight trajectories in plurality of directions. The duration of the passage of a straight trajectory from top to bottom of the layers equals to that of a ray's passage. However, this duration of straight trajectory in a layer is regulated through a transformation of velocity in the layer. The transformed velocity equals the square of the propagation velocity in that layer, and scaled to the velocity of the upper layer. We prove for precritical model, i.e. a medium with monotonously decreasing velocities with depth, that rays can be stretched to straight trajectories by an addition transformation on the thickneses of the layers.

The main advantage of the straight trajectory concept lies in its simplicity. We have used it as a fast way to compute the response of a stratified layered medium due to a point source. There is no need to consider complex reflection coefficients such as those occurring for post critical angles as a consequence of Snell's law of refraction.

HIGH RESOLUTION MINI - SPECTROGRAPH

Haim Lotem* and Mario Dageanais

Photonic Switching and Integration Optoelectronics Laboratory
Department of Electrical Engineering
University of Maryland, College Park 20742, USA

The spectral resolution of spectrographs based on a diffraction grating and a diode-array detector, is a function of the spectrograph f-number. It can be shown that the grating spectral resolution is matched with the diode-array resolution when the system f-number is larger than $1.5xP/\lambda$, where P is the pixel separation of the detector-array and λ the wavelength. Therefore, the corresponding f-number for high resolution systems in the visible range is quite large, even when high resolution arrays with P = 10 μm are employed. This means that the required spectrograph length, for a common system, such as the Czerny-Turner, with about 10 cm wide grating, is about 3 m. We propose a novel geometry for a grating spectrograph employing a diode-array detector, that is characterized by high spectral resolution while having very small dimensions. The compact spectrograph is based on double diffraction by a grating at grazing incidence combined with a tuning mirror. A typical system is expected to show a resolving-power of $3x10^5$ and dimension of only $15x15x2$ cm^3. Due to the large angle of incidence and the double diffraction by the grating, the transmission is lower by about a factor of 5 than that of equivalent common spectrographs.

* On leave from NRCN, Israel.

FREE SPECTRAL RANGE IN A DIFFRACTION-GRATING LITTROW CAVITY

Haim Lotem

Laser Department, NRCN, P. O. Box 9001
Beer-Sheva 84190, Israel

Diffraction gratings are commonly used to tune and narrow the resonance of optical cavities. In a Littrow grating cavity, the grating which acts as a retro-reflector, is aligned at an angle with the cavity axis. In such a geometry there is no unique cavity axial length, and therefore, the usual cavity free spectral range cannot be defined. We discuss the performance of grating cavities using both geometrical ray tracing and the result of the scalar diffraction theory for the phase of a plane wave diffracted at a grating[1]. It is shown that the grating cavity is axially symmetric and under certain conditions may be modeled by an equivalent tilted mirror Fabry-Perot. The tilt angle magnitude is linear with wavelength deviation from the cavity resonant Littrow wavelength, and the mirror separation is equal to the central axis length of the grating cavity. The model interprets the axial modes spectral spacing and predicts a mode broadening effect which is linearly dependent on the wavelength difference between the mode and the central resonant mode. Resonant effects were experimentally studied in a passive grating cavity by an interferometric method. The cavity mode spacing was investigated using a tunable probe laser, and the cavity axial symmetry was demonstrated using a compensating-plate.

(1) Patrick McNicholl and Harold J. Metcalf, "Synchronous cavity mode and feedback wavelength scanning in dye laser oscillators with gratings", Appl. Opt. 24, 2757-2761 (1985).

Electromagnetic modeling of a coaxial, large-bore copper vapor laser

Pinhas Blau

Laser Department
Nuclear Research Center - Negev
P.O.Box 9001, *Beer-Sheva*

The copper-vapor laser is a pulsed-electric-discharge pumped laser.
Modeling of the electric field is essential both for optimization of the pumping process and for development of the excitation circuit. Analysis has shown[1] that the laser impedance cannot be characterized by constant resistance and inductance, however constant conductivity can be assumed if the temporal dependence of the current density profile is accounted for.
In the model, the temporally and spatially resolved electric field is calculated considering skin effect and transmission-line effect. The plasma conductivity is calculated using estimated electron temperature, and measured,[2] radially resolved, electron density and gas temperature. The current density profile and total current are obtained. Very good agreement exists between calculated and measured laser current in a 100 W, 8 cm diameter, copper-vapor laser.

[1]P. Blau, "Analysis of the impedance of a coaxial, large-bore copper-vapor laser", submitted for publication.

[2]P.Blau, I.Smilanski, S.Gabay, and S.Rosenwaks, "Radially and temporally resolved measurements of electron density and gas temperature in a copper-vapor laser", accepted for publication, CLEO 93.

Growth and Characterization of Ti:Sapphire

A. Cohen, S. Biderman, M.P. Dariel A. Horowitz, M. Nahmani and M. Weiss

Crystal Growth Department

A. BenAmar

Laser Department

Nuclear Research Center Negev
P.O.Box 9001
84190 Beer Sheva , Israel

High quality Ti:Sapphire crystals of ϕ 32 x 150 mm were grown using a modified commercial Czochralsky puller. The modifications included: (a) A chamber compatible with high temperature ($>2000^{o}$ C) growth and (b) Gas sealing of the puller in order to enable inert growth conditions. Post annealing in a reducing ambience was required to further reduce the residual Ti^{4+} in order to get high quality Ti:Sapphire laser rods. Laser rods of ϕ 9 x 15mm with Brewster angles were fabricated according to strict specifications.

Mechanical and optical characterizations were performed on the laser rods. Lasing experiments served as the ultimate test for the quality of the Ti:Sapphire. The Ti:Sapphire rods were pumped longitudinally both by a copper vapor laser (reported in a parallel paper) and by a frequency doubled Nd:YAG laser.

Pumping with a copper vapor laser produced an output power of 3 W with a total efficiency of 25 %. Pumping with the Nd:YAG laser produced an output energy of 20 mJ with a total efficiency of 35 %.

- We wish to acknowledge the support of the ministry of Science and Technology

Status Report of the Israeli Tandem-FEL Project

M. Draznin, A. Eichenbaum, A. Gover, Y. Pinhasi, Y. Yakover
Faculty of Engineering, Tel-Aviv University,
Tel-Aviv 69978, Israel
Tel.: 972-3-6408149

J. Sokolowski,
Weizmann Institute of Science, Rehovot, Israel

B. Mandelbaum, A. Rosenberg, Y. Shiloh
RAFAEL, Haifa, Israel

G. Hazak, L.M. Levine, O. Shahal,
N.R.C., Beersheva, Israel

The first year of funded operation of the Israeli Tandem electrostatic accelerator FEL was directed towards reconditioning, upgrading the accelerator and demonstration of high current e-beam transport throughout the entire system, and the deisgn of a resonator system.

In addition to experimental work, theoretical and numerical studies were done on e-beam transport simulations, resonator design and FEL performance. Beam transport codes which were used include Hermansfeldt E-Gun, SCAT, TRANSPORT and TRACE.

Small signal gain calculations show that reasonable gain at mm wavelengths can be achieved with various waveguide resonators. Curved parallel plates and metal dielectric waveguides show relatively low losses and are therefore favored. We are presently developing a full 3-D nonlinear FEL code which is valid also in the nonlinear collective regime.

The recent experimental results of electron beam transport without internal focusing at currents $20 - 550 mAmp$ and efficiency of 100% to 55% showed good correspondence to numerical simulations. Experiments on optical transmission of curved parallel plates waveguide showed very small losses at 100 GHz.

Prebunched FEM Experiment at TAU

M. Arbel, D. Ben-Haim, M. Cohen,
M. Draznin, A. Eichenbaum, A. Gover,
A. Kugel, H. Kleinman, Y. Pinhasi, and Y. Yakover

Faculty of Engineering
Tel Aviv University
69978 Tel Aviv, Israel

The status of an experimental project aimed to demonstrate an electrostatic free electron maser (FEM) with prebunching in a depressed collector configuration is presented. The FEM utilizes a $1A$ prebunched electron beam obtained from a convergent Pierce-type gun which is part of a commercial traveling-wave-tube (TWT). The electron beam is bunched by the TWT section following the gun at $5.5GHz$, and then accelerated to $70KeV$. The bunched beam is injected into a planar wiggler ($B_w = 300G$, $\lambda_w = 4.4cm$) constructed in a Hallbach configuration with 17 periods and utilizes two long permanent magnets for horizontal focusing. The quasi-CW FEM is designed to operate as an amplifier in the centimeter wavelength region. We plan to study the FEM gain enhancement and radiation features due to the prebunched (superradiant) mode of operation, startup from noise, high harmonics emission, and evolution of the spatial and temporal coherence of radiation. Simulation of the FEL operation shows promise of a gain of approximately 10 and r.f. power of $5KW$. In this presentation we review the design of the main parts of the experimental set-up, and present some analytical, numerical, and experimental results.

Design, Simulation, and Measurements of Wiggler Field and Electron Trajectories for FEM Experiment at TAU

R. Kost, M. Refaeli, A. Kugel, M. Draznin, M. Cohen, and A. Gover

Faculty of Engineering
Tel Aviv University
69978 Tel Aviv, Israel

Beam injection and transport inside a wiggler in FEL experiments of low energy and high current require a careful design of the wiggler field and magnetic focusing elements. This includes provisions for steering magnets at the entrance and exit of the wiggler and leteral focusing fields along the wiggler (in planar wigglers). We build the desired wiggler field and measure field errors which may have detainmental effects on FEL operation (such as phase shifts and beam walkoff) by using the pulsed-wire technique. In this article we present the experimental design and measurements of the entrance and propagation of the electron beam ($2A$, $70KeV$) in a planar wiggler ($B_w = 300G$, $\lambda_w = 4.4cm$) constructed in Hallbach configuration with 17 periods and two long permanent magnets for horizontal focusing. The measurements were used to find the wiggler field and to estimate the electron trajectories. We also present the calculation of the wiggler field gradient required for focusing the electron beam in horizontal direction and the electron trajectories in such a field. A comparison of the analytical formulae results of this calculation with 3D numerical simulation is presented.

AUTHOR INDEX

*No abstract available.

*No abstract available.